Bioabsorbable Materials for Osteosynthesis and Small Joint Arthroplasty in the Hand

Eero Waris

Department of Hand Surgery, Helsinki University Central Hospital;
Institute of Biomedicine/ Anatomy, University of Helsinki;
Department of Medicine, Helsinki University Central Hospital;
ORTON Orthopaedic Hospital of the Invalid Foundation, Helsinki, Finland

Academic Dissertation

To be presented, with the permission of the Faculty of Medicine of the University of Helsinki,
for public examination in the auditorium of Töölö Hospital,
on October 17th, 2008, at 12 noon.

Helsinki 2008

Supervisor	Professor Yrjö T. Konttinen, MD, PhD Department of Medicine/ Invärtes medicin Helsinki University Central Hospital Helsinki, Finland
Reviewers	Professor Christer Sollerman, MD, PhD Department of Hand Surgery Sahlgrenska University Hospital Gothenburg, Sweden
	Docent Ilkka Antti-Poika, MD, PhD Orto-Lääkärit Medical Center Helsinki, Finland
Opponent	Docent Eero Belt, MD, PhD Rheumatism Foundation Hospital Heinola, Finland

Tieteellinen tutkimus ORTONin julkaisusarja, A:25
Publications of the ORTON Research Institute, A:25
http://ethesis.helsinki.fi

ISBN 978-952-9657-41-4 (paperback)
ISBN 978-952-9657-42-1 (PDF)
ISSN 1455-1330

Yliopistopaino
Helsinki 2008

To Krista and Juhana

CONTENTS

ABSTRACT

Fractures and arthritic joint destruction are common in the hand. Surgical interventions are required to minimise functional impairment in more severe cases. A reliable and stable fracture fixation can be achieved by metal implants, which however, become unnecessary or even harmful after consolidation. The silicone implant arthroplasty is the current method of choice for reconstruction of metacarpophalangeal joints in rheumatoid patients. However, the outcome tends to worsen with long-term follow-up and implant-related complications become frequent. To address these problems, bioabsorbable implants were designed for the hand area. The bone fixation stability provided by bioabsorbable implants is of concern in the hand. Bioabsorbable joint scaffold arthroplasty offers a concept for small joint arthroplasty, but the histology is unknown.

Aims of the studies were: 1) to evaluate the biomechanical stabilities provided by self-reinforced (SR) bioabsorbable poly-L/DL-lactide 70/30, polylactide-polyglycolide 80/20 and poly-L-lactide implants in a transverse and an oblique osteotomy of small tubular bones and to compare them with those provided by metal implants; 2) to evaluate the SR poly-L/DL-lactide 70/30 plate for osteosynthesis in a proof-of-principle type of experiment in three cases of hand injuries; and 3) to evaluate the poly-L/D-lactide (P(L/D)LA) 96/4 joint scaffold, a composite joint implant with a supplementary intramedullary Polyactive® 1000PEO70PBT30 stem and Swanson silicone implant in an experimental small joint arthroplasty model.

Methods used were: 1) 112 fresh frozen human cadaver bones and 160 pig metacarpal bones osteotomised transversally or obliquely, respectively, and tested *ex vivo* in three point bending and in torsion; 2) three patient cases of complex hand injuries; and 3) the fifth metacarpophalangeal joints reconstructed in 18 skeletally-mature minipigs and studied radiologically and histologically.

Results of bioabsorbable fixation: In a transverse osteotomy, a 2.0 mm bioabsorbable plate system provided fixation stability comparable to that of a 1.7 mm titanium plate system but lower than that of a 2.3 mm titanium plate system. In an oblique osteotomy, 1.5 mm bioabsorbable pins provided fixation rigidity comparable with 1.5 mm Kirschner wires in dorsal and palmar apex bending, but torsional rigidity was lower. 2.0 mm bioabsorbable screws provided rigidity comparable with that of 1.5 mm Kirschner wires in all directions, but with lower rigidity than the titanium screws. The bioabsorbable plate considerably enhanced the bending stability for the fixation construct, but a single bioabsorbable screw provided only minor torsional stability. In patient cases, a bioabsorbable plate and screws were successfully used for osteosynthesis resulting in consolidation.

Results of bioabsorbable joint scaffold arthroplasty: P(L/D)LA 96/4 joint scaffold formed a porous interposition spacer, which maintained the arthroplasty space and induced fibrous tissue in-growth *in situ*. The scaffold was initially filled with vascular, loose connective tissue. Along with the degradation of the scaffold, the in-grown connective tissue matured and condensed turning into dense fibrous connective tissue. After three years, the scaffold had almost completely degraded and been replaced by well-organised dense fibrous tissue. Patches of

loose connective tissue with few macrophages and foreign-body giant cells were seen as a last sign of the polymer degradation process. In the composite joint implant, the Polyactive® 1000PEO70PBT30 stem caused deleterious, osteolytic tissue reaction.

Conclusions: The initial fixation stabilities provided by bioabsorbable implants in the tubular bones of the hand were comparable with currently-employed metal fixation techniques, and were sufficient for fracture stabilisation in three preliminary cases in the hand. However, in torsion the stabilities provided by bioabsorbable implants were lower than that provided by metal counterparts. The bioabsorbable plate enhanced the bending stability for the bioabsorbable fixation construct. P(L/D)LA 96/4 joint scaffolds demonstrated good biocompatibility and were shown to enable fibrous tissue in-growth *in situ* and finally formation of a functional, stable pseudarthrosis with dense fibrous connective tissue. However, due to deleterious tissue reaction, a supplementary Polyactive® 1000PEO70PBT30 stem can not be applied to the composite joint implant. The bioabsorbable implants have potential for use in clinical hand surgery, but have to await validation in clinical patient series and controlled trials.

LIST OF ORIGINAL PUBLICATIONS

This thesis is based on the following publications, which will be referred to in the text by their Roman numerals.

I Waris E, Ashammakhi N, Happonen H, Raatikainen T, Kaarela O, Törmälä P, Santavirta S, Konttinen YT. Bioabsorbable miniplating versus metallic fixation for metacarpal fractures. Clin Orthop Rel Res 2003;410:310-319.

II Waris E, Ashammakhi N, Raatikainen T, Törmälä P, Santavirta S, Konttinen YT. Self-reinforced bioabsorbable versus metallic fixation systems for metacarpal and phalangeal fractures. A biomechanical study. J Hand Surg [Am] 2002;27:902–909.

III Waris E, Ninkovic M, Harpf C, Ninkovic M, Ashammakhi N. Self-reinforced bioabsorbable miniplates for skeletal fixation in complex hand injury. Three case reports. J Hand Surg [Am] 2004;29:452-457.

IV Waris E, Ashammakhi N, Lehtimäki M, Tulamo RM, Kellomäki M, Törmälä P, Konttinen YT. The use of biodegradable scaffold as an alternative to silicone implant arthroplasty for small joint reconstruction: an experimental study in minipigs. Biomaterials 2008;29:683–691.

V Waris E, Ashammakhi N, Lehtimäki M, Tulamo RM, Törmälä P, Kellomäki M, Konttinen YT. Long-term bone tissue reaction to polyethylene oxide/ polybutylene terephthalate copolymer (Polyactive®) in metacarpophalangeal joint reconstruction. Biomaterials 2008;29:2509-2515.

ABBREVIATIONS

ANOVA	analysis of variance
CMC	carpometacarpal
CT	computerised tomography
DIP	distal interphalangeal
IP	interphalangeal
MC	metacarpal
MCP	metacarpophalangeal
PBT	polybutylene terephtalate
PDS	polydioxanone
PEO	polyethylene oxide
PEO/PBT	co-polymer of polyethylene oxide and polybutylene terephtalate
1000PEO70PBT30	co-polymer of polyethylene oxide and polybutylene terephtalate with a PBT content of 30 mol-% and an initial PEO segment length of 1000 Da
PIP	proximal interphalangeal
PGA	polyglycolic acid or polyglycolide
PDLA	poly-D-lactide
PDS	polydioxanone
PLA	polylactic acid or polylactide
PLGA	co-polymer of lactide and glycolide
P(L/DL)LA	poly-L/DL-lactide
P(L/D)LA	poly-L/D-lactide
PLLA	poly-L-lactide
PTMC	polytrimethylene carbonate
ROM	range of motion
SD	standard deviation
SR	self-reinforced

1 INTRODUCTION

Hand function is important for the human being. The delicate and complex anatomy of the hand is reflected in its sophisticated mechanical and sensory functions. Because of active use, the hand is susceptible to disorders such as traumatic injuries and arthritic joint destruction. They may lead to impairment of hand function affecting quality of life, work ability and social communication. Optimal management of hand injuries and arthritis can prevent a significant amount of morbidity and disability.

In the unstable fractures or complex injuries of hand, internal fixation is often needed. Metal implants provide reliable and stable fixation allowing early mobilisation, but they become unnecessary or even harmful after consolidation [20, 49, 125, 127, 174, 175]. Prominent implants may interfere with surrounding tissues causing tendon irritation and disturbing joint movement [127, 175]. Problems may arise from pin track infections and loosening [20, 174]. Hence, the metal implants are often removed in a secondary operation [20, 174, 175].

Small joint arthroplasty is a challenging problem in hand surgery. In advanced metacarpophalangeal (MCP) joint destruction, silicone implant arthroplasty – the current method of choice – provides satisfactory results in rheumatoid patients, which, however, tend to worsen over time [33, 53]. Silicone-implant related complications include implant breakage, fragmentation and wear, as well as osteolysis around the implant [9, 33, 47, 53, 188]. The use of current biostable hardware in the operative treatment of hand fractures and small joint arthroplasty, does not yield optimal functional outcomes and may lead to complications necessitating repeated surgical procedures.

Bioabsorbable implants are increasingly used for bone fixation in trauma, orthopaedic [158, 219] and craniomaxillofacial surgery [6, 219]. The aim with their use is to retain tissue-supporting properties for a certain period of time to guarantee regeneration of damaged tissues and to guide the growth of new tissue, while at the same time allowing degradation and finally replacement of the implant by host tissue. This helps limit possible long-term adverse effects of implants and avoid the necessity for further surgical intervention.

The biomechanical properties of bioabsorbable fixation implants have not been well validated in hand bones, where small implants of good mechanical properties are required. Bioabsorbable poly-L/D-lactide (P(L/D)LA) 96/4 joint scaffold arthroplasty is a recent, clinically-introduced concept in the reconstruction of small joints [64, 65], but experimental *in vivo* studies are needed to validate this concept.

In the present study, the applicability of bioabsorbable polymers for hand osteofixation and for small joint arthroplasty was studied.

2 REVIEW OF THE LITERATURE

2.1 Anatomy and biomechanics of the hand

The skeleton of the hand consists of carpal, metacarpal and phalangeal bones. The metacarpals are the most proximal of the long bones of the hand and form the support structure for the palm. Their shafts are curved longitudinally so that they are convex dorsally and concave on their volar aspect. Four of the fingers contain three phalanges each, but the thumb only has two. The joints of the fingers are metacarpophalangeal (MCP), proximal interphalangeal (PIP) and distal interphalageal (DIP) joints. In the thumb there is only one interphalangeal (IP) joint.

The MCP joint is integral for the normal function of the hand. It is a condylar joint, in which the convex metacarpal head articulates with the shallow concave cavity of the proximal phalanx base. The articular surface of the head of the metacarpal bone has a wider volar surface, which arrangement leads to the tightening of the collateral ligaments when the joint is brought in flexion. There is a volarly-moving axis of rotation, when the MCP joint comes into flexion. The stability is achieved via the collateral ligaments on the radial and ulnar sides of the joint, more volarly via accessory collateral ligaments and via the volar plate on the volar side of the joint. Dorsally, the joint is reinforced by the expansion of the digital extensor tendon (extensor hood). Additionally, the deep transverse metacarpal ligaments connect the medial four joints to each other and hold the heads of the metacarpal bones together. Normal synovial membrane is attached around the margins of the articular cartilage with volar and dorsal capsular reflections. The range of motion (ROM) for the MCP joint is normally described to be 90-100° for active flexion-extension, and a maximum of 60° for abduction-adduction with extension but decreasing with flexion. The combination of these movements also allows restricted axial rotation. The MCP joint deviates slightly in the ulnar direction with flexion of the digits.

The IP joints are hinge joints located between the phalanges, and their movement is limited to flexion and extension. The volar plate and collateral ligaments provide stability to the joint. The metacarpal bones articulate to carpal bones by carpometacarpal (CMC) joints of 2nd to 5th finger with little or no mobility. The CMC joint of the thumb (CMC I, trapeziometacarpal joint) is a biconcave-convex saddle-shaped joint with good mobility and, for example, enables the thumb to be positioned in opposition to the other fingers. Its elaborate ligamentous system is essential for its stability and allows high force transmission during routine pinch and grasp [12]. The movements of the hand occur primarily in the wrist, which articulates the hand to the forearm and includes eight carpal bones arranged in two rows of four each: trapezium, trapezoid, capitate, hamate; scaphoid, lunate, triquetrum and pisiform.

The musculature moving the fingers falls into two groups: 1) the extrinsic muscles, the flexors and extensors which pass from the upper forearm to the hand; and 2) the intrinsic muscles, the interossei and lumbricals which are situated close to the metacarpal bones. The deep and superficial flexors, respectively, produce flexion of the DIP and PIP joints. There are five annular pulleys and four cruciate pulleys, which prevent bowstringing of the flexor tendons across the joints. The interossei and lumbrical muscles exert a flexion force on the MCP joint through their attachments into the extensor hood and proximal phalanx. The flexor tendons

can also exert a flexion moment on the MCP joint, but their insertions on the phalanges require this to occur after IP joint flexion. The thumb has only a single extrinsic tendon for the flexion of IP joint, and three pulleys.

The extrinsic extensors are primarily responsible for MCP extension. An inconstant pattern of intertendinous connections (juncturae tendinum) exists at the metacarpal level. Unlike other fingers, both the index and small finger have dual extensor system. The sagittal bands aid in extension of the MCP joint through their insertion into the volar plate, as well as stabilising the extensor tendons over the joint itself. The interossei and lumbrical muscles are the principal extensors of the IP joints of the fingers. The interossei muscles also work as abductors and adductors of the fingers. The extensor mechanism of the thumb is different from that of the fingers in that each joint has an independent tendon for extension. The intrinsic muscles of the thumb primary provide rotational control, but also contribute to MCP flexion and IP extension.

The function of the hand is assessed by recording the total active ROM of the affected finger, recorded as the summation of flexion range of the MCP and IP joints. The normal range for thumb has been recorded to be 140° and for other fingers 260° [39, 48].

The internal forces acting in the bones, joints and soft tissues during hand function have been analysed [9, 37, 222]. The maximum force generated by the flexor tendons [80] has been calculated to create an average bending moment of 0.35 Nm to metacarpals [202]. The average pinch strength has been reported to be 70 N for men and 50 N for women [9], whereas for arthritic patients only 5-20 N [222]. From the external forces exerted on finger pad, the internal forces that act on the MCP joint have been estimated by splitting the internal force into three vectors, which are perpendicular to the metacarpal bone (X), volar (Y) and ulnar (Z) force components. These internal force components have been reported to be on average 6, 3, and 2 times the external force in the pinch grip, and 12, 6 and 4 times the external force in the full power grip, in each X, Y and Z direction respectively [9]. Thus, according to these three dimensional models, the average maximum pinch strength of male and female yields compressive forces of 420 N and 300 N on the MCP joint surface, respectively. Experimental measurements have shown that a pinch force of 1 kg at the thumb tip translates a 12 kg compression force at the CMC I joint, but compression forces up to 120 kg may occur at the CMC I joint during a strong grasp [37].

Fractures of the metacarpals and phalanges may be associated with variable degrees of angulation, shortening and rotation. Typically, metacarpal shaft fractures tend to angulate apex dorsally because of the deforming pull of the flexor tendons and the intrinsic muscles (Fig. 1A). On the other hand, shaft fractures of the proximal phalanges tend to angulate apex palmarly secondary to pull of the intrinsic muscles proximally and extensor tendon distally (Fig. 1B).

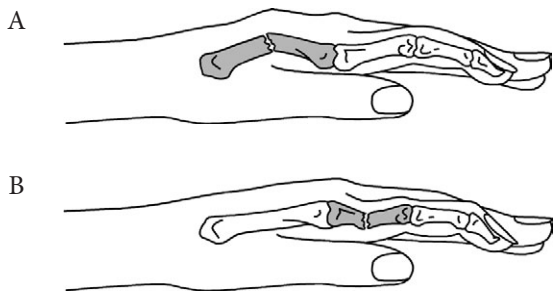

Figure 1. A typical displacement pattern of A) metacarpal fractures is dorsal apex angulation and that of B) proximal phalangeal fractures palmar apex angulation.

2.2 Internal fixation of metacarpal and phalangeal fractures

Metacarpal and phalangeal fractures are common, comprising approximately 17% of all fractures [199]. Most of these fractures are stable and can be treated with a cast or splint. However, unstable fractures or complex hand injuries require internal skeletal fixation to restore optimal hand function. The internal fixation is commonly provided with metal implants, which are generally made of stainless steel, titanium or titanium alloys.

2.2.1 Biomechanical test methods

In most biomechanical studies regarding metacarpal and phalangeal fixation stabilities, denuded bone specimens have been used, although surrounding soft tissues contribute to the stability of system [124]. On the other hand, there are reference values for the biomechanical stabilities of various fixation implants and biomaterials in such system. The specimens most utilised have been human cadaver metacarpal [13, 45, 104, 107, 124, 139-141, 202] and proximal phalangeal [14, 46, 50, 107, 140, 159, 204] bones, pig metacarpal bones [2, 105, 106] and synthetic bones [22, 171]. Fresh frozen bone specimens [2, 106, 139-141] have been demonstrated to most closely maintain the mechanical properties of bone [192], but also various preservatives such as formaldehyde or ethanol [13, 14, 45, 46, 104, 124, 159, 202, 204] have been used to preserve bone specimens. The bone specimens should be kept in hydrated conditions, preferably in physiological saline to maintain the mechanical properties of bone [192].

Fracture models used in the biomechanical studies include transverse [2, 13, 22, 46, 50, 104-106, 124, 139-141, 171, 202, 204], oblique [14, 45, 46, 105, 204] or spiral [107] osteotomy, and less frequently, standard techniques have been used to create a standardised fracture or comminution [159].

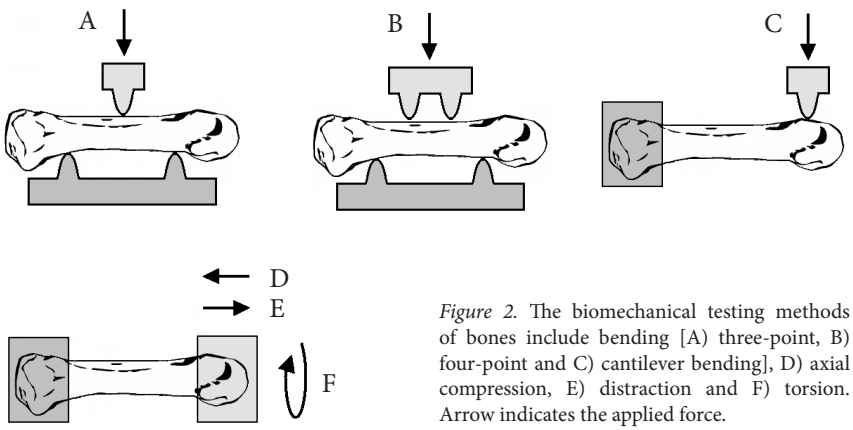

Figure 2. The biomechanical testing methods of bones include bending [A) three-point, B) four-point and C) cantilever bending], D) axial compression, E) distraction and F) torsion. Arrow indicates the applied force.

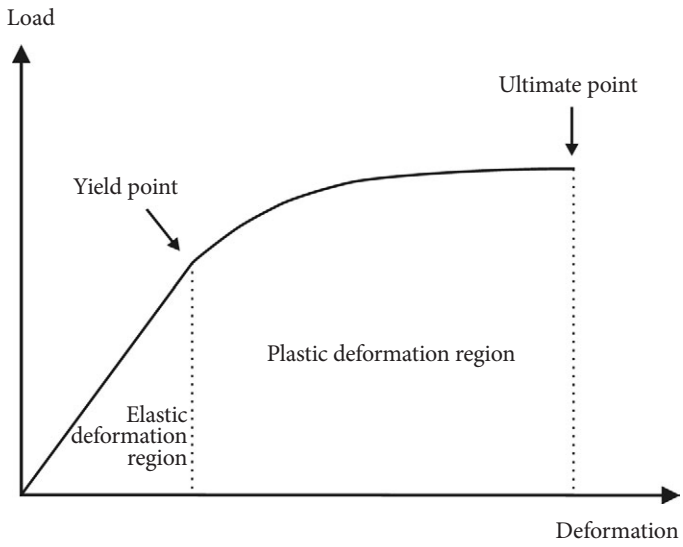

Figure 3. Schematic presentation of load-deformation behaviour of a bone specimen.

The testing methods of bone specimens include bending [2, 13, 14, 22, 45, 46, 50, 104-107, 124, 139-141, 159, 171, 202, 204], torsion [13, 45, 46, 107, 139, 141, 159, 204], axial compression [45, 46, 159] and distraction [204] tests (Fig. 2). Three types of bending testing have been described: three-point bending [13, 14, 124, 139-141] four-point bending [2, 22, 45, 46, 104-106, 159, 204] and cantilever bending [50, 107, 171, 202] (Fig. 2).

The relationship between the load applied to an object and the deformation in response to this load is called the load-deformation curve (Fig. 3). The load-deformation curve can be typically divided into two regions: the elastic deformation region and the plastic deformation region [192]. In the elastic deformation region, the deformation in the bone shows a linear increase, as load increases. The slope of the elastic region of the load-deformation curve represents the extrinsic stiffness or rigidity of the object. The elastic deformation and plastic deformation regions are separated by the yield point. Stress subjected *in vivo* in the specimen must be safely below the yield point, since above that point load applied to the specimen causes permanent damage to the shape and creates a potential for complications such as malunion or nonunion in fracture healing. In the plastic deformation region, the slope of the curve is reduced, but the load often continues to increase to the maximum point of the curve - the ultimate point. The breaking point at which the bone actually breaks is often the same value as the ultimate point.

Fatigue properties can be measured by applying cycling loading to the objects. In fatigue tests, the specimen is repetitively loaded, with loads within the elastic deformation region of the load-deformation curve, and the decrease of its mechanical properties over a certain period of time or number of cycles is recorded [45]. In the bone, the cause of fatigue failure is attributed to creep, or the accumulation of cracks in bone [192].

2.2.2 Biomechanical studies

The fixation stabilities provided by various techniques of metal internal fixation have been intensively studied in hand bones. Stable fixation is usually preferred in the hand to facilitate early ROM exercises. These decrease the hand stiffness, joint contractures, and tendon adhesions associated with prolonged immobilization. However, there is experimental evidence that rigid fixation is not always the most desirable method with respect to fracture healing [181]. Furthermore, there is no data indicating exactly what is the minimal fixation rigidity required to achieve functional stability in the hand. Failure of the osteosynthesis usually leads to non-union or malunion.

Biomechanical studies on human denuded metacarpal and phalangeal bone specimens have shown that metal plate fixation with an interfragmentary screw is biomechanically superior to other fixation methods, including a plate alone, two interfragmentary lag screws, Kirschner wire fixation, or interosseous wiring [13, 14, 45]. For oblique and spiral osteotomies, screw fixation enhances fixation stability by using the lag screw technique to achieve interfragmentary compression [14, 107].

After a transverse osteotomy, a dorsal plate fixation provided more rigidity than crossed Kirschner wires or a single interosseous wire with or without a Kirschner wire in torsion and in dorsal apex bending [13]. In palmar apex bending and corresponding cantilever bending direction, two crossed Kirschner wires, or a Kirschner wire combined with an interosseous wire provided rigidity similar to [13, 14, 202] or higher [50] than a dorsal plate alone. A dorsal plate alone is at a mechanical disadvantage in palmar apex bending, which isolates the plate and allows only the plate to support the load. The volar, rather than dorsal, placement of the plate allows the bone to share the mechanical load and thus increases the rigidity in palmar apex bending [105], but respectively decreases the stability in dorsal apex bending [140]. Three-dimensional plate design increases the rigidity of plate fixation [141, 171].

The stability of Kirschner wire fixation is dependent on the configurations and diameter of the Kirschner wires. For transverse osteotomies, crossed Kirschner wires provide the highest resistance to torsion and distraction [204], whereas crossed and longitudinal configurations provided comparable stability against bending [204]. For oblique osteotomy, bending, torsion and distraction are best resisted by Kirschner wires placed perpendicular to the fracture [204], whereas compressive loading is best resisted by wires placed perpendicular to the shaft. Therefore, using multiple Kirschner wires in different orientations is preferred [105, 106, 204]. A supplementation of stainless-steel cerclage wire with Kirschner wires, a technique termed tension band wiring, provides additional stability and achieves compression at the fracture site [14, 202].

The fatigue performance of various metal fixation techniques has been studied by Firoozbakhsh *et al.* [45]. In cyclic loading, the plate and screw fixation had the highest fatigue stiffness in bending, torsion, and axial loading, followed by two interfragmentary lag screws, crossed Kirschner wires with tension bands, and intramedullary Kirschner wires after oblique osteotomy [45].

2.2.3 Clinical results and problems related to metal fixation implants

The results vary as regards the post-operative outcomes after operative treatment of metacarpal and phalangeal fractures. Functional outcome is optimised when anatomic restoration and stable fixation are achieved; active ROM exercises can be initiated early in the post-operative period, and soft-tissue damage is minimised.

The Kirschner wire fixation is often preferred because of the relatively easy technique and the possibility for percutaneous introduction. In a retrospective consecutive case series of 22 metacarpal shaft fractures, multiple intramedullary Kirschner wires provided good results, but in two patients the Kirschner wires bent at the fracture site producing 20° angular deformities [44]. In a prospective study on 277 digital fractures, Pun *et al.* [142] reported in 1989 unsatisfactory results with 109 unstable digital fractures treated with Kirschner wire fixation, most of which were associated with a soft-tissue injury. Only 30.3% of these operated digits achieved total active ROM ≥ 210°. The reported complication rate associated with the use of Kirschner wires has usually been 15-18% [20, 174]. The most common complications were pin tract infection, pin loosening, and loss of reduction. Rare complications included osteomyelitis, tendon impalement or rupture, nerve lesion, non-union, pin protrusion and migration [20, 174]. The majority of the complications resolved following Kirschner wire removal without permanent sequelae [20, 174]. There have been reports of Kirschner wires migrating from the hand as far as the heart [55, 58]. Fractures with segmental bone loss or extensive comminution often cannot be treated effectively with Kirschner wires.

A randomised prospective study of 32 patients with an oblique proximal phalangeal shaft fracture showed that percutaneous Kirschner wires and open lag screw fixation provided similar outcomes as regards union, functional recovery or residual deformity [67]. A retrospective case study of 50 metacarpal and 40 proximal phalangeal fractures reported better results with open screw fixation than with percutaneous Kirschner wire fixation [41]. This was explained by the fact that the screw fixation allows earlier mobilisation. In 32 patients with a fracture dislocation of the base of the thumb metacarpal (Bennett's fracture) with a large fracture fragment, percutaneous transarticular Kirschner wire fixation and open reduction with a lag screw yielded similar clinical outcomes [99].

Following metal plate and screw fixation, several studies have demonstrated favourable recovery of function in metacarpal and phalangeal fractures [17, 39, 48, 189]. Dabezies and Schutte [39] reviewed their series of 52 unstable metacarpal and phalangeal fractures without any significant soft-tissue injury and reported excellent results with average total active ROM ranging from 233° in the condylar group to 252° in the metacarpal group. In a retrospective series of 22 patients with 26 unstable metacarpal fractures treated with screws and plates, 20 of the involved fingers achieved total active ROM ≥ 220°, but in 6 cases with an open, intra-articular or extensor tendon injury the movement was restricted [48]. In a retrospective consecutive series of 56 closed, extra-articular metacarpal and phalangeal fractures treated with titanium miniplates and screws, the patients achieved average total active ROM of 256° of the involved finger and all but one of the 44 patients fully regained their previous activity, and subjective impairment was totally absent in 39 of the patients [189].

After metal plate and screw fixation, less encouraging results have also been reported [31, 125, 127, 143, 175]. Pun *et al.* [143] reported in 1991 unsatisfactory results with stainless-steel plate and screw fixation in a prospective study of 52 unstable phalangeal fractures, most

of which were open or comminuted or associated with significant soft-tissue injury. The functional outcome was unsatisfactory since only 26.9% of the involved digits reached good results with a total active ROM ≥ 210°. The authors concluded that these results were similar to the comparator group from an earlier study by the same authors, in which Kirschner wire fixation was used in the same institute [142]. Stern *et al.* [175] reported complications in 16 of 38 (42%) proximal phalangeal and metacarpal shaft fractures treated with stainless-steel plate fixation. Total active ROM ≥ 210° was achieved in 76% of all digits, but in only 5 of 9 (56%) phalangeal fractures.

Through metallurgical advances, lower-profile plates made of titanium have become available. However, Page and Stern [127] could not demonstrate any improvement in the clinical outcomes or complication rates (57%) following low-profile titanium plate fixation of 105 metacarpal and phalangeal fractures compared to results of earlier studies by Stern *et al.* [175] and Pun *et al.* [143]. In two more recent retrospective studies, major complications were registered in 32% of metacarpal [49] and in 52% of phalangeal [92] fractures following plate fixation. The use of minicondylar plate for unstable intra-articular and periarticular fractures of the phalanges and metacarpals resulted in complication rate of 57%, and 38% of the fractured fingers achieving total active ROM ≥ 221° [125]. The most common complications related to the use of metal plates have been stiffness, malunion or consolidation problems, but also plate loosening or breakage, plate prominence, infection and tendon rupture have been reported [31, 125, 127, 143, 175]. The plate fixation itself is not necessarily the prime determinant of the poor clinical outcomes, but rather the frequent use of plates, in particular in complex injuries [31, 125, 127, 143, 175]. The unfavourable prognostic factors that have been reported to adversely affect the functional outcome are an open or comminuted fracture, intra-articular or periarticular involvement, multiple fractures and associated soft-tissue injury, particularly tendon injury [32, 125, 127, 142, 175]. The complications and poor outcomes are more frequent for phalangeal than for metacarpal fractures [125, 127, 175, 189].

The metal fixation implants become unnecessary or even harmful after the consolidation of metacarpal and phalangeal fractures [20, 49, 125, 127, 174, 175] that typically occurs after 4 to 7 weeks [212]. The disadvantage of metal plate fixation in the hand is that they may cause irritation and adhesion of tendon and surrounding tissue [35], palpability, pain and disturbance of the function of a nearby joint. The high elastic modulus of metals causes stress shielding and bone loss beneath the applied plate, especially in weight-bearing bones [63, 126]. Metal implants cause signal interference with radiologic and magnetic resonance imaging. Growth aberrations can emerge as a result of the use of metal implants in children [6, 124]. *In vivo* corrosion and metal sensitivity have been reported as a potential disadvantage of the metal implants, especially of stainless-steel implants [60]. The advantages of titanium over stainless steel include decreased implant stiffness and increased biocompatibility [60].

A second intervention is often performed to remove metal implants in the hand. It implies additional surgical discomfort, risks, and associated sosio-economic costs [158]. Kirschner wires are often left in place only until consolidation [20]. In earlier series, as many as 25% of metal plates were removed in a secondary procedure [175], but the advances in plate profile and design, use of titanium and lateral placement of the implants to avoid the extensor mechanism have decreased the need for plate removal [49, 189].

2.3 Small joint arthroplasty in the hand

2.3.1 Arthritic hands

The etiologies of the articular destructions of the finger joints include most often rheumatoid arthritis, osteoarthritis, and trauma.

Rheumatoid arthritis is a chronic, systemic, autoimmune inflammatory disease of unknown etiology with a prevalence of approximately 1% [61]. Symmetrical involvement of the small joints of the hands is typical. It often leads to involvement along the entire kinetic chain from the wrist to the PIP joint, but the MCP joint is the most commonly involved joint, arthroplasty of which is an established procedure. The MCP joint involvement typically falls along a spectrum involving a progression of joint destruction and deformity. Typical deformities in MCP joints are volar subluxation and ulnar deviation. The factors that contribute to the development of an ulnar deviation include dislocation of the extensor tendons in an ulnar direction, exaggeration of the ulnar shift of the long flexors, pressure of the thumb against the fingers during lateral pinch, ulnar intrinsic pull, and carpal collapse associated with radial deviation of the metacarpals. Volar subluxation, with eventual dislocation of the MCP joints, may occur when the volar force of the flexor tendons, unopposed by the extensor tendons dislocated in an ulnar direction, acts on the attenuated capsular structures. Other characteristic deformities are hyperextension of the PIP joint with flexion of the DIP joint (swan-neck deformity), flexion of the PIP joint with hyperextension of the DIP joint (boutonnière deformity), and Z-shaped deformity of the thumb from volar subluxation of the first MCP joint and compensatory hyperextension of the IP joint. Muscle involvement may lead to contractures and weakness. Inflammation in and around the tendons may distend tendon sheaths and cause tendon ruptures.

Osteoarthritis is the most common form of arthritis. The exact etiology is unknown, but it leads to a disturbance of the normal balance of degradation and repair of articular cartilage and subchondral bone [61]. It occurs usually as a primary disorder, but can also occur secondarily to infection or trauma. A series of factors, such as age, sex, heredity, occupation, injuries, and the level of activities, are related to the development of hand osteoarthritis. The most commonly affected joints are DIP and CMC I joints, but other types including PIP, MCP, sesamoid, scaphotrapezial-trapezoid and pisiform-triquetral osteoarthritis are seen. In joints with osteoarthritis, inflammation may be present; however, it is usually mild and may only involve the periarticular tissues. Secondary displacement and contracture are usually more limited than in rheumatoid arthritis. Radiological features are joint-space narrowing, osteophytes, subchondral sclerosis, bone cysts, deformation of bone heads, and cortical collapse [61].

2.3.2 Advances in small joint arthroplasty

Small joint arthroplasty is a major challenge in hand surgery. A variety of arthroplasty techniques have been developed in attempt to address this issue, with varying results. The currently-used arthroplasty methods include joint resection and the interposition of soft tissues or alloplastic material, and surface replacement prostheses. Vascularized toe joint transfer is used as an alternative form of treatment for reconstructing traumatic injury of finger joints and is indicated in a young patient to maintain the epiphyseal growth plate [173]. Joint fusion is considered an alternative salvage procedure to relieve pain and to create stability, but it leads to loss of joint motion.

Resection arthroplasty techniques without and with interposition of soft-tissues [156], including the extensor tendon [193, 194] or volar plate [156, 191] were pioneering inventions in small joint arthroplasty. In Vainio's arthroplasty, the extensor tendon over the MCP joint is sectioned, and its distal end is interpositioned between the proximal phalanx and the resected metacarpal head and sutured to the volar plate; the proximal extensor stump is sutured over the distal stump [193, 194]. In volar plate arthroplasty described by Tupper [191] the volar plate is released proximally and brought over the metacarpal head excision, and sutured dorsally as an interposition material. The data on the results of the soft-tissue arthroplasty procedures for MCP joints varies. After Swanson silicone implants became available, the use of soft-tissue arthroplasties has become only occasional. However, there are no comparative studies showing their inferiority compared to silicone implant arthroplasty. Tendon interposition with or without ligament reconstruction after partial or complete trapezium excision is commonly used to alleviate pain in thumb basal joint osteoarthritis [183], although some surgeons prefer a temporary Kirschner wire fixation instead of tendon interposition to distract and maintain the arthroplasty space and to allow fibrous tissue invasion [56].

Since Swanson presented his concept of silicone implant arthroplasty in the mid 1960s, the use of flexible silicone implants for deformity and destruction of MCP joints in rheumatoid arthritis has been studied extensively and the method has become well accepted [33, 96]. Encouraged by success of silicone implants in the MCP joints, similar hinge silicone implants were also developed to reconstruct radiocarpal and PIP joints, with less favourable results [81, 179]. The silicone implants to resurface the radial head or the base of the thumb metacarpal, or to replace scaphoid, trapezium and lunate have also been used in the past but their use is currently sparse because of high rate of failures and problems with silicone wear, synovitis and osteolysis [28, 81]. During the last decades a number of biological [10, 190] and alloplastic materials such as ceramics [7], pyrolytic carbon, Gelfoam [123], expanded polytetrafluoroethylene [119], polypropylene [119], and polyurethane [172] have been used as an interposition material in small joint arthroplasty, but none of the large number of procedures is completely satisfactory and some cause major complications [7, 10, 119].

A large number of different designs of constrained implants have been developed for small joint replacement arthroplasty. The first MCP prostheses were metal hinges [9, 96], followed by various types of cemented or non-cemented constrained implants with metal and polymeric components [9, 96], but a high incidence of complications such as implant breakage, loosening, recurrence of deformity, progressive loss of mobility, bone erosion, deposition of debris and perforation through the cortex were reported [9, 96].

Most recently, surface replacement MCP and PIP prostheses with separate proximal and distal components (for insertion with or without cement), which come into contact to form bearing surfaces, have become available [96]. These prostheses simulate normal joint kinematics. They are now increasingly performed and may be adequate for implantation in patients without inflammatory disease or with less advanced rheumatoid disease. A wide variety of biomaterials have been utilised, including cobalt-chrome alloys, stainless steel, titanium, titanium alloys, ceramics, ultra-high molecular weight polyethylene and more recently pyrolytic carbon [23, 36, 96, 173]. However, none of the surface replacement designs has shown consistently successful clinical results and become widely accepted. There are several reasons why transferring the successful large joint arthoroplasty technology to the hand joints is difficult. The small joints of the hand are anatomically precise and delicate joints, and function within a very narrow tolerance of friction and mechanical balance of bone and soft-tissue forces. The stabilising soft tissues and ligaments, which are necessary for surface replacement prostheses, are often destroyed in late-stage rheu-

matoid arthritis. Positive long-term results with pyrolytic carbon surface replacement MCP prostheses have been reported in 26 mostly rheumatoid patients with little deformity and subluxation [36]. However, early data suggest that pyrolytic carbon surface replacement arthroplasty does not demonstrate superiority over silicone implant arthroplasty in osteoarthritic and post-traumatic patients [23, 173]. This surface replacement concept has been applied also for arthroplasty of the basal joint of the thumb, but high complication rates have been reported [96, 215].

2.3.3 Silicone implant arthroplasty in metacarpophalangeal joints

Silicone is a chemically-inert polymer of dimethylsiloxane that can be prepared as a liquid, gel or elastomer [220]. The Swanson silicone MCP implant is a one-piece silicone rubber implant with a double stem inserted into the opposing diaphyses, and a rectangular body between them in the middle. The body of the implant acts as a dynamic joint spacer between the bone ends, providing strength and flexibility. The stems of the implants are allowed to act like pistons within the intramedullary canals of metacarpal and proximal phalanx during movements of the joint, which is thought to spread the stresses over a greater implant area and thus to make the implant more durable. The implant induces fibrous tissue formation around it, a reaction that has been termed "encapsulation" [177]. The fibrous capsule undergoes functional adaptation and is oriented during a period of early motion [177]. Once a sufficient amount of fibrous capsule has formed around the implant, its integrity is of decreasing importance.

A number of studies with Swanson silicone implant arthroplasty have shown satisfactory results in the short to intermediate term in patients with rheumatoid arthritis in terms of pain relief and increased ROM [33, 53]. The reported active ROM values after silicone MCP joint arthroplasty are usually 40-50° [33, 53, 173]. The passive motion is typically greater but is not recorded in most clinical studies. The immediate post-operative ulnar deviation is usually corrected to less than 5° [33, 53]. However, the outcomes tend to worsen with long-term follow-up, regarding joint stiffening and recurrence of deformity [33, 53]. The complications encountered with silicone implants are breakage, fragmentation and wear of the implant, subsidence, bone changes (bone-shortening, erosion) and less frequently infection [9, 33, 47, 53, 188].

The rates of complication and breakage of Swanson implants vary considerably in the literature. In long-term follow-up, two-thirds of the implants have been reported to have broken [53, 188]. The loss of silicone implant integrity does not necessarily result in loss of joint function as regards ROM and hand function measures [53, 177]. However, recurrent ulnar deviation [53, 188] and osteolysis [130] have been related to silicone implant breakage. The pistoning movement of the Swanson implant releases silicone particles. This may cause osteolysis around the implant and, less frequently, silicone-induced particle synovitis [47, 53, 81, 188] or lymphadenopathy [47]. The loss of bone stock may be an enormous challenge in revision arthroplasty. Due to these limitations, silicone elastomer implants have usually been used only for rheumatoid arthroplasty and they are not recommended in osteoarthritis or after trauma.

Based on the concept of Swanson, modifications of flexible silicone MCP implant designs, such as Avanta (formerly Sutter) with more anatomical centre of rotation, have been introduced without significantly better clinical outcomes [116, 129]. Modifications of silicone implants with titanium grommets [9, 167, 188], Dacron reinforcement [40] or osseointegrable titanium fixtures [115] have not shown improved results. The results of the silicone implant arthroplasty are far from normal and far from ideal. Need for implants with improved biocompatibility and prolonged life in service in small joint artroplasty is evident [53, 131, 173].

2.4 Bioabsorbable materials

Exploration of the use of synthetic bioabsorbable polymers in medicine started in the 1960s [6, 158, 216, 219]. Early clinical applications of the polymers in this family were for sutures, but later implants for internal bone fixation were also developed. The bioabsorbable polymers have been applied for controlled release of drugs and proteins, and developed also in the forms of porous scaffolds for tissue engineering [79, 221].

The most widely used synthetic bioabsorbable polymers in surgery are aliphatic polyesters of α-hydroxy acid derivates, especially polyglycolide (polyglycolic acid, PGA) and polylactide (polylactic acid, PLA) and their co-polymers. However, a variety of synthetic polymers have been studied including polycaprolactone, polydioxanone (PDS) and polytrimethylene carbonate (PTMC). A segmented block co-polymer of polyethylene oxide (PEO) and polybutylene terephtalate (PBT) is one of the recent bioabsorbable polymers being under research.

2.4.1 Polyglycolide (PGA), polylactide (PLA) and their co-polymers

Polyglycolide or polyglycolic acid (PGA) (Fig. 4) of a high molecular weight is a hard, tough, highly crystalline polymer synthesised by ring-opening polymerisation from the glycolide, a cyclic diester of glycolic acid [79]. The first bioabsorbable synthetic polymer used clinically, in the form of sutures, was made of PGA [219]. A clinical limitation of PGA implant in bone fixation is the rapid degradation rate that may not always allow complete bone healing and may cause adverse tissue reactions [19, 135, 216, 219]. Self-reinforced (SR) PGA implants lose all mechanical strength *in vivo* within 4-7 weeks [203] and completely vanish in the cancellous bone of rabbits within 36 weeks [128]. Pure PGA implants are no longer used in osteosynthesis.

Polylactide or polylactic acid (PLA) (Fig. 4) of a high molecular weight is a polymer, synthesised by ring-opening polymerisation from cyclic diesters of lactic acid. Compared with PGA, PLA is more hydrophobic and has a slower degradation rate. Due to the chiral nature of lactic acid, it exists in two stereoisomeric forms, L- and D- lactic acid. Accordingly, the cyclic diester of lactic acid, lactide, occurs in three forms, namely L- (actually LL-), D- (actually DD-) and DL- lactide.

Poly-L-lactide (PLLA) is a partially crystalline polymer. The crystallinity and hydrophobicity make PLLA resistant to hydrolysis and degradation. The bending strength of SR-PLLA rods decreases to the level of cancellous bone in 36 weeks *in vivo* [100], but complete strength loss does not occur until 2 years *in vitro* [187]. The total loss of PLLA implant mass takes several years so that the remnants of SR-PLLA plates can been detected as long as 5 years after fixation of mandibular body osteotomies in sheep [176].

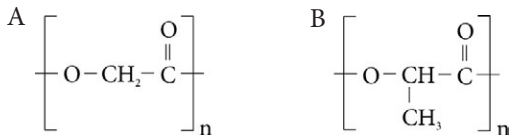

Figure 4. Chemical structure of A) polyglycolide and B) polylactide.

The polymerisation of a mixture L-, D- and DL-lactides leads to the synthesis of poly-D/L-lactides. Their strength and degradation rate depend on the relative amounts of L- and D-monomers in the polymer chain. Because of decreased crystallinity, the stereoco-polymers have lower strength and they are more susceptible to hydrolysis than pure PLLA. SR-P(L/DL)LA 70/30 is practically completely amorphous due to the high D-content in the polymer structure. The bending strength of the SR-P(L/DL)LA 70/30 pins started to decrease significantly after 18 weeks *in vitro*, losing all strength within 48 weeks [187]. *In vivo* the strength retention of SR-P(L/DL)LA 70/30 pins was longer in the rat subcutis, since about 40% of the initial bending and shear strengths were remaining at one year [73]. The complete absorption time of SR-P(L/DL)LA 70/30 is unclear, but it is estimated to occur *in vivo* in 2–3 years.

By co-polymerising L-lactide and glycolide, PLGA co-polymers with a variety of physicochemical properties can be obtained depending on their compositional ratios. The relationship between the co-polymer composition and the mechanical and degradation properties of the corresponding co-polymers is not, however, linear [112]. The SR-PLGA 80/20 co-polymer has substantially amorphous structure and the strength properties of pins decrease significantly after 6 weeks *in vitro* [138] and *in vivo* [101]. After 1.5 years some PLGA remnants were seen intracellularly in microscopic examination in rabbit cranial bone [182].

2.4.2 Mechanical properties and fabrication of implants

PGA and PLA exhibit the highest mechanical properties of all synthetic bioabsorbable polymers. However, implants manufactured from PGA, PLA or their co-polymers using the traditional melt-moulding techniques (such as extrusion and injection moulding) exhibit only modest mechanical properties. The values reported for strength are usually 40-140 MPa and for elastic modulus typically 2-5 GPa [187]. These values are lower than those of cortical bone, for which bending and shear strength values of 180-195 MPa and 68 MPa respectively, and elastic modulus of 6-20 GPa have been measured [155, 184].

Mechanical improvement of bioabsorbable implants was achieved when the self-reinforced (SR) manufacturing technique was invented [185, 187]. It significantly increases the strength, ductility and elastic modulus of bioabsorbable polymers. This involves the formation of a composite structure made of polymeric material comprised of oriented reinforcing units and a binding matrix, with both the matrix and reinforcing elements having the same chemical structure. A high degree of similar molecular orientation makes SR implants stiff and strong in the direction of their long axis. The most effective SR method is to die-draw the melt-moulded polymer sample into a partially-oriented form at controlled temperatures above the glass transition temperature of the polymer [187]. For SR-PLLA pins, an initial bending strength of 300 MPa and a shear strength of 220 MPa have been reported [185]. The bending strength values for SR-P(L/DL)LA 70/30 and SR-PLGA 80/20 pins have been reported to be 214 MPa [73] and 226 MPa [138], respectively. The initial shear strength values of 121 MPa [73] and 115 MPa [138] have been reported for these SR co-polymers, respectively. The elastic modulus of SR pins is 6-10 GPa [73, 138, 185, 187], being close to that of cortical bone. Due to increased ductility, the self-reinforcement enables molding of the bioabsorbable plates at room temperature.

A number of fabrication technologies have been developed to process bioabsorbable polymers into tissue engineering scaffolds [79, 221]. These techniques include textile technologies, solvent casting and particulate leaching, gas foaming, freeze-drying, compression moulding, phase separation and rapid prototyping (solid free fabrication) [79, 221].

2.4.3 Degradation, absorption and biocompatibility

The degradation of PLA, PGA and their co-polymers occurs by non-specific hydrolysis in an aqueous environment. First, water diffuses into the material. Hydrolytic scission of polymer chains occurs first in the amorphous regions of the polymer after which it continues on the crystalline domains. This leads to a fall in molecular weight and strength properties and to implant fragmentation. Eventually, during the last phase of degradation, the mass of the polymer disappears. Polymer fragments are hydrolyzed into smaller and smaller fragments and finally to its monomer glycolic and lactic acid, which are further metabolised in the citric acid cycle to carbon dioxide and water. A part of the glycolic acid is also excreted by urine. (Fig. 5).

The loss of strength and degradation of bioabsorbable polymers *in vivo* depends on microstructural (chemical composition and structure, molecular weight and molecular weight distribution, crystallinity vs. amorphous composition, hydrophilicity vs. hydrophobicity, molecular orientation, porosity, purity, surface quality) and macrostructural (size and geometry of the implant, weight/surface area ratio) factors, as well as environmental factors such as storage conditions and implantation site (cancellous/cortical bone, vascularity, mechanical stress) [79, 187, 203]. The degradation rate is generally more rapid for polymers with lower molecular weight, with a more hydrophilic and amorphous structure. The degradation process is enhanced *in vivo* and enzymes are supposed to play a role in the degradation [6].

The degradation and resorption process of bioabsorbable implants elicits a localised inflammatory reaction characterised by an invasion of macrophages, foreign-body giant cells, and neutrophilic polymorphonuclear leukocytes [19]. This was considered to represent an inherent biologic tissue response, as occurs with every implanted material [19]. Macrophages and foreign-body giant cells are responsible for the ultimate digestion of the polymeric debris [128]. Proliferating fibroblasts produce collagen around the polymer material leading to the formation of a fibrous capsule [82-84, 93].

The biocompatibility of bioabsorbable poly-α-hydroxy-acid implants is strongly influenced by the degradation behavior of the polymer used. They are generally well-tolerated by living tissues. However, sometimes adverse tissue reactions have been reported to have manifested, especially if using pure PGA implants [19]. The clinical characteristics of the adverse tissue reaction vary from local swelling to a painful, erythematous, fluctuant nodule, or in some

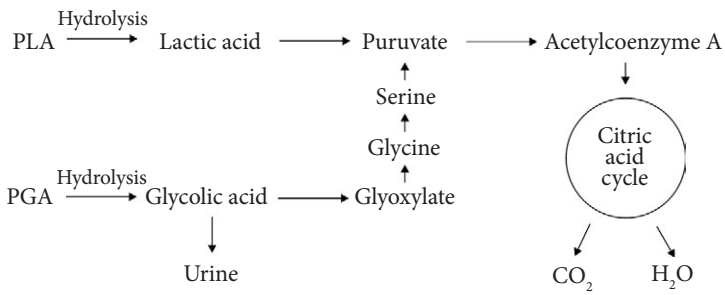

Figure 5. Degradation of polylactide and polyglycolide.

instances fluid accumulation or sterile sinus track at the implant site [19]. Radiographs obtained at the time of this manifestation may show osteolytic lesions with cystic extensions of implant track [19]. Histologically, there is an increased inflammatory foreign-body reaction composed mainly of neutrophilic polymorphonuclear leukocytes and foreign-body giant cells phagocytising the polymer debris with adjacent bone resorption [18]. The adverse tissue reaction is transient and typically occurs during the second phase of the degradation process of the implants when the mass of the polymer is disappearing [19]. This reaction has not been found to disturb the bony consolidation [19, 158]. In an attempt to determine any possible immunologic component in these foreign-body reactions, PGA was found to be an immunologically-inert implant material in cytological and immunological studies [165]. However, some studies suggest that degradation of PLA and PGA may activate complement system [30, 180].

The clinically-manifested adverse tissue reactions are seen most frequently with implants made of pure PGA, the incidence varying from 2.0 to 46.7% in the orthopaedic literature [19]. It is likely to result from rapid degradation of the PGA and subsequent increasing number of hydrolysed polymeric debris that exceed the clearance capacity of the surrounding tissue [135]. It has also been suggested that the degradation may lead to an increased osmotic pressure and local pH drop at the implant site [19]. Increased risk of manifestation of adverse tissue reactions has been documented to be related to use of a quinone dye as an additive in the PGA polymer, implant geometry with large surface area and implantation site with poor vascularisation such as scaphoid [19, 135]. During the last decade, the pure PGA implants have been set aside to give way for newer implant polymers with significantly better biocompatibility.

The incidence of clinically-manifested adverse tissue reaction is generally low for implants made of PLA [19]. The biocompatibility of SR-PLLA implants with molecular weights of 45,000–65,000 Da has been documented in numerous clinical [1, 6, 19, 75, 76, 89, 137, 158, 205, 213, 214, 219] and experimental [103, 133, 134, 206-209] studies. Occasionally, a temporary sterile discharge without clinical signs of inflammation can be observed in x-rays post-operatively [1]. No clinically-manifested adverse tissue reactions have been recorded in craniomaxillofacial patients with SR-PLLA implants [6], and only one such case was recorded among 491 orthopaedic patients [19]. However, the use of PLLA with very high molecular weight up to 10^6 Da, such as in the materials used by Bergsma *et al.*, resulted in subcutaneous swelling at the ankle fracture operation site in all patients, 3-5 years post-operatively [11]. The problem with these specially-prepared, bulky PLLA implants was thought to be that due to the high molecular weight, partially-crystalline PLLA disintegrates into polymer fragments with high crystallinity. These, hydrolytically relatively stable, particles may trigger phagocytosis and therefore provoke a prolonged inflammation and foreign-body reaction [219].

The use of SR-P(L/DL)LA 70/30 and SR-PLGA 80/20 co-polymer implants with substantially amorphous structures has reduced the intensity of the inflammatory reaction, and they have been reported to have good biocompatibility [6, 219]. In experimental *in vivo* studies, SR-PLGA 80/20 and SR-P(L/DL)LA 70/30 co-polymer implants have been documented to histologically evoke only a mild inflammatory reaction [73, 145, 182], and no clinically-manifested adverse tissue reactions have been reported in clinical studies, to the best of our knowledge [6, 219].

2.4.4 Bioabsorbable implants in bone surgery with special reference to hands

Bioabsorbable fixation implants have gained popularity and are strengthening their position in bone surgery. They are available for stabilisation of fractures, osteotomies, bone grafts and fusions particularly in cancellous bones, as well as for reattachment of ligaments, tendons, meniscal tears and other soft tissue structures [137, 158, 219]. In the upper extremity, bioabsorbable pins have been popularised in radial head fractures [62, 137, 219], but implants have also been used successfully in the fixation of distal humeral fractures [66, 102, 132], distal radial fractures [29, 51], and for a radioulnar joint fusion in Sauvé-Kapandji procedure [121]. In craniomaxillofacial surgery, especially in pediatric craniofacial operations, P(L/DL)LA and PLGA miniplating systems have been popularised [6, 219].

The overall results in clinical use of SR-PLLA and PLA co-polymeric osteofixation implants have been favourable [6, 158, 219]. Most of the studies are, however, retrospective or case series reviews. Regarding the fixation of bone segments in bone surgery only a few (randomised) controlled clinical studies are available which investigate the benefits of bioabsorbable osteofixation over conventional treatment methods.

Experimental in vivo studies

Experimental studies have been carried out intensively with bioabsorbable implants in bone. The properties of SR-PLLA, SR-P(L/DL)LA 70/30 and SR-PLGA 80/20 pins and screws have been shown to be suitable for the fixation of small fragments of cancellous bone [73, 101, 145, 206, 208, 209]. Viljanen *et al.* [209] fixed transcondylar osteotomies of rat distal femurs with either a SR-PLLA pin or a Kirschner wire. Both implants appeared to have suitable properties for the fixation of small cancellous bone fragments, but new bone formation was more vigorous at the osteotomy site in the SR-PLLA group. Both implants caused similar mild foreign-body reactions during the 48-week observation. Viljanen *et al.* [206] also noted that a decrease in cortical bone density in rabbits was avoided when distal femoral osteotomies were fixed with SR-PLLA screws rather than metal screws.

SR-PLLA and SR-P(L/D)LA 96/4 rods were strong enough to be used as intramedullary nails for femoral shaft osteotomies in rabbits, and resulted in good bone healing and biocompatibility [103, 162, 207]. Compared with metal intramedullary rods, SR-PLLA rods seemed to have only a minor stress-shielding effect [207]. SR-P(L/DL)LA 70/30 and metal screws were applied in the fixation of mandibular body osteotomies in sheep [77]. In both groups all osteotomies consolidated at similar rate and no adverse tissue reactions were seen during 24-week observation. Consolidation of 2.5 mm-wide sheep craniotomy lines has been shown to proceed more effectively under a wide SR-PLLA plate than under a narrow titanium plate [133]. The SR-PLLA plate was surrounded by a dense connective tissue and no signs of significant inflammatory reactions occurred during the two-year follow-up. In frontal bone craniotomies in growing sheep, the absorption of a punched P(L/D)LA 96/4 plate was complete at two years, the bone surface being smooth and covered with dense connective tissue [134]. The suitability of a PLGA sheet as a separating agent between extensor tendon and metacarpal bone after controlled trauma in monkeys has been studied [38]. The sheet degraded in 50 days, and the tissue reaction was minimal. Extensor tendon mobility was attained quickly and was better than in control hands without implants. The PLGA sheet prevented the development of fibrosis and adhesions between the traumatised tendon and subjacent bone.

Biomechanical studies

The fixation stabilities provided by bioabsorbable implants intended for use in the hand osteosynthesis have been studied earlier. In a biomechanical study by Fitoussi *et al.* [46], 1.5 mm SR-PGA pins coated with PDS provided comparable rigidity to 1.5 mm Kirschner wires for transverse and oblique human proximal phalangeal osteotomies in bending and axial loading, but the torsional rigidity provided by these SR pins was very weak. Maruyama *et al.* [104] reported more limited results with two crossed 1.5 mm SR-PGA pins, which provided 61% of the bending strength provided by 1.2 mm Kirschner wires in transverse human metacarpal osteotomies.

The pullout strength of SR-PLLA pin was higher than that of Kirschner wires in bovine femur [160]. In contrast, titanium screws presented higher torque strength and interfragmentary compression compared with bioabsorbable screws [26, 169]. When two parallel SR pins combined with bioabsorbable suture were compared with two parallel Kirschner wires and metal tension band fixation in a rabbit knee fusion model, the bending tests did not show any statistical difference [117].

Bozic *et al.* [22] studied the biomechanics of 6-hole non-reinforced P(L/DL)LA 70/30 plate (thickness 1.5 mm, length 39 mm, width 9.0 mm; written communication, Bozic KJ 2001) and 2.5 mm screws in a synthetic metacarpal bone model and reported that the 6-hole titanium plate and 2.0 mm screws provided over 2.5 times higher stiffness and failure load in dorsal apex bending. Prevel *et al.* [139] studied the biomechanical characteristics of non-SR PLGA (Lactosorb®) plates in the fixation of transverse metacarpal osteotomies, but the comparative analysis to titanium platings [141] can not be considered valid in that study [218]. Of seven currently commercially available bioabsorbable PLA co-polymeric plate-and-screw systems, SR-P(L/DL)LA 70/30 (BioSorb™ FX) implants provided the strongest and stiffest fixation when polymethylmethacrylate blocks simulating bone segments were fixed and tested in tensile, bending and torsion tests [25]. Titanium plate and screws, however, proved to be the most superior [25].

Alexander *et al.* [2] developed an intramedullary PLLA-carbon fibre composite device for phalageal fracture fixation, and reported that in pig metacarpals there was higher bending rigidity and maximum bending moment than obtained using two crossed Kirschner wires. Furthermore, non-SR P(L/D)LA 95/5 intramedullary rods (Ø 3 mm) provided similar rigidity to that obtained using two longitudinal crossed 1.1 mm Kirschner wires in bending, compression and torsion tests in a comminuted phalangeal fracture model [159]. By combining interlocking Kirschner wires with the P(L/D)LA 95/5 rods, torsional rigidity was further increased.

In the fixation of cadaver scapholunate and lunotriquetral intercarpal joints, two parallel non-SR PDS pins (1.3 mm) provided an average of 46% of the fixation stiffness of Kirschner wire (1.1 mm) fixation for the treatment of wrist ligament injuries [144]. In an experimental scapholunate dissociation, application of a dorsal P(L/D)LA plate stabilised the scaphoid and lunate and restored their kinematics for 1,000 cycles of motion [170]. In the smallest and most osteoporotic cadavers, however, the failure of fixation was noticed partly due to technical problems.

Clinical studies in the hand

In the field of clinical hand surgery, reports on the use of bioabsorbable osteofixation implants are increasing in number (Table 1). Various authors have reported the use of bioabsorbable implants for fixation of metacarpal and phalageal fractures and osteotomies [4, 24, 43, 52, 57, 59, 68, 69, 72, 87, 90, 91, 97, 111, 136, 137, 161, 201, 223, 225], for scaphoid fractures and non-union [1, 89, 98, 108, 135, 136, 146, 225], and for arthrodeses of IP, thumb MCP, CMC I [4, 5, 72, 75, 110, 210, 211, 223], and wrist joints [75, 213, 214] (Table 1). In a prospective randomised study with 23 patients, non-SR PDS pins (OrthoSorb®) were compared with Kirschner wires in the fixation of metacarpal and phalangeal fractures, osteotomies and arthrodeses [72]. No differences were seen in outcomes with respect to time to union and complications, but additional procedures were needed more often in the Kirschner wire group (Table 1).

The implants used for hand osteosynthesis thus far have been mostly pins and rods made of PGA, PDS or PLLA. Cases of clinically-manifested adverse tissue reactions have been reported, most of which have been related to older generation implants made of pure PGA. In recent years, mostly PLLA, PLGA and P(L/D)LA implants have been used and have shown good biocompatibility [1, 4, 5, 43, 89, 97, 213, 214]. A few cases of transient mild osteolysis in x-rays or soft-tissue swelling have been reported without disturbing bone healing [1, 4, 5, 43, 52, 68]. Recently, non-SR PLGA 82/18 (LactoSorb®) [43, 97] and PLLA/PDLA/PGA/PTMC co-polymeric [52] plate systems were introduced clinically for the fixation of unstable metacarpal fractures.

A variety of bioabsorbable implants are available for attaching soft tissue structures to bone [8, 27, 219]. Originally designed to reattach the labrum to the glenoid in the shoulder surgery [8, 27], suture anchors are also used for reattachment of ligaments, tendons and capsule-ligamentous structures in the hand. Recently, bioabsorbable suture anchors have also become available for hand applications, but clinical reports on their use are missing. For the reinsertion of total rupture of the ulnar collateral ligament of the MCP joint in the thumb, successful results have been reported on using a SR-PLLA tack [76, 205] (Table 1). For the repair of triangular fibrocartilage complex tears, the all-inside arthroscopic use of bioabsorbable clips has been described [15, 16].

Table 1. A literature search of publications on the clinical use of bioabsorbable implants in the hand osteosynthesis.

Publication	Number of pts	Type of fixation	Indication for surgery (number of cases)	Control	Postop. immobilization	Follow-up time	Results
Meyer-Clement *et al.* 1984 [111]	NA	PGA suture (2 USP)	Condylar, subcapital, intra-articular or epiphyseal fracture of phalanx (18)	-	2 wks	NA	No later reosteosynthesis or corrective osteotomy needed
Haas *et al.* 1986 [59]	11	PDS splints (Ø 1.3 mm) alone or with a metal cerclage	Open fracture (including replantations) (13) of the base or head of phalanx, or head of MC	-	2 wks, after which gradual activity	NA	No healing problems
Wüstner *et al.* 1986 [223]	10	PDS splints (Ø 1.3 mm)	Arthrodesis of DIP (1), PIP (3), or thumb MCP joint (1); fracture of phalanx (6); (3 replantations, 4 open fractures)	-	2-3 wks, after which gradual activity	NA	Radiological consolidation in all cases within 6 weeks
Rustemeier and Ganβmann 1986 [161]	5	two PDS splints (Ø 1 mm) + PDS suture	Mallet finger avulsion fracture (5)	-	3-4 wks	6 mo	In 4/5 pts no limitation of joint movement, one dislocation resulting to 10° extension lack
Pihlajamäki *et al.* 1992 [137] *(a)*	7	SR-PLLA pin (Ø 1.5 or 2.0 mm)	Fracture of MC (4) or proximal phalanx (3)	-	NA	8-37 mo	Uneventful functional recovery, no redisplacement, no signs of adverse tissue reactions
Kumta *et al.* 1992 [91]	15	Intramedullary SR-PGA rod (Ø 1.5 or 2.0 mm) and a metal wire loop	Unstable extra-articular fracture of MC or phalanx (20)	K-wire with a metal wire loop (15 pts, 18 fractures)	NA	24 wks	One redisplacement in both study groups requiring re-operation, no non-unions, no significant difference in the groups at 24 mo, transient mild tissue reaction to SR-PGA
Voche and Merle 1992 [210] *(b)*	23	Intramedullary PLA rod (triangular cross-section, 3 mm on a side) and a metal oblique pin (Ø 1 mm)	Arthrodesis of thumb MCP joint (24)	-	Gradual activity after 4 d	mean 19.8 mo	In 22/24 cases radiological consolidation in 9 mo, one case of infection at 10 wks, no adverse tissue reactions
Vihtonen *et al.* 1993 [205] *(c)*	70	SR-PLLA tack (Ø 1.15 mm)	Rupture of ulnar collateral ligament of thumb MCP joint (70)	-	4 wks	6 mo	In 69/70 joints the stability was restored, radiological union in all 22 cases with a avulsion fragment, normal movement was restored in 58 pts, two re-operations: pain in the scar and local infection

Table 1—cont'd. A literature search of publications on the clinical use of bioabsorbable implants in the hand osteosynthesis.

Publication	Number of pts	Type of fixation	Indication for surgery (number of cases)	Control	Postop. immobilization	Follow-up time	Results
Merle and Voche 1994 [110] *(b)*	50	Intramedullary PLA rod (triangular cross-section, 3 mm on a side) and a metal oblique pin (Ø 1 mm)	Arthrodesis of thumb MCP joint (52)	-	Gradual activity after 4 d	mean 22.4 mo	In 50/52 cases radiological consolidation in 7-11 wks (mean 9 wks), no adverse tissue reactions, one case of sepsis
Yamamuro *et al.* 1994 [225] *(a)*	14	PLLA screws, pins and nails	Fracture of IP (2) or MCP (1) joint, delayed union of scaphoid fracture (6)	-	NA	2-6 yrs	Bone union, radiology and clinical course good in all cases, one case of mild tendovaginitis
Juutilainen and Pätiälä 1995 [75] *(a, d)*	NA	Two crossed SR-PLLA rods (Ø 1.5-2.0 mm) for MCP and IP arthrodesis, one SR-PLLA rod (Ø 3.2 mm) for wrist arthrodesis	Arthrodesis of IP (12), thumb MCP (5), CMC I (1), or wrist (18) joint in RA pts	-	6 wks (MCP and IP arthrodesis), 8 wks (wrist)	6 mo	No nonunions, one superficial infection
Voche *et al.* 1995 [211]	12	Intramedullary PLA rod (triangular cross-section, 5 mm on a side) and one or two PLA pins (Ø 1.3 mm)	Arthrodesis of thumb MCP joint (13)	-	Gradual activity after 4 d	19-31 mo (mean 23)	12/13 thumbs healed within 6-8 weeks (radiologically within 8-10 wks), one case of delayed union, one case of extrusion of the pin at 8 mo, no sign of inflammation
Pelto-Vasenius *et. al.* 1995 [135]	20 (6 were lost to follow-up)	One (12 cases) or two (2 cases) SR-PGA pins (quinone dye-coloured) coated with PDS layer (Ø 2.0 mm)	Nonunion or delayed union of scaphoid fracture (14)	Herbert screw (4.0 mm, 14 pts, 4 of which were lost to follow-up)	6-12 wks (mean 7)	57-77 mo (mean 68)	Union rate 64% in PGA pin group and 60% in Herbert screw group, transient sinus formation in 5/20 pts in PGA pin group, functional outcome better in Herbert screw group
Juutilainen *et al.* 1996 [76] *(c)*	140	SR-PLLA tack (Ø 1.15 mm)	Rupture of ulnar collateral ligament of thumb MCP joint (140)	-	4 wks	6 mo	In 138/140 joints the stability was restored, radiological union in all 34 cases with a avulsion fragment, normal movement was regained in 118 pts, 5 re-operations were needed
Pelto-Vasenius *et al.* 1996 [136]	32 (12 lost to follow up)	SR-PGA pins alone or with SR-PLLA pins (Ø 1.1-2.0 mm)	Fracture of MC other than Bennett (8), MC Bennett (5), phalanx (5), trapezium (1), scaphoid (1)	-	0-5 wks (mean 3.6)	11 mo – 8.5 yrs (mean 4.5 y)	Pt satisfaction 15/20 pts, adverse tissue reaction 3/20, normal work capacity 7/8 (MC other than Bennett), 2/5 (Bennett) and 5/5 (phalanx), 0/1 (trapezium), 1/1 (scaphoid)

Jensen and Jensen 1996 [72]	11	PDS pin (Ø tapered 1.3-1.35 mm, non-tapered 2.0 mm)	Fracture of phalanx (4); arthrodesis of IP or MCP joint (5); osteotomy of MC (1) or phalanx (1)	K-wire (12 pts)	12-42 d, (mean 28 d)	6 mo	No difference in union time or complications rate between the groups, failure of 1/4 of fixation and 2/5 of fusions in the PDS pin group, the number of additional operative procedures higher in the K-wire group.
Vandenberk *et al.* 1996 [201]	3	PDS pin	Fracture of proximal (2) or middle (1) phalanx	-	5 d – 3 wks	8 mo – 2 yrs	Good functional recovery, one slight displacement
Matsusue *et al.* 1997 [108] *(a)*	NA	PLLA screws or pins	Delayed union of scaphoid fracture (2)	-	NA	4-9 yrs	Good bone union in both cases, no adverse tissue reactions
Kumta *et al.* 1998 [90]	46	SR-PGA or SR-PLLA pins (Ø 1.5 or 2.0 mm)	Unstable fracture of MC or phalanx	-	NA	NA	Union in 42/46, no adverse tissue reactions
Brüser *et al.* 1999 [24] *(e)*	66	2/0 PGA suture	Fracture of MC (79)	-	1.5-6 wks (mean 3.7 wks)	4-7.5 wks (mean 6.1 wks)	One delayed union due to premature loading, no adverse tissue reactions, ROM 98%
Krein *et al.* 2000 [87] *(e)*	78	2/0 PGA (76 pts) or PDS (2 pts) suture	Fracture of MC (92)	-	1.5-6 wks (median 3.4)	4–7.5 wks (median 6.1 wks)	One delayed union due to premature loading, no adverse tissue reactions, ROM 98%
Voutilainen *et al.* 2001 [214] *(d)*	18	SR-PLLA rod (Ø 3.2 mm)	Arthrodesis of wrist (21) in 17 RA and 1 psoriatic arthritis pts	-	8 wks	3.0-8.0 yrs (mean 5.4)	One nonunion, painless 15/21 cases, good subjective function 19/21 cases
Lionelli and Korentager 2002 [97]	1	PLGA 82/18 plate and 4 screws (Ø 2.0 mm)	Fracture of MC shaft (1)	-	NA	NA	Plate shattered and fixation failed, non-compliant pt
Voutilainen *et al.* 2002 [213]	18	SR-PLLA rod (Ø 3.2 mm)	Arthrodesis of wrist (24) in RA pts	-	2-3 wks + 6-7 wks	0.5-3.4 yrs (mean 1.7)	3 cases of nonunions, one of which required a reoperation, pt satisfaction 21/24 cases, satisfactory pain relief 22/24 cases
Arata *et al.* 2003 [4]	22	PLLA rod	Arthrodesis of IP joint (15) or phalangeal shaft fracture (11) in digital replantation	-	3-4 wks	5-50 mo (mean 14)	No cases of non-union or infection, one case of transient bone resorption
Arata *et al.* 2003 [5]	16	PLLA rod	Arthrodesis of DIP (15) or thumb IP (1) joint	-	3 wks	2-25 mo	No cases of nonunion or infection, 2 cases exhibited minor, transient swelling
Qi *et al.* 2003 [146] *(a, f)*	4	SR-PGA and SR-PLLA screws, SR-PLLA rods	Delayd union of scaphoid fracture (4)	-	2 wks	3-78 mo	All cases healed without dislocation, infection or local effusion

Table 1—cont'd. A literature search of publications on the clinical use of bioabsorbable implants in the hand osteosynthesis.

Publication	Number of pts	Type of fixation	Indication for surgery (number of cases)	Control	Postop. immobilization	Follow-up time	Results
Akmaz *et al.* 2004 [1]	12	SR-PLLA screw (6 pts), two SR-PLLA pins (6 pts)	Nonunion of scaphoid fracture (12)	-	5-10 wks (mean 9 wks)	22-35 mo (mean 25)	Union in all pts in 3.5-7 (mean 4.5) mo. 4 cases of temporary sterile discharge, no sinus formation
Kujala *et al.* 2004 [89]	6	SR-PLLA screw (Ø 2.0 mm, 4 pts), two SR-PLLA screws (Ø 2.7 mm, 1 pt), SR-PLLA screw (Ø 2.0 mm) and stainless steel compression pin (Ø 2.5 mm, 1 pt)	Fracture of scaphoid (3) or nonunion of scaphoid fracture (3)	-	4-9 wks (mean 8 wks)	12-30 mo (mean 17)	Union in 5 cases, one nonunion persisted in once previously operated case, no adverse tissue reactions/ radiological discharge
Huang *et al.* 2004 [68] *(f)*	60	Intramedullary PDLLA *(g)* nail (24 pts); intramedullary PDLLA-chitosan (g) wire (36 pts) (Ø 1.0-3.5 mm)	Open (52) or closed (8) fracture of MC (24), proximal (22) or middle (14) phalanx	-	3-4 wks	4-11 mo (mean 6 mo)	Consolidation in 6-16 wks (mean 8 wks), primary healing in 16/24 pts in PLDLA group, 8/24 pts showed adverse tissue reaction 3-4 wks postop and 6 of them needed refixation with K-wires, primary healing in 35/36 pts in PLDLA+chitosan group, 1 case of adverse tissue reaction 19d postop
Yajima *et al.* 2004 [224]	2	Bioabsorbable pin(s) *(g)*	Scaphocapitate joint fixation after lunate excision and tendon interposition in Kienböck's disease	-	Case I: 1 mo, case II: NA	Case I: 29 mo, Case II: NA	Asymptomatic osteoarthritic change at the scaphocapitate joint in case I
Huang *et al.* 2005 [69] *(f)*	28	Intramedullary PDLLA-chitosan *(g)* nail (Ø 1.0-2.0 mm)	Fracture of proximal (15), middle (11) or distal (2) phalanx in replantation	-	3-4 wks	3-10 mo (mean 4 mo)	One case of adverse tissue reaction 3 wks postop, consolidation was obtained in other cases, 27/28 pts excellent or good function of the replantated finger
Guo *et al.* 2006 [57] *(a, f)*	NA	SR-PGA screws and SR-PLLA rods	Intra-articular fracture of MCP (3) or IP (2) joint	-	2-6 wks	3-60 mo	Bone healing in 1-3 mo, no dislocation, infection or local effusion, satisfying functional recovery
Dumont *et al.* 2007 [43]	12	PLGA 82/18 plating (2.0 mm system, 12 cases), PLGA 82/18 lag screws (Ø 2.5 mm, 2 cases)	Unstable fracture of MC (14)	-	1 wk or 3 wks	26 wks	Consolidation within 6 weeks, mean ROM 234°, implant failure in 2 pts (one wk splint in these pts) one of which with a comminuted fracture needed refixation, transient soft-tissue swelling in 3 pts

Liu *et al.* 2008 [98] *(f)*	18	One or two PLDLA screw(s) (Ø 3.5 mm) *(g)*	Nonunion of scaphoid fracture (18)	-	8 wks	13-50 mo (mean 17.3 mo)	Union in all cases in 3-8 mo (mean 4.5 mo), 16/18 pts painless and good function, no infection or failure of fixation.
Givissis et al. 2008 [52] *(a)*	7	PLLA/PDLA/PGA/ PTMC co-polymeric plate and screws	Displaced fracture of MC (9)	-	2 wks	1.2-2.7 yrs	Union in all cases of MC fractures with "excellent final outcome", 2 cases of local swelling and sterile abscess formation 10 and 15 mo postop. resolved by surgical debridement.

a) Bioabsorbable implants were used to stabilise bone fixation in many body areas in the series. Only cases with a hand operation were included in the table
b) These two publications are from the same institute in France so it is probable that the patient data is partly overlapping
c) The first 70 patients published by Vihtonen *et al.* 1993 [205] were also included in the later publication by Juutilainen *et al.* 1996 [76]
d) The patient data is partly same in these two publications (written communication, Voutilainen N, 2007)
e) These two publications are from the same institute in Germany and it is probable that the patient data is partly overlapping
f) Article is in Chinese. Data is based on English abstract and article translation by Guofeng Ma, MD
g) No details of the implant material given

Abbreviations: K-wire = Kirschner wire, mo = month, NA = not available, pt = patient, postop. = post-operative(ly), MC = metacarpal, RA = rheumatoid arthritis, ROM = range of motion, USP = United States Pharmacopeia, indicates designation of suture sizes, d = day, wk = week, yr = year.

2.4.5 Bioabsorbable joint scaffold arthroplasty

The bioabsorbable joint scaffold arthroplasty is a clinically-introduced concept in the reconstruction of small joints of the rheumatoid and osteoarthritic hands [79, 186]. The first clinical study for the reconstruction of MCP joints was performed using scaffolds folded of Vicryl® (co-polymer of 90% PGA and 10% PLLA) or Ethisorb® (made of PDS and the co-polymer of 90% PGA and 10% PLLA) fleeces [94]. The complete degradation of these fleeces turned out to be too rapid, leading to sinus formation and a premature collapse of the arthroplasty space in some patients [94].

Since 1997, the bioabsorbable joint scaffolds have been made of P(L/D)LA 96/4. *In vitro*, the half-life of the tensile strength of P(L/D)LA 96/4 filament is approximately 13 weeks (Fig. 6) [64]. The complete absorption time of P(L/D)LA 96/4 scaffolds is unclear.

The mean porosity of P(L/D)LA 96/4 scaffolds has been reported to be 69-79% varying according to the size of the scaffold [120]. *In vitro* compression testing along the axis of the scaffold disclosed a compression modulus, which should be able to withstand *in vivo* stresses and loading in the MCP joints of the human hand [120]. With the compression force of 80 N the P(L/D)LA 96/4 scaffolds showed mean relative compression of 47-22% depending on the size of the scaffold [120]. The histology of the P(L/D)LA 96/4 joint scaffold arthroplasty was unknown before the current thesis.

Preliminary clinical results have been reported on the use of P(L/D)LA 96/4 joint scaffolds for the reconstruction of MCP joints in rheumatoid arthritis patients. Honkanen *et al.* [64] reported a prospective study on 80 MCP joint arthroplasties with P(L/D)LA 96/4 scaffolds in 23 rheumatoid patients (40% of the patients represented revisions of failed silicone implant arthroplasties with bone defects). The follow-up of 15 patients exceeded one year, and they demonstrated good pain alleviation, decrease of ulnar deviation from pre-operative 26° to 6°, extension deficit from 29° to 18° and active flexion from 75° to 69°. Volar subluxation exceeded half of the bone thickness in 6% of the joints, whereas pre-operative it was observed in 56% of joints. Recently, the same 23 patient cohort was re-analysed and after an average of

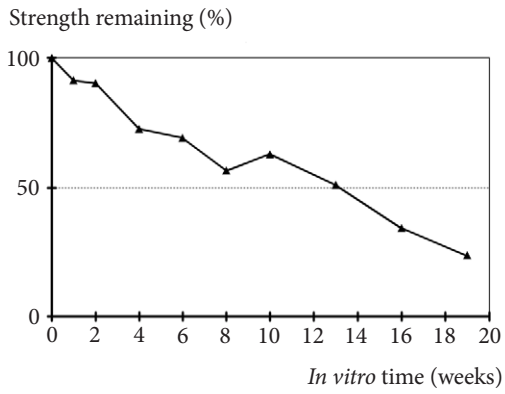

Figure 6. Tensile strength of P(L/D)LA 96/4 4-ply multifilament *in vitro* (Reprinted, with permission [64]).

4.9 year follow-up, volar subluxation was seen in 11% of joints, whereas the mean ulnar deviation was 5°, extension deficit 15° and active flexion 63° [65]. The authors concluded that the good primary result in the correction of deformities did not disappear upon complete degradation of the scaffold. The results were comparable with published data on silicone implant arthroplasties without risk for implant fracture and without any significant periprosthetic osteolysis. As an advantage, the use of the P(L/D)LA 96/4 joint scaffold enabled intramedullary bone grafting in revision arthroplasties. In a prospective follow-up study of 21 patients with 52 failed silicone implant MCP arthroplasties and severe osteolysis and soft-tissue deficiencies, the P(L/D)LA joint scaffolds showed promising clinical and radiological results one year after the revision operation with intramedullary bone packing [70]. The active ROM, ulnar deviation and recurrent volar subluxation were greater in this follow-up than in the study by Honkanen *et al.* [64].

A randomised multi-centre trial comparing silicone implant MCP arthroplasty with P(L/D)LA 96/4 implant MCP arthroplasty is in progress. Another multi-center study is investigating the use of P(L/D)LA 96/4 joint scaffolds in other small joint arthroplasties including CMC I, PIP and metatarsophalangeal joints. A similar concept of biodegradable T-shaped woven spacer (Artelon®) made of polyurethaneurea fibres has been applied in the treatment of CMC I osteoarthritis [122]. In a prospective study, ten patients with partial trapezium resection and a polyurethaneurea spacer showed significantly better pinch strength than five patients with abductor pollicis longus tendon arthroplasty after 3 years' follow-up [122].

2.4.6 Co-polymer of PEO/PBT (Polyactive®)

A segmented block co-polymer of polyethylene oxide (PEO) and polybutylene terephtalate (PBT) (commonly known with Polyactive® trade name) is one of the recently introduced bioabsorbable polymers (Fig. 7). It has been under intensive investigations in orthopaedic surgery and tissue engineering applications, such as for bone substitute and for bone and cartilage tissue engineering [34, 114, 118].

By varying the PEO/PBT ratio and using PEO of different molecular weight, co-polymers with a variety of mechanical, physicochemical and biological properties can be obtained [195]. The hydrophilic PEO segment is soft and amorphous (Fig. 7A). The hydrophobic PBT segment shows harder, crystalline properties (Fig. 7B). By increasing the content and the molecular weight of PEO segment in the co-polymer structure, the polymer becomes more elastomeric [164], more rapidly degradable [151, 164], and more hydrogel-like, i.e. it swells in an aqueous environment [195]. The mechanism of degradation has not been completely resolved but hydrolysis seems to play an important role in it [154].

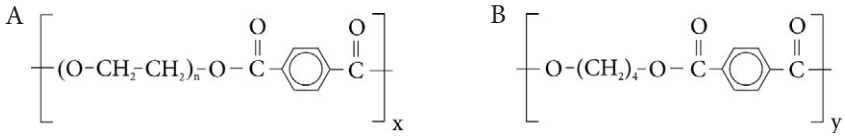

Figure 7. Chemical structure of a A) polyethylene oxide (PEO) segment, and B) polybutylene terephtalate (PBT) segment of the PEO/PBT co-polymer.

In *in vivo* experimental studies, the PEO/PBT co-polymer has shown osteoconductive and bone-bonding properties, if the PEO content is 55 mol-% or higher [21, 88, 109, 149-151, 153, 163, 196, 197]. Its mechanism is not fully clarified, but the calcification of the polymer surface is considered to be crucial [95, 147, 149, 195]. The calcium phosphate crystals are believed to be formed through electrostatic forces and hydrogen bonds around carboxyl groups, produced from PEO segments during the hydrolysis of the co-polymer [95, 148]. The calcification also continues into the surrounding bone, forming a crystal continuity at the interface [195]. The co-polymers with the higher PEO content and PEO molecular weight show higher calcification and stronger bone-bonding properties [149, 152, 153, 195-197]. The hydrogel-like property of the co-polymer is also considered an important factor in creating a strong interface bond between polymer and bone, creating the claimed good osteoconductivity [149, 150, 152, 153, 163, 195]. In a histological study on goats, dry press-fit inserted PEO55PBT45 implants with a PBT content of 45 mol-% showed good implant-bone contact during 25 weeks follow-up, whereas similar wet, fully pre-swollen implants were all encapsulated by a thin layer of fibrous tissue interposed between the bone and implant [163]. In *in vitro* studies, the swelling pressures generated by PEO/PBT co-polymers in the surrounding bone reached over 2 MPa [163, 195].

The Polyactive® 1000PEO70PBT30 co-polymer with a PBT content of 30 mol-% and an initial PEO segment length of 1000 Da is initially highly elastomeric [78, 164]. However, its mechanical properties decrease rapidly in an aqueous environment due to the high swelling typical for hydrogels and later also due to degradation [78]. The initial shear strength of the gamma-sterilised Polyactive® 1000PEO70PBT30 was 7.0 MPa, but more than 50% of the initial strength was lost in a week in hydrolytic conditions *in vitro* [78]. Respectively, the diameter of the stems increased by 20% due to swelling [78].

The osteoconductive and bone bonding properties of Polyactive® 1000PEO70PBT30 composition have been documented in several *in vivo* studies with various animal models [88, 149-151]. In a distal diaphysis of goat femur, over 95% of bone contact was reported with Polyactive® 1000PEO70PBT30 cylinders at early post-operative weeks, after which the bone contact decreased but remained over 80% during the follow-up of 52 weeks [149]. However, some of the experimental studies and a preliminary clinical study have failed to show any osteoconductive effect [3, 157]. In various *in vitro* and *in vivo* studies in which the polymer has also been implanted in bone, this polymer family has been documented as having good biocompatibility [21, 88, 109, 149, 151-153, 157, 163, 198] and only a mild or no inflammatory reaction in the surrounding tissue has been reported [149, 151, 152, 157]. No adverse tissue reactions such as tissue necrosis or osteolysis have, to our knowledge, earlier been reported in the literature.

3 AIMS OF THE STUDY

The overall objectives of the present thesis were to investigate the stabilities of bioabsorbable implants when used for fixation of tubular bones of the hand, and the histology of bioabsorbable joint scaffold arthroplasty. The specific objectives were:

- To study the initial fixation stabilities provided by SR-PLGA 80/20 and SR-P(L/DL)LA 70/30 plates and screws for fixation of transverse metacarpal osteotomy, and to compare the results with those of metal fixation methods (I).

- To study the initial fixation stabilities provided by SR-P(L/DL)LA 70/30 plates and screws, and SR-PLLA pins for fixation of oblique osteotomy of small tubular bone, and to compare the results with those of metal fixation methods (II).

- To study preliminarily if SR-P(L/DL)LA 70/30 plate systems can be used clinically in the fixation of unstable fractures and fusions of the hand in a small proof-of-principle type study (III)

- To evaluate a bioabsorbable P(L/D)LA 96/4 joint scaffold in an *in vivo* experimental design to find out its histology, biocompatibility, effect on tissue replacement and rate of bioabsorption in a small joint arthroplasty model in minipig (IV)

- To compare radiological results between the P(L/D)LA 96/4 joint scaffold, a composite joint scaffold with a double-sided Polyactive® 1000PEO70PBT30 stem and Swanson implant arthroplasties in a small joint arthroplasty model in minipig (IV-V)

- To assess the biocompatibility and applicability of a double-sided Polyactive® 1000PEO70PBT30 stem in a composite joint implant in a small joint arthroplasty model in minipig (V)

4 MATERIALS AND METHODS

4.1 Bioabsorbable fixation

4.1.1 Bone specimens

In paper I, 56 pairs of second metacarpal bones were collected from human cadavers (44 males and 12 females). The approval for using cadaver bones was received from the National Authority for Medicolegal Affairs in Finland. None of the donors had a known history of musculoskeletal illness. The donors had died at age of 25–90 years (mean 64, SD 14). The harvest was done 1–7 days (mean 4, SD 1) *post mortem*. The mean length of the bones was 69.9 mm (SD 4.7), the midshaft cross-sectional height was 9.7 mm (SD 1.1) and width was 9.1 mm (SD 0.8), and the cortical thickness was 2.4 mm (SD 0.5). There was no difference in the covariates between the tested study groups ($p < 0.05$).

In paper II, 160 fresh pig second metacarpal bones were used. The specimens were dissected from fresh fore limbs obtained from a local slaughterhouse at the time the animals were killed and stored at +4 °C before harvesting. The harvest was done 1 – 3 days after killing. The mean length of the bones was 59.3 mm (SD 1.4), the midshaft cross-sectional height was 9.1 mm (SD 0.6) and width was 6.4 mm (SD 0.4), and the cortical thickness was 1.8 mm (SD 0.4). There was no significant difference in the covariates between the groups ($p < 0.05$).

The bones were dissected free of soft tissues, wrapped in a normal saline-soaked gauze and frozen to –70 °C. The frozen specimens were thawed at room temperature for 12-24 hours before laboratory studies. The bones were immersed in normal saline and kept moist throughout the experiment. A transverse osteotomy (paper I) or an oblique osteotomy ulnar distal to radial proximal orientation at a 30° angle to the long axis of the bone (paper II) was made in the mid-diaphyseal region, using a circular diamond saw (Ø 30 mm, thickness 0.30 mm, Giflex-TR diamond disc, Bredent, Senden, Germany). In both papers, intact bone specimens served as controls.

4.1.2 Implants

The bioabsorbable implants were made of SR-PLGA 80/20 (BioSorb™ PDX, Bionx Implants Ltd, Tampere, Finland), SR-P(L/DL)LA 70/30 (BioSorb™ FX, Bionx Implants Ltd, Tampere, Finland), or SR-PLLA (SmartPin™, Bionx Implants Ltd, Tampere, Finland). The raw material used for manufacturing the implants was purified medical-grade polymer (Purac Biochem, Gorinchem, Netherlands). All implants were sterilised with gamma irradiation of a minimum dose of 2.5 MRads. The metal implants studied were commercially-available titanium plates and screws (Howmedica Leibinger, Freiburg, Germany) and stainless steel Kirschner wires (Synthes, Mathys Medical, Bettlach, Switzerland; Medicon eG, Tuttlingen, Germany). The geometries of the implants are shown in Table 2.

Table 2. Geometry and properties of plates and screws used in the biomechanical studies (paper I and II).

	SR-PLGA 80/20 plate system	SR-P(L/DL)LA 70/30 plate system	1.7 mm titanium plate system	2.3 mm titanium plate system
Plate				
Thickness (mm)	1.0	1.2 (I), 1.0 (II)	0.55	1.0
Width (mm)	5.5	5.5	3.6	4.5
Length (mm)	25.5	25.5 (I), 35 (II)	17.4	26
Screw				
Head	cruciate	cruciate	cruciate	cruciate
Head height (mm)	1.75	1.75	0.85	0.85
Thread pitch (mm)	1.0	1.0	0.6	0.8
Outer diameter (mm)	2.0	2.0	1.7	2.3
Inner diameter (mm)	1.45	1.45	1.2	1.6
Thread depth (mm)	0.275	0.275	0.25	0.35
Tapping	pretapping	pretapping	self-tapping	self-tapping

In paper I, the human metacarpal bone specimens with a transverse osteotomy were randomized and fixed by using one of the seven fixation methods: dorsal (Fig. 8A) or dorsolateral (Fig. 8B) SR-PLGA 80/20 plate with 2 mm screws, dorsal (Fig. 8A) or dorsolateral (Fig. 8B) SR-P(L/DL)LA 70/30 plate with 2 mm screws, dorsal titanium plate (S plate) with 1.7 mm screws (Fig. 8C), dorsal titanium plate (M plate) with 2.3 mm screws (Fig. 8D), or crossed 1.25 mm Kirschner wires (Fig. 8E) fixed by the retrograde method across the osteotomy site.

In paper II, the pig metacarpal bone specimens with an oblique osteotomy were randomised and fixed by using one of the following methods: two SR-PLLA pins with a diameter of 1.5 mm (Fig. 8a); two stainless steel Kirschner wires with a diameter of 1.25 mm; two stainless steel Kirschner wires with a diameter of 1.5 mm (Fig. 8b); two SR-P(L/DL)LA 70/30 screws with a outer diameter of 2.0 mm (Fig. 8c); two titanium lag screws with a diameter of 1.7 mm (Fig. 8d); SR-P(L/DL)LA 70/30 plate and an 2.0 mm interfragmentary screw (Fig. 8e), or a titanium plate with an interfragmentary lag screw (outer Ø 2.3 mm) (Fig. 8f).

4.1.3 Fixation technique

The reduction of transverse osteotomy was achieved by hand and that of oblique osteotomy with reduction clamps. Both titanium and bioabsorbable plates were bent at room temperature to contour them to the convex shaft of the bone. When a plate was combined with an interfragmentary screw in an oblique osteotomy, the interfragmentary screw was first passed perpendicularly to the osteotomy in the mid-lateral plane of the bone, after which the plate was fixed to the dorsal aspect of the bone with four bicortical screws. In contrast to titanium screws, bioabsorbable screws needed tapping. The insertion of a bioabsorbable pin also required pre-drilling of the bone with a Kirschner wire of corresponding diameter. In an oblique osteotomy, interfragmentary Kirschner wires, bioabsorbable pins and screws were inserted slightly non-parallel across the osteotomy line. After insertion, Kirschner wires and titanium screws were cut flush with the bone surface with metallic cutter, whereas bioabsorbable pins and screws were shortened with a hot wire loop.

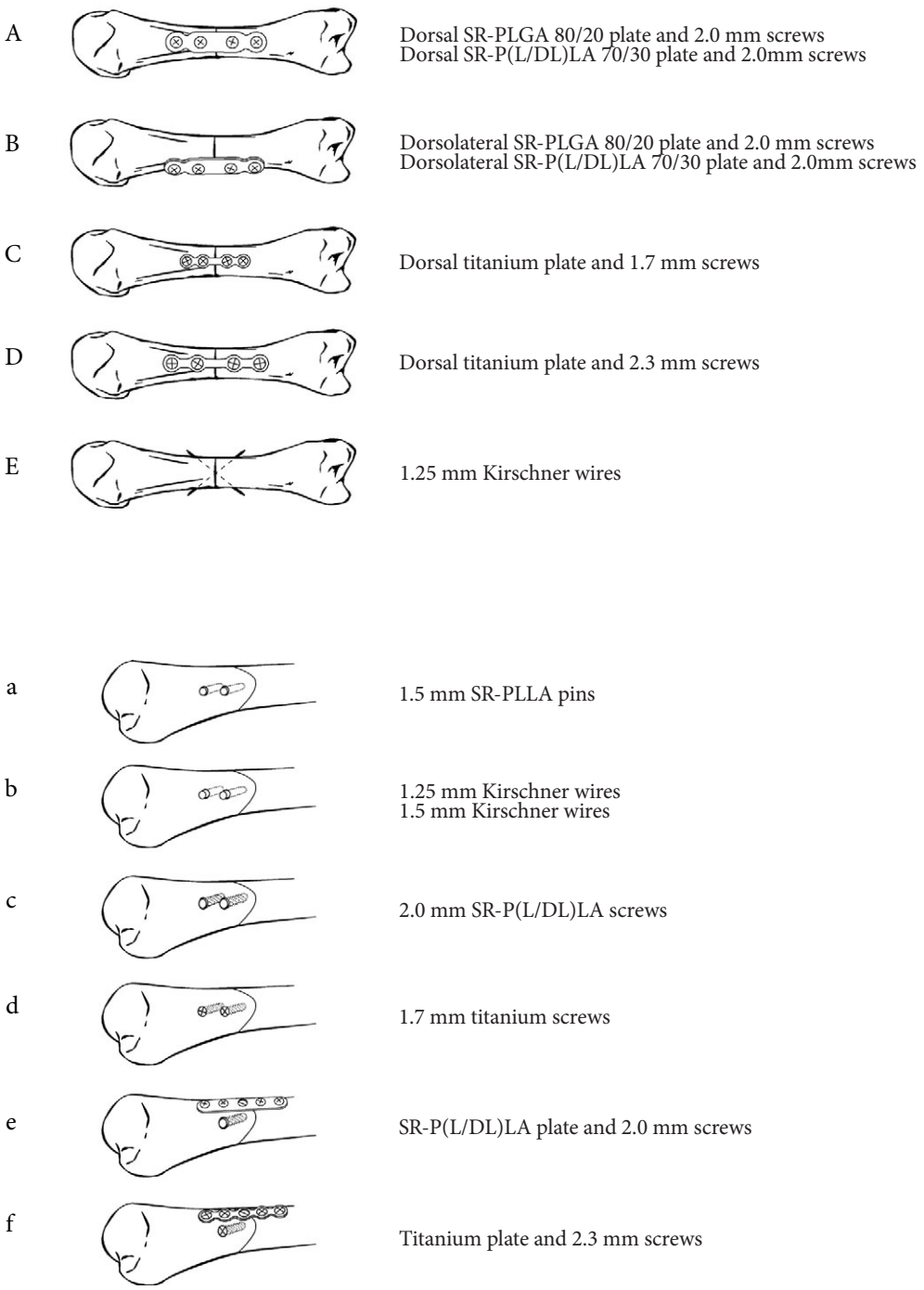

Figure 8. Fixation configurations of transverse osteotomy (I) (A-E) and oblique osteotomy (II) (a-f).

4.1.4 Biomechanical testing

Biomechanical testing was done using bending and torsion tests. The tests were performed using Lloyd testing machine (Lloyd Instruments Ltd, Fareham, England) at room temperature. Eight specimens were tested in the transverse osteotomy model (paper I) and ten specimens in the oblique osteotomy model (paper II), both in bending and in torsion.

Bending tests

The palmar and dorsal apex bending were applied to the specimens using a three-point loading [13, 14, 139-141]. In paper II, lateral apex bending was also applied. The loading crosshead was centred over the osteotomy site in the middle of support span of 30 mm. The span was chosen to represent the longest possible span not interfering with the ends of the bones. The cross-head speed was constant 1 mm/min. The radius of each support span and crosshead was 5 mm.

First, the specimens were non-destructively tested in palmar apex by applying a 1.0 mm crosshead displacement. In paper II, the specimens were then similarly non-destructively tested in apex lateral bending. Finally, the specimens were loaded until failure in the dorsal apex bending. The load-displacement curve was plotted for each specimen.

Flexural rigidity (extrinsic stiffness) of the bone illustrates the slope the load-deformation curve in the elastic region where the deformation increases linearly with increasing load before the yield point. It is equal to EI, where E is the elastic modulus and I the cross-sectional moment of inertia. Flexural rigidity was calculated using the equation 1 where F/x is the force-deflection curve of initial linear section (N/m) and L the length of the span (m) [192].

$$EI = \frac{F}{x}\frac{L^3}{48}, \qquad (1)$$

The ultimate point in dorsal apex bending was defined as a decrease in load with increasing displacement. The maximum bending moment at ultimate point was calculated using equation 2, where F is force at the ultimate point (N) and L the length of the span (m).

$$M = \frac{FL}{4}, \qquad (2)$$

In paper I, failure modes were observed visually and recorded (site of bending, presence of screw pull-out, evidence of fracture lines).

Torsion test

The bones selected for torsional tests were placed in bone cement (Palacos® R, Schering-Plough) in circular plastic form (diameter 30 mm, depth 15 mm) at both of their ends. After the cement was allowed to dry, the specimens were fastened vertically into the testing machine and loaded to torque with external rotation (i.e. distal epiphysis rotates externally compared with proximal epiphysis) (Fig. 3F), thus in the direction that opens up the oblique osteotomy (paper II). The angular velocity was constant 0.25 rad/min. The torque-twist relationship was determined.

The torsional rigidity (extrinsic stiffness) was calculated from torque-twist curve using the equation 3, where T/θ is the slope of torque-twist curve of initial linear section (Nm/rad), and

L the length of the unembedded portion of the specimen (m).

$$GJ = \frac{T}{\theta} L \ , \qquad (3)$$

4.1.5 Statistical methods

Mean values and standard deviations (SD) were calculated for each study group and for intact bones. Differences among the groups were compared using analysis of variance (ANOVA) and if differences were found to be relevant, pairwise comparisons were done with the t test for normally-distributed variables and the nonparametric Mann-Whitney U test was done for skewed distributions. The level of statistical significance was set at $p < 0.05$. Statistical analyses were done using SPSS 10.0 program (Chicago, IL, USA).

4.1.6 Patient cases

Three patients with complex hand injury were osteosynthesised with bioabsorbable SR-P(L/DL)LA 70/30 plate and screws.

Patient 1

A 22-year-old man crushed his right hand in a dough-kneading machine. He suffered a large laceration of the dorsal aspect of the hand, including a soft-tissue defect with laceration of the extensor tendons of thumb, index, middle and ring fingers, and a displaced fracture of the shaft of the third metacarpal bone (Fig. 9). Fracture stabilisation was achieved with a 6-hole SR-P(L/DL)LA 70/30 plate (thickness 1.2 mm) and four 2.0 mm screws (inner Ø 1.5 mm, pitch 1.0 mm) (Fig. 9). The extensor digitorum tendon of the index finger and the superficial branch of the radial nerve were repaired. An extended lateral arm free flap and a full thickness skin graft were designed and transferred to cover the soft-tissue defect (Fig. 9). Post-operative management consisted of the application of an extensor tendon splint for three weeks, physical rehabilitation and compressive dressing.

Patient 2

A 61-year-old man sustained a traumatic complete amputation of the right thumb at the MCP joint level while working with a wood-splitting machine (Fig. 10). Thumb replantation and arthrodesis of the MCP joint were undertaken using an H-shaped SR-P(L/DL)LA 70/30 plate (thickness 1.2 mm) and seven 2.0 mm screws (inner Ø 1.5 mm, pitch 1.0 mm) (Fig. 10). Post-operatively, a cast was applied for three weeks.

Patient 3

A 24-year-old female patient suffered a severe bone defect in the proximal phalanx of the left thumb secondarily to trauma in childhood (Fig. 11). Exploration of the left thumb revealed 15° of active movement of the IP joint and intact soft tissues except for extensor tendon rupture. A corticocancellous graft of 20 x 10 x 7 mm was harvested from the iliac crest and used to fill the bone defect. It was fixed with a SR-P(L/DL)LA 70/30 plate (thickness 1.0 mm) and three 1.5 mm screws (inner Ø 1.0 mm, pitch 0.8 mm) (Fig. 11) in conjunction with three weeks stabilisation of the MCP and IP joints with two 0.8 mm Kirschner wires.

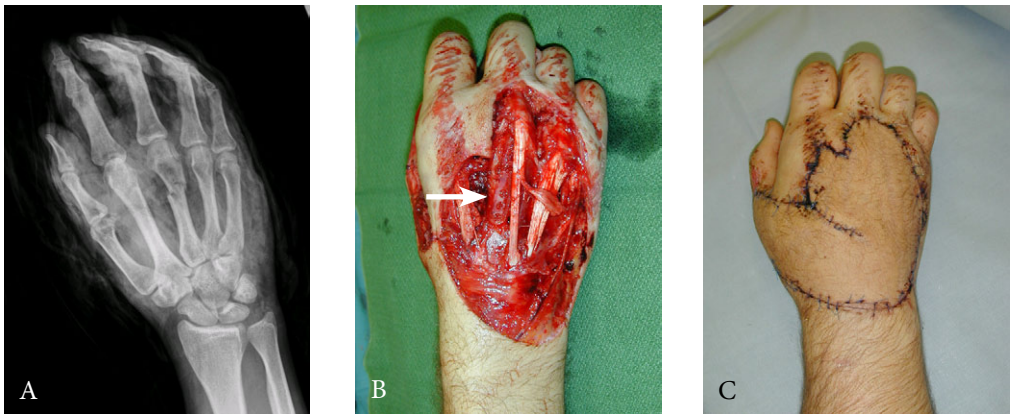

Figure 9. Patient 1: A) Initial radiological findings show a displaced fracture of the third metacarpal; B) Intraoperative view showing internal fixation with a SR-P(L/DL)LA 70/30 plate (arrow); and C) Final appearance after an extended lateral arm free flap and full thickness skin graft.

Figure 10. Patient 2: A) Pre-operative view of complete thumb amputation; B) Arthrodesis of the metacarpophalangeal joint was carried out with a SR-P(L/DL)LA 70/30 plate (arrow).

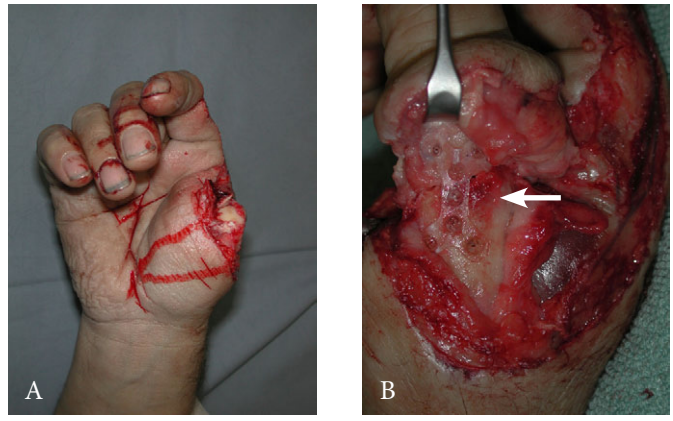

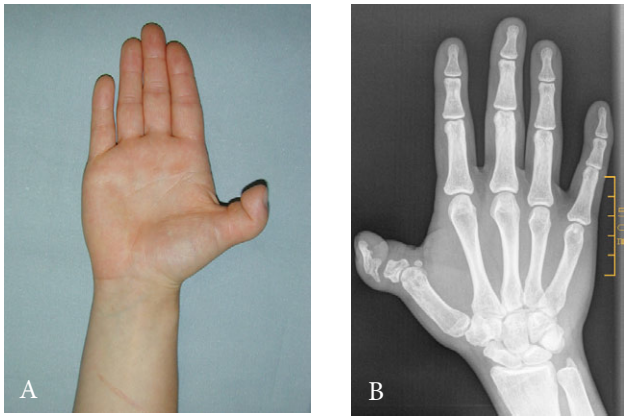

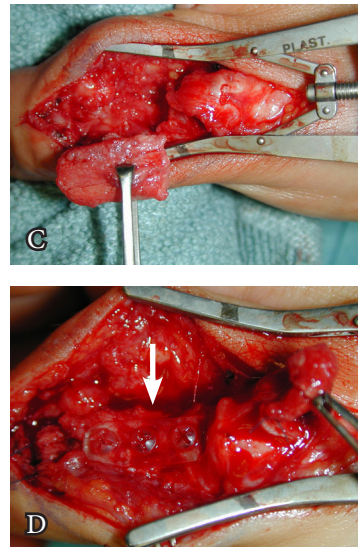

Figure 11. Patient 3: A-B) Pre-operative appearance. A bone defect in the proximal phalanx and limited movement of the interphalangeal joint in the right thumb were observed; C-D) A corticocancellous bone graft from the iliac crest was fused to adjacent bone structures with a SR-P(L/DL)LA 70/30 plate and screws (arrow).

4.2 Bioabsorbable joint scaffold arthroplasty

4.2.1 Experimental animals

The experiments on minipigs were approved by the Research Animal Committee of the Faculty of Veterinary Medicine, Helsinki University, and by the Provincial Administrative Board. Eighteen skeletally-mature female minipigs (Ellegaard Göttingen Minipigs Aps, Dalmose, Denmark) with a mean age of 3.6 years (range 2.1-4.5) and a mean weight of 43.3 kg (range 29-57) were used.

4.2.2 Implants

The P(L/D)LA 96/4 scaffolds (Fig. 12A) were manufactured of purified, medical-grade (residual monomer < 0.5%) poly-L/D-lactide co-polymer with an L/D isomer ratio of 96/4 (Purac Biochem b.v., Gorinchem, The Netherlands). Raw P(L/D)LA 96/4 polymer was melt-spun to 4-ply multifilament using Gimac microextruder (Gimac, Castronno, Italy) having a die temperature of 265°C and oriented by drawing in a two-step process to a draw ratio of 4.2. The 4-ply multifilament was knitted to a tubular jersey structure using a tubular jersey knitting machine (Textilmaschinenfabrik Harry Lucas, Neumünster, Germany) and rolled to a cylindrical scaffold 8 mm in diameter and 3.5 mm thick (Fig. 12A) and heat-treated above the glass transition temperature in the molds. The scaffolds were washed with ethanol, dried in vacuum overnight and packed separately into double pouches before they were sterilised with gamma irradiation of a minimum dose of 2.5 MRads. The fabrication method of the P(L/D)LA 96/4 scaffold is described in more detail elsewhere [79, 120]. The material data of the polymer is given in Table 4. The mean porosity of P(L/D)LA 96/4 scaffolds has earlier been reported to be 69.5% defined by comparing the mass of the scaffold to the corresponding mass of a solid P(L/D)LA 96/4 piece [120].

The composite joint implant was composed of a P(L/D)LA 96/4 scaffold combined with an intramedullary double-sided Polyactive® 1000PEO70PBT30 stem (Fig. 12B). The stems were fabricated of a segmented block co-polymer of polyethylene oxide (PEO) and polybutylene terephtalate (PBT) with a PEO/PBT ratio of 70/30 and an initial length of the PEO segment of 1000 Da (trade name Polyactive® 1000PEO70PBT30, IsoTis b.v., Bilthoven, The Netherlands). The molecular weight of the used co-polymer was 80,000 – 125,000 dl/g (manufacturer's information). The polymer was thermally stabilised with 0.55-0.85 wt% vitamin E. The stems were injection-moulded at 150°C using a pilot-scale Battenfeld injection molding machine.

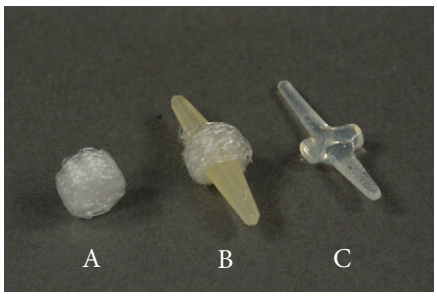

Figure 12. Implants used were A) P(L/D)LA 96/4 scaffold, B) P(L/D)LA 96/4 scaffold with a 1000PEO70PBT30 stem, and C) Swanson silicone implant.

Table 4. Material data of raw P(L/D)LA 96/4 polymer before and after processing.

	Raw P(L/D)LA 96/4	Processed P(L/D)LA 96/4 scaffold
Inherent viscosity (chloroform, 25°C)	4.98 dl/g	3.17 dl/g
Heat of fusion	30.2 J/g	26.2 J/g
Glass transition temperature	66°C	59°C

The final quadrangular stems were 25.4 mm in length with an edge of 3.0 mm in the base and 1.5 mm in the tip, and with a groove in the central part. The P(L/D)LA 96/4 scaffold part of the composite joint implant was fabricated of raw P(L/D)LA 96/4 (Purac Biochem b.v., Gorinchem, Netherlands). P(L/D)LA 96/4 was melt-spun to 4-ply multifilament and knitted to tubular single jersey which was rolled onto its place in the central groove in the midway of the Polyactive® 1000PEO70PBT30 stem. The resulting composite joint implant produced thus consists of a P(L/D)LA 96/4 scaffold in the middle part (having an outer diameter of 8 mm and thickness of 3.5 mm), flanked by intramedullary double-sided Polyactive® 1000PEO70PBT30 stem 12.3 mm long on the metacarpal side and 9.6 mm long on the proximal phalangeal side (Fig. 12B). Finally the implants were packed separately before they were sterilised with gamma irradiation using a minimum dose of 2.5 MRads.

The Swanson silicone finger joint implant (Wright Medical Technology, Inc., Arlington, Tennessee, USA) of size 00 was appropriate to meet the anatomical requirements (Fig. 12C). The size of the midsection was 7.9 mm (width) x 3.0 mm (depth) x 3.3 mm (height).

4.2.3 Anaesthesia

The animals were sedated with 0.5 mg/kg midazolam (Dormicum®, Roche Oy, Espoo, Finland) intramuscularly and 4 mg/kg azaperone (Stresnil, Janssen-Cilag Pharma, Vienna, Austria) intramuscularly. After premedication with 0.01 mg/kg of glycopyrrone (Robinul®, John Wyeth and Brother Ltd., New Lane, Havant, Hantfordshire, England) intramuscularly, anesthesia for surgery was induced and after intubation maintained with isoflurane (Forene®, Abbott Scandinavia, Solna, Sweden). During operation, 500-1000 ml of fluid (Ringersteril, Baxter Ltd, Vantaa, Finland), bentzylpenicillin natrium 35 000 IU/kg (Geepenil, Orion Pharma, Espoo, Finland) and 2.2 mg/kg flunixine meglumine (Finatyde, Schering-Plough Sante Animal, Segre, France) were administered intravenously. Analgesia was employed by 0.1 mg/kg butorphanoltartrat (Torbugesic Vet, Fort Dodge Laboratories, Fort Dodge, Iowa, USA) intramuscularly.

4.2.4 Surgical technique and post-operative care

The operation was performed in sterile conditions on both forelimbs, under tourniquet control. The implants used were randomly implanted, so that two different implants were implanted in the forelimbs of each animal. A longitudinal skin incision was made on the dorsum of the fifth MCP joint. After the joint was exposed by a longitudinal capsular incision between the common digital extensor and extensor digiti quinti tendons, the metacarpal head and the base of proximal phalanx were resected piecemeal with bone rongeurs and chisel, leaving the collateral ligaments intact. The resected joint space was thoroughly irrigated with saline and care was taken to remove all cartilage. Sesamoid bones were not removed.

The joint reconstruction was achieved with one of three different implants described above: 1) P(L/D)LA 96/4 scaffold (Fig. 12A), 2) P(L/D)LA 96/4 scaffold with a double-sided Polyactive® 1000PEO70PBT30 stem (Fig. 12B), or 3) Swanson silicone implant (Fig. 12C). The plain P(L/D)LA 96/4 scaffold without a stem was fixed in its place by two PDS (PDS II, 4/0 USP, Ethicon®, Norderstedt, Germany) knots, one for each collateral ligament. The silicone arthroplasty was done following the accepted principles as proposed by Swanson [177]. For Swanson and P(L/D)LA 96/4 scaffold with a double-sided Polyactive® 1000PEO70PBT30 stem, the intramedullary canals of the metacarpal and proximal phalanx were reamed in a rectangular shape to accommodate the stem of the implant. The joint capsule and skin were closed with interrupted and continuous intracutaneous 4/0 PDS sutures, respectively. The tourniquet was released. The wound was covered by teat bandage (Animal Soft, Snøgg Industri As, Mosby, Norway) and sterile gauzes followed by self-adherent wrap (Coban™, 3M Health Care, Borken, Germany) for ten days post-operatively.

4.2.5 Follow-up and examination methods

Clinical follow-up consisted of radiological examinations (anterior-posterior radiograph) and ROM measurements with a goniometer pre-operatively, immediately after the operation, and at follow-up time points until sacrifice. The animals were harvested at 10, 26, and 52 weeks post-operatively to obtain three specimens in each group, as well as at three years to obtain two specimens in each arthroplasty group. Harvesting was made by giving an overdose of pentobarbital (Mebunat vet, Orion-yhtymä Oyj, Espoo, Finland) following administration of the euthanising agent (T61 vet.inject., Intervet International GmbH, Unterschleissheim, Germany) intravenously.

After harvesting, the operated areas were dissected free of soft tissues and inspected before the radiographs were taken. The arthroplasty space width and volar subluxation were measured from anterior-posterior and lateral radiographs, respectively. The operated areas were excised as specimens, fixed in a series of ethanol immersions of rising concentrations (70% to 90%) and embedded in methylmetacrylate. For histological analysis, 20 µm uncalcified whole mount sections were cut through the longitudinal axis of the bones and the joint by using a cutting and grinding method [42] and stained by a modified Masson-Goldner trichrome method [54]. For the scaffold porosity measurements, three unimplanted intact P(L/D)LA 96/4 scaffolds were prepared as controls similarly for the microscopic analysis. A light microscope was used for histological evaluation. The quantitative measurements were performed with the use of computer-assisted image-analysis software (analySIS pro 3.0, Soft Imaging System GmbH, Münster, Germany). Since the P(L/D)LA 96/4 is highly birefringed, its retention and degradation over time were assessed using a polarising microscope. The porosity of the scaffold was calculated on the basis of positive birefringence areas of photographs made under low-power magnification.

4.2.6 Statistical methods

ANOVA or for non-normal data Kruskal-Wallis test was used to assess differences between groups. If such differences were found, pair-wise comparisons using t-tests or Mann-Whitney U-tests (if non-normal data) were carried out to locate the differences. Two-tailed P values < 0.05 were considered significant. Statistical analyses were done using SPSS 12.0 program (Chicago, IL, USA).

5 RESULTS

5.1 Bioabsorbable fixation

5.1.1 Transverse osteotomy

Palmar apex bending

The rigidity (Fig. 13) of dorsal SR-P(L/DL)LA plating was higher than that of dorsal SR-PLGA ($p = 0.011$) and 1.7 mm titanium plating ($p = 0.032$). There was no significant difference in rigidity between dorsal SR-PLGA and 1.7 mm titanium plating ($p = 0.340$). Both types of dorsolateral bioabsorbable plating were more rigid than the corresponding dorsal platings ($p < 0.001$). Of the plated bones, dorsal 2.3 mm titanium plating had the highest rigidity ($p = 0.020$, versus the second highest), whereas crossed Kirschner wires provided the highest stability when analysing all fixation groups ($p < 0.001$). Intact control bone had a mean rigidity of 0.427 Nm^2 (SD = 0.063).

Dorsal apex bending

In rigidity (Fig. 14A), both dorsal bioabsorbable platings (SR-PLGA, $p = 0.005$; SR-P(L/DL)LA, $p < 0.001$) were weaker than dorsal 2.3 mm titanium plating. Of the two, SR-PLGA plating was more rigid than SR-P(L/DL)LA plating ($p = 0.005$) and it was equal in rigidity to the dorsal 1.7 mm titanium plate ($p = 0.491$). Both types of dorsal bioabsorbable plating were more rigid than crossed Kirschner wires (SR-PLGA, $p < 0.001$; SR-P(L/DL)LA, $p = 0.001$). When applying the bioabsorbable plates dorsolaterally, the rigidity decreased (SR-PLGA, $p < 0.001$; SR-P(L/DL)LA, $p = 0.006$) compared with the corresponding dorsal plating. There was no difference in rigidity between the dorsolateral bioabsorbable platings and crossed Kirschner wires ($p = 0.284$).

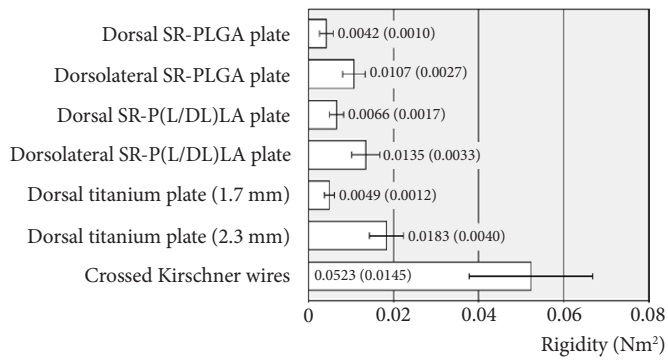

Figure 13. Rigidity of transversally-osteotomised bones in palmar apex bending. Values are presented as means (and standard deviations).

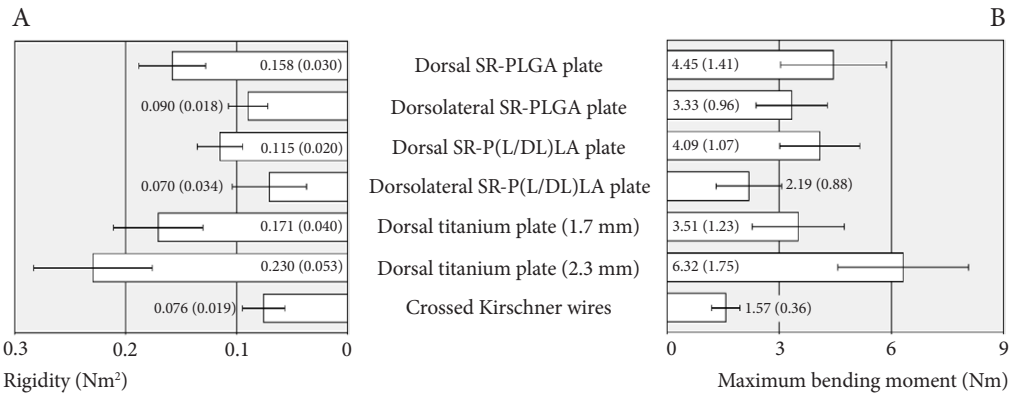

Figure 14. A) Rigidity and B) maximum bending moment of transversally-osteotomised bones in dorsal apex bending. Values are presented as means (and standard deviations).

Analysis of the maximum bending moment (Fig. 14B) revealed that both types of dorsal bioabsorbable plating had higher values than crossed Kirschner wires ($p < 0.001$), but there was no difference when compared with 1.7 mm titanium plating ($p = 0.331$). The values measured in the dorsal bioabsorbable plate groups did not differ ($p = 0.567$). When intact bone was excluded, dorsal 2.3 mm titanium plating had the highest maximum bending moment ($p = 0.034$, versus the second highest) among the fixation methods studied. A tendency toward lower values was seen when dorsolateral bioabsorbable plating was compared with corresponding dorsal plating (SR-PLGA, $p = 0.084$; SR-P(L/DL)LA, $p = 0.002$). The mean value for crossed Kirschner wires was the lowest, but the difference compared with dorsolateral SR-P(L/DL)LA was not significant ($p = 0.090$). Intact control bone had a rigidity of 0.477 Nm^2 (SD = 0.099) and a maximum bending moment of 9.04 Nm (SD = 2.07).

Visual evaluation of failure mechanisms revealed that osteotomies plated dorsally with SR-PLGA plates were broken either at the plate (five of eight specimens) or the bone cortex (three of eight specimens). Dorsal SR-P(L/DL)LA plates were stretched slightly at the screw hole site, after which the fixation failed as above (three of eight specimens at the plate, and three of eight specimens at the cortex) but in two specimens the dorsal SR-P(L/DL)LA plate stretched without breaking. Dorsolateral bioabsorbable plates broke (SR-PLGA, eight of eight specimens; SR-P(L/DL)LA, four of eight specimens) or were stretched without breaking (SR-P(L/DL)LA, four of eight specimens) at the screw hole site. Bones plated dorsally with 1.7 mm titanium plate failed because of plate breakage (five of eight specimens) or because the titanium screws came out of the bone (three of eight specimens), whereas all bones plated dorsally with 2.3 mm titanium could not resist the force created around the screws, leading to broken cortex (four of eight specimens) or longitudinal splitting of the diaphysis (four of eight specimens). Kirschner wires broke through the cortex (eight of eight specimens) when angulation at the osteotomy site was increased. The areas subjected to the highest stress in plating systems were on the bone adjacent to the screws and at the screw hole sites of the plate nearest to the osteotomy. The screws and their heads did not break in any instance.

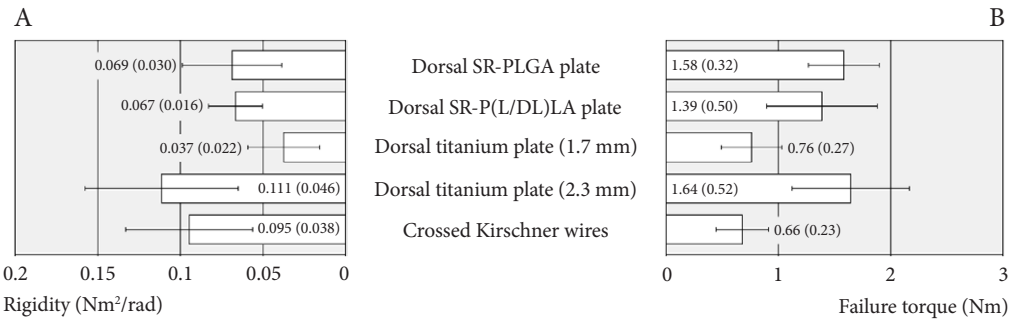

Figure 15. A) Torsional rigidity and B) failure torque of transversally-osteotomised bones. Values are presented as means (and standard deviations).

Torsional loading

In torsional loading (Fig. 15A) both types of dorsal bioabsorbable plating were more rigid than dorsal 1.7 mm titanium plating (SR-PLGA, $p = 0.036$; SR-P(L/DL)LA, $p = 0.011$) but weaker than 2.3 mm titanium plating (SR-PLGA, $p = 0.046$; SR-P(L/DL)LA, $p = 0.022$). The bioabsorbable platings were statistically equivalent ($p = 0.721$) and they did not differ from Kirschner wire fixation ($p = 0.178$). Torsional rigidity of intact control bone was 1.05 Nm^2/rad (SD = 0.25).

In terms of failure torque (Fig. 15B), the bioabsorbable and 2.3 mm titanium platings were statistically equal ($p = 0.510$). Furthermore, the bioabsorbable platings had higher failure torque than 1.7 mm titanium plating ($p = 0.008$, versus dorsal SR-P(L/DL)LA plating) or crossed Kirschner wires ($p = 0.002$, versus dorsal SR-P(L/DL)LA plating). Failure torque of intact control bone was 5.89 Nm (SD = 1.35).

5.1.2 Oblique osteotomy

Palmar apex bending

1.5 mm SR-PLLA pins, 1.5 mm Kirschner wires and SR-P(L/DL)LA screws (outer Ø 2.0 mm, inner Ø 1.45 mm) provided similar rigidities ($p = 0.643$) in palmar apex bending. The SR-P(L/DL)LA plate with an interfragmentary screw provided rigidity equal to that of titanium lag screws ($p = 0.148$) and was found to be more rigid than any of the Kirschner wires, SR-PLLA pins or SR-P(L/DL)LA screws ($p < 0.001$). The titanium plate with an interfragmentary lag screw showed the most resistance of all the fixation devices tested ($p < 0.001$). Intact bone had a rigidity of 0.255 Nm^2 (SD = 0.026) (Fig. 16A).

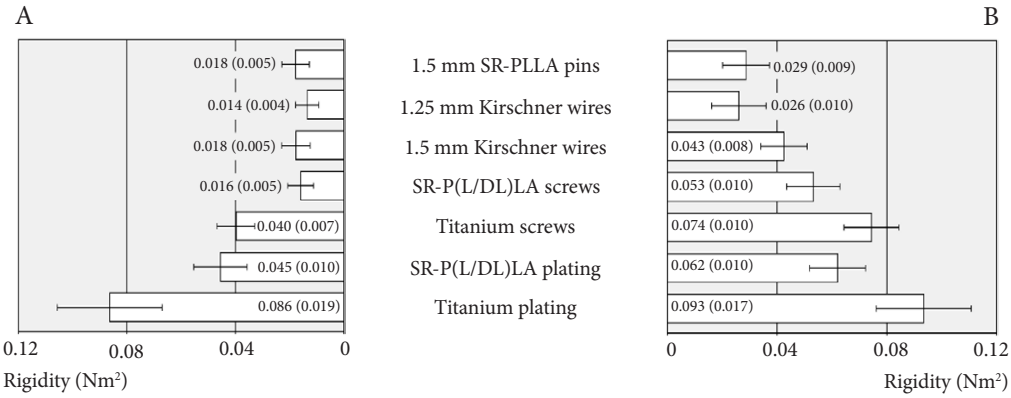

Figure 16. Rigidity of obliquely-osteotomised bones in A) palmar and B) lateral apex bending. Values are presented as means (and standard deviations).

Lateral apex bending

1.5 mm SR-PLLA pins provided rigidity comparable to that of the 1.25 mm Kirschner wires ($p = 0.532$), whereas 1.5 mm Kirschner wires provided higher values than 1.5 mm SR-PLLA pins ($p = 0.002$). SR-P(L/DL)LA screws provided higher rigidity than 1.5 mm Kirschner wires ($p = 0.018$) or 1.5 mm SR-PLLA pins ($p < 0.001$). No statistically significant difference was found between the rigidities provided by SR-P(L/DL)LA screws and SR-P(L/DL)LA plating ($p = 0.064$), but titanium lag screws provided higher rigidity than SR-P(L/DL)LA screws ($p < 0.001$). Titanium plate fixation showed the highest rigidity of all fixation methods tested ($p = 0.008$ vs. titanium lag screws). Intact bone had a rigidity of 0.202 Nm^2 (SD = 0.032) (Fig. 16B).

Dorsal apex bending

1.5 mm SR-PLLA pins, 1.5 mm Kirschner wires, SR-P(L/DL)LA screws (outer Ø 2.0 mm, inner Ø 1.45 mm) and titanium lag screws (outer Ø 1.7 mm) provided equal rigidities ($p = 0.338$). SR-P(L/DL)LA plating was more rigid than titanium lag screws ($p = 0.005$) but less rigid than titanium plating ($p = 0.001$). Intact bone had a rigidity of 0.213 Nm^2 (SD = 0.045) (Fig. 17A). The rigidities of SR-P(L/DL)LA plating ($p = 0.671$) and titanium plating ($p = 0.179$) did not reveal any significant differences when the values in dorsal and palmar apex bending tests were compared.

The maximum bending moments (Fig. 17B) of 1.5 mm SR-PLLA pins and 1.5 mm Kirschner wires were similar ($p = 0.576$). SR-P(L/DL)LA screws resisted force better than SR-PLLA pins ($p < 0.001$) or titanium lag screws ($p = 0.038$). The plated bones had the highest values among the fixation configurations ($p < 0.001$), titanium plate fixation having a higher value than the bioabsorbable one ($p < 0.001$). The maximum bending moment of intact control bone was 4.48 Nm (SD = 0.95).

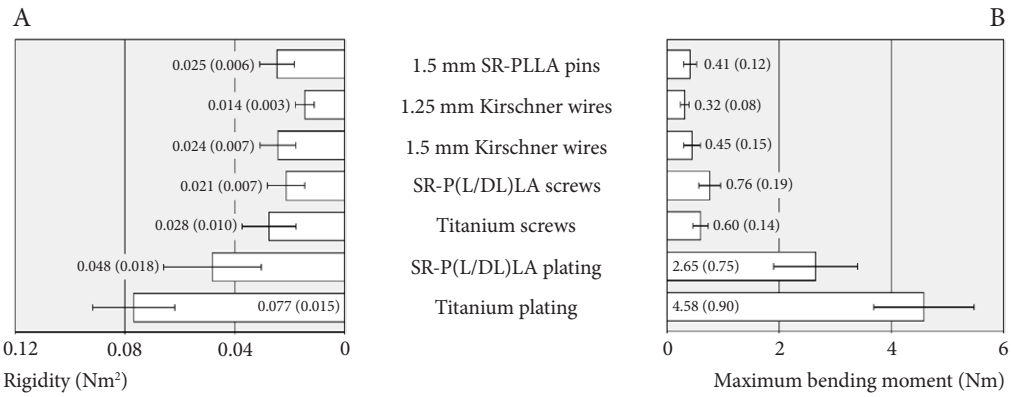

Figure 17. A) Rigidity and B) maximum bending moment of obliquely-osteotomised bones in dorsal apex bending. Values are presented as means (and standard deviations).

Torsional loading

The torsional rigidity (Fig. 18A) values of 1.5 mm SR-PLLA pins and 1.25 mm Kirschner wires were statistically similar (p = 0.613), and comparison between 1.5 mm SR-PLLA pins and an SR-P(L/DL)LA 70/30 plate with an interfragmentary screw did not reveal any statistical difference (p = 0.155). SR-P(L/DL)LA screws provided rigidity equal to that of 1.5 mm Kirschner wires (p = 0.737) and higher than that of 1.5 mm SR-PLLA pins (p = 0.003). SR-P(L/DL)LA screws did not show any statistically significant difference from titanium lag screws (p = 0.088), but titanium plating had greater rigidity (p = 0.003). Intact bone had a rigidity of 0.275 Nm (SD = 0.037).

The failure torque (Fig. 18B) values of SR-PLLA pins, SR-P(L/DL)LA screws and titanium lag screws were similar (p = 0.967). Furthermore, SR-PLLA pins did not show any statistically significant difference from Kirschner wires with diameters of 1.25 mm (p = 0.395) or 1.5 mm (p = 0.056). SR-P(L/DL)LA and titanium plating showed the highest mean values of failure torque, which did not differ statistically from each other (p = 0.418). The difference between SR-P(L/DL)LA plating and 1.5 mm Kirschner wires was not statistically significant (p = 0.063). The failure torque of intact bone was 2.03 Nm (SD = 0.28).

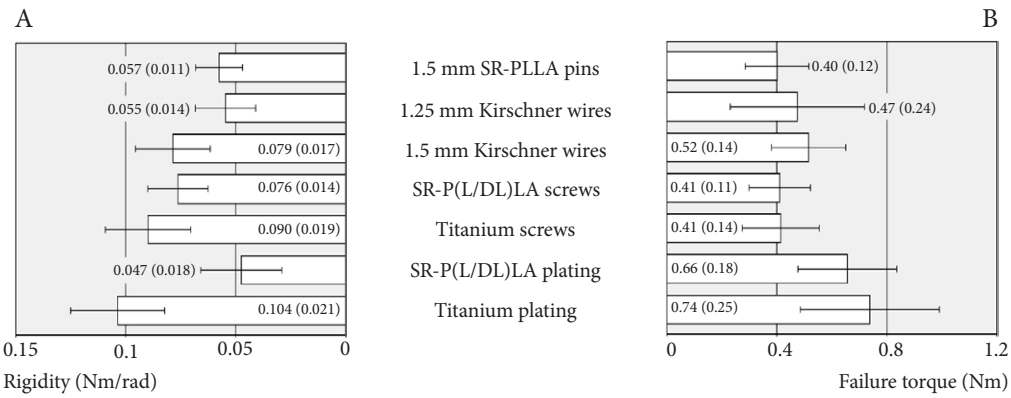

Figure 18. A) Torsional rigidity and B) failure torque of obliquely-osteotomised bones. Values are presented as means (and standard deviations).

5.1.3 Patient cases

Patient 1

Reduction remained (Fig. 19) and uneventful union ensued, but there was a little scar contracture of the thumb, and a bulky flap. At a follow-up 15 months post-operatively, the patient was free of pain and demonstrated good overall function of the hand. The active motion of the MCP joint of the middle finger was 20° to 60°, and that of the index and ring fingers was 0° to 30°.

Patient 2

Radiographic union was evident at six weeks (Fig. 20A). On the last visit, 20 months after surgery (Fig. 20B-C), the thumb was painless and he was able to perform his daily activities without restriction. The active motion of the interphalangeal joint was 25° to 35°, whereas the carpometacarpal joint regained 10° flexion and 30° hyperextension. The thumb demonstrated active abduction of 45°.

Patient 3

Bone consolidation occurred at 6 weeks. At the final follow-up after 12 months, the contours of the thumb were satisfactory (Fig. 21A-B) and the patient had regained function of her thumb except for slight lateral instability owing to laxity of the lateral collateral ligaments.

5.2 Bioabsorbable joint scaffold arthroplasty

All minipigs recovered uneventfully from the operation, stood up after the anesthesia and put weight on and used all limbs normally without any signs of limping. No swelling or thickening of the tissues was macroscopically seen in the skin or subcutaneous layers. The extensor tendons above the reconstructed joint could be freely moved. However, in the Swanson implant group belonging to the 26-week follow-up, one minipig developed a sinus at the operation site two months post-operatively, followed by an implant extrusion and sinus healing. This forelimb was excluded from the study. No differences in the joint stiffness or stability were found between the arthroplasty groups in manual examination.

5.2.1 Range of motion

The mean pre-operative and post-operative passive ROMs of the joints are shown in Table 5. The mean ROM of each study group decreased significantly from the pre-operative mean values of 130-140° to the mean values of 89-94° in the early post-operative weeks ($p < 0.001$). No further statistically significant changes in ROM were observed during the three-year follow-up ($p > 0.05$). No differences were found between the study groups ($p > 0.05$).

Figure 19. Patient 1: X-ray 1 month after surgery.

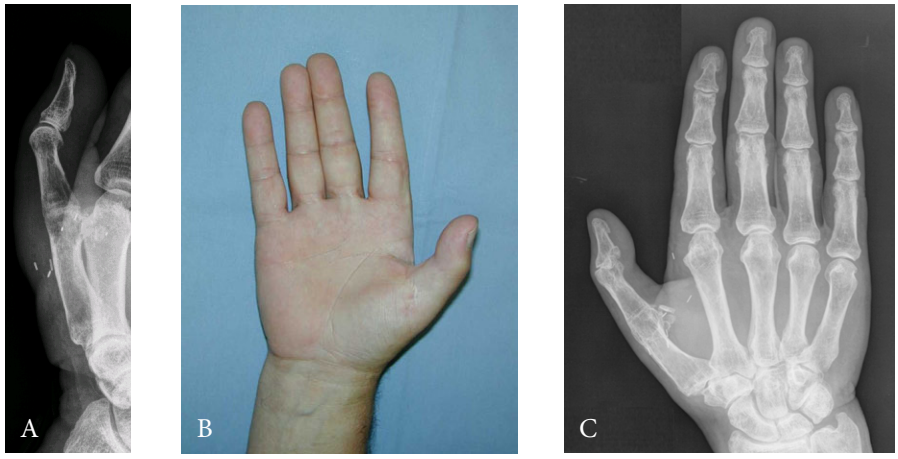

Figure 20. Patient 2: A) X-ray 6 weeks after surgery showing solid union of fusion of the thumb MCP joint; B-C) Thumb contour 20 months after surgery.

Figure 21. Patient 3: A) A view of the hand 8 months after surgery and B) an x-ray 12 months after surgery showing good thumb contour.

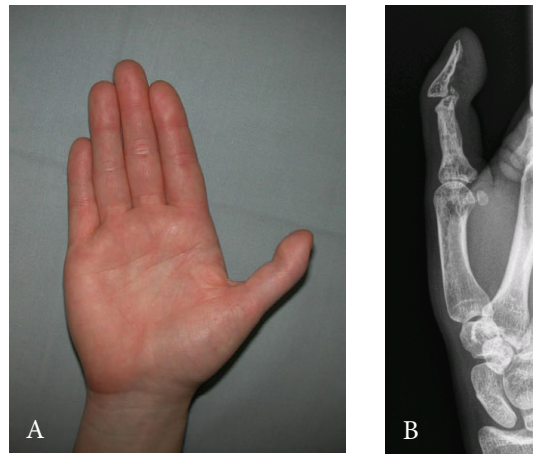

Table 5. Mean passive range of motion and radiological evaluation of arthroplasty space width, volar subluxation and maximum diameter of cavity around the intramedullary stem after P(L/D)LA 96/4 joint scaffold, Swanson silicone implant, and P(L/D)LA 96/4 joint scaffold with a Polyactive® 1000PEO70PBT30 stem at follow-ups. Values are presented as means (and standard deviations).

	Preoperative	10 weeks	26 weeks	1 year	3 years
Passive range of motion (degree)					
P(L/D)LA scaffold	140 (8)	89 (11)	98 (10)	94 (10)	86 (2)
Swanson implant	140 (7)	94 (15)	96 (18)	90 (7)	74 (6)
P(L/D)LA scaffold with Polyactive® stem	135 (6)	94 (16)	100 (8)	92 (9)	70 (1)
Arthroplasty space width (mm)					
P(L/D)LA scaffold		4.9 (1.1)	4.5 (0.8)	4.3 (1.0)	3.9 (0.3)
Swanson implant		4.4 (1.0)	4.0 (0.5)	3.5 (0.5)	2.7 (0.5)
P(L/D)LA scaffold with Polyactive® stem		5.4 (1.1)	5.1 (0.6)	3.4 (0.5)	4.7 (1.9)
Volar subluxation (mm)					
P(L/D)LA scaffold		0.4 (0.3)	0.5 (0.9)	0.7 (0.2)	0.8 (0.5)
Swanson implant		0.2 (0.3)	0	0	0
P(L/D)LA scaffold with Polyactive® stem		0.6 (0.5)	0.7 (0.1)	0.6 (0.4)	0
Maximum diameter of cavity around the intramedullary stem (mm)					
Swanson implant		3.5 (0.5)	3.8 (0.5)	3.3 (0.2)	3.6 (0.3)
P(L/D)LA scaffold with Polyactive® stem		7.1 (1.0)	5.5 (1.1)	8.2 (0.7)	-

5.2.2 Radiography

In the P(L/D)LA scaffold and Swanson silicone implant groups, the contours of the resected bone ends were both initially sharp (Fig. 22 and 23A and a), but gradually became uneven and sclerosed during the 3-year follow-up (Fig. 23B-D and b-d). At 10 weeks, a periosteal reaction was seen at the resected bone ends in both groups (Fig. 23A and a). In the P(L/D)LA scaffold group after 26 weeks, the end of the metacarpal bone had remodeled into a rounded and convex shape, whereas the proximal phalanx had become concave due to new bone formation at the edges of the proximal phalanx (Fig. 23B). In the Swanson implant group, bony spurs were noted at 10 weeks at the metacarpal bone end on the volar and dorsal aspects (Fig. 23a). They became gradually more pronounced so that at three years the Swanson silicone implant was almost completely surrounded by bony spurs (Fig. 23d).

In the Polyactive® 1000PEO70PBT30 stem group, radiographs showed severe osteolytic changes around the stem in all specimens during the first post-operative year (Table 5, Fig. 22C and 23a'-c'). The maximum diameter of osteolytic stem cavity averaged 7.1 mm, 5.5 mm and 8.2 mm in 10, 26 and 52 week specimens, respectively. The widest diameter of the stem cavity was usually found in the central part of the stem site adjoining the arthroplasty space. The bone cortex around the Polyactive® 1000PEO70PBT30 stem site was often less than 1 mm in thickness and occasionally even perforated. At 3 years, the radiographs showed clear regression of the osteolytic area with traces of new trabecular bone (Fig. 23d'), but small osteolytic cysts, 2-3 mm in diameter, were still visible. However, no single and continuous osteolytic implant cavity could be identified anymore. The resected bone ends were highly more sclerosed in the Polyactive® 1000PEO70PBT30 stem group than in the P(L/D)LA scaffold and Swanson implant groups.

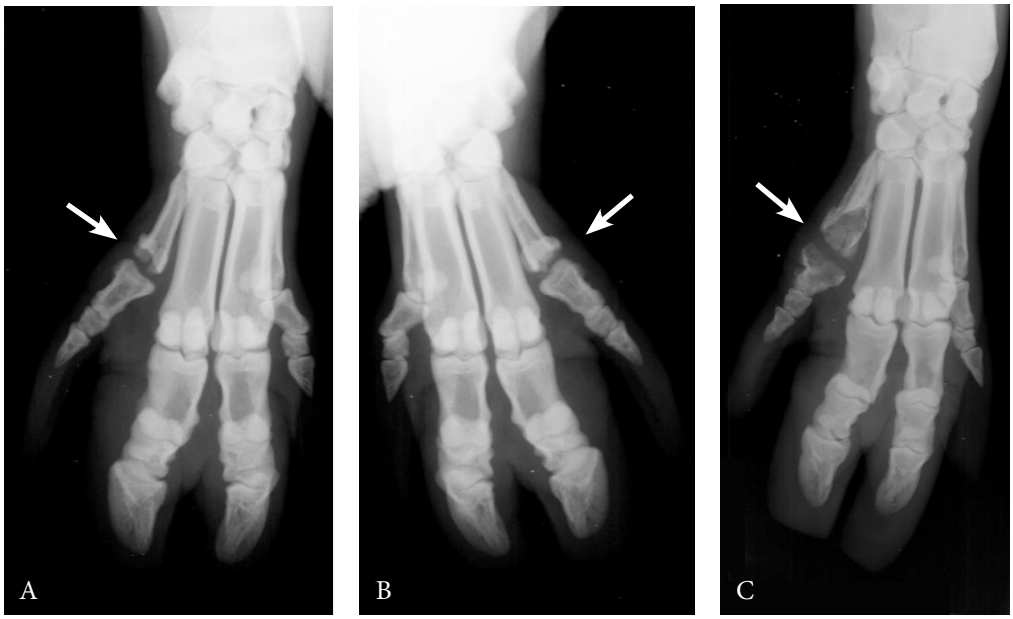

Figure 22. Radiograph at one year follow-up showing A) P(L/D)LA 96/4 joint scaffold, B) Swanson silicone implant, and C) P(L/D)LA 96/4 joint scaffold with a Polyactive® 1000PEO70PBT30 stem in the fifth MCP joint of the fore limb of a minipig (arrows)

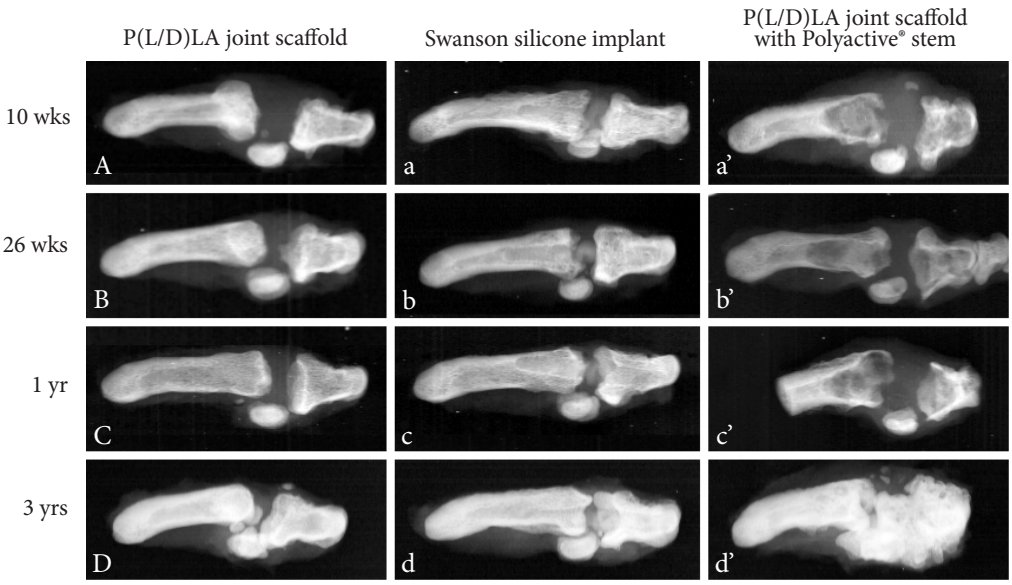

Figure 23. Radiographs of the arthroaplasty after P(L/D)LA 96/4 joint scaffold, Swanson silicone implant and P(L/D)LA 96/4 joint scaffold with a Polyactive® 1000PEO70PBT30 stem in lateral projection examined post-operatively at 10 weeks, 26 weeks, 1 year and 3 years. On the left metacarpal bone and on the right proximal phalanx in each radiograph.

In the Swanson implant group, only minimal bone erosion was seen around the intramedullary silicone stems (Fig. 23a-d), the mean value of the widest diameter being 3.6 mm (SD = 0.4) (Table 5). This was similar to or only slightly greater in value than the original reamed bone channel diameter. The difference was significant when this value was compared to the mean diameter of Polyactive® 1000PEO70PBT30 stem group ($p < 0.001$). Bone remodeling was frequently seen at the end of the silicone stems where the cortical bone became very thin (Fig. 23c and d). No breakage of the silicone implant could be seen in the radiographs. The specimens reconstructed with a plain P(L/D)LA scaffold without a stem and without intramedullary reaming showed normal structure of the bone without any osteolytic changes.

The mean arthroplasty space width ranged being 4.9–3.9 mm and 4.4–2.7 mm in the P(L/D)LA scaffold and Swanson silicone implant groups during the follow-up, respectively (Table 5). The mean values were higher in the P(L/D)LA scaffold group, but the difference was not statistically significant ($p = 0.077$). During the follow-up, no statistically significant decrease in arthroplasty space width was seen in either group ($p = 0.516$, $p = 0.13$, respectively). In the Polyactive® 1000PEO70PBT30 stem group the values of arthroplasty space width were misleading high due to severe osteolytic changes (Fig. 23a'-c') (Table 5).

Volar subluxation was present at all follow-up time points in the joints reconstructed with a P(L/D)LA scaffold (Table 5), the mean value being 0.56 mm (range 0.0–1.1 mm). No statistically significant increase towards higher values of subluxation were seen during the follow-up ($p = 0.790$). Similar volar subluxation was present also in the Polyactive® 1000PEO70PBT30 stem group. In the Swanson implant group, volar subluxation was seen only in one joint (Table 5).

5.2.3 Light microscopy of P(L/D)LA 96/4 joint scaffold arthroplasty

The P(L/D)LA scaffold remained in the correct position between the resected bone ends during the whole study period. All histological sections showed fibrous connective tissue formation in the scaffold without any cartilage except for the articular surfaces of the sesamoid bones, which had been left untouched in the operation. The mean porosity of the unimplanted P(L/D)LA scaffold was 69% (SD 1.0) with a range from 62% to 74% (Fig. 24). The mean filament diameter of the unimplanted scaffold was 113 μm (SD 2.1).

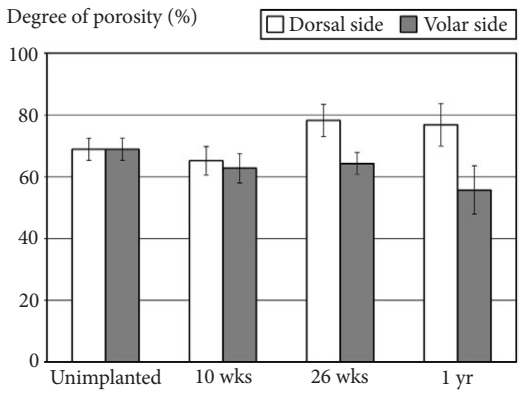

Figure 24. The porosity of P(L/D)LA 96/4 scaffold before implantation and at follow-up in the dorsal and volar sides of the joint scaffold.

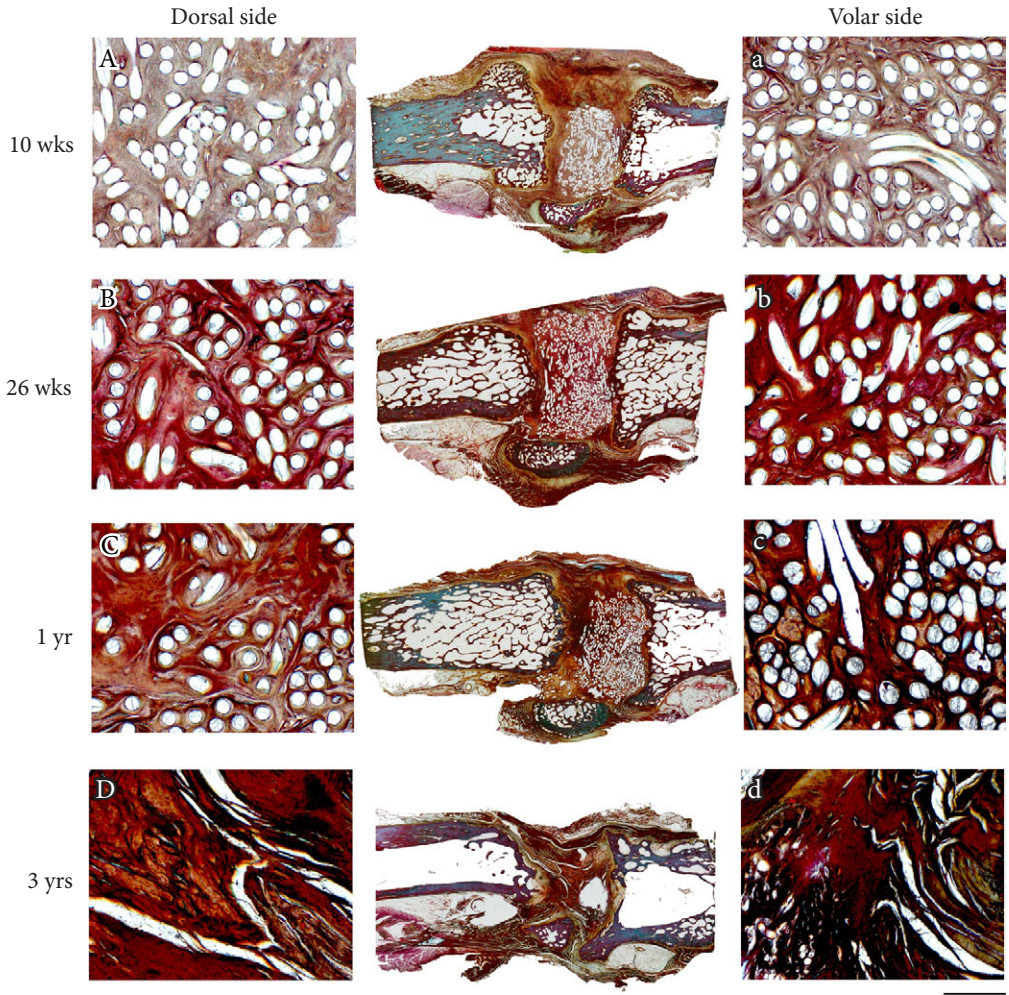

Figure 25. Sagittal photomicrograph of the joints reconstructed with P(L/D)LA 96/4 scaffold at A) 10 and B) 26 weeks and C) 1 and D) 3 years post-operatively. A histological detail of the P(L/D)LA 96/4 joint scaffold is presented in the dorsal (left column) and volar side (right column) of the reconstructed joint. Masson-Goldner trichrome; scale bar 500 μm in the microscopic view.

Ten-week follow-up

At 10 weeks, the P(L/D)LA scaffold was surrounded by a fibrous tissue capsule and became completely invaded by loose connective tissue rich in fibroblasts and capillaries (Fig. 25A and a). The polymer filaments were practically intact when observed by the light microscope and only few cracks were seen. Their mean filament diameter throughout the scaffold was 112 μm (SD 2.7). The mean degree of porosity was 65% (SD 4.1) dorsally in the scaffold and 63% (SD 5.0) volarly in the scaffold (Fig. 24). This did not statistically differ from the porosity of the unimplanted PL(D/L)LA scaffold ($p = 0.19$). Volarly, the in-grown connective tissue had matured and condensed forming now a dense collagen framework between the polymer filaments (Fig. 25a). Each individual filament was encapsulated by 3-7 layers of fibroblasts. In some parts of the scaffold, the 4-ply P(L/D)LA multifilament structure of the knitted scaffold was distinguishable. Dorsally in the scaffold, mainly unorganised cell-rich loose connective tissue was seen (Fig. 25A). A few macrophages were detected on the surface of the P(L/D)LA

filaments, but neither lymphocytes nor neutrophils were present. The fibrous interface area between the scaffold and the resected bone end was approximately 1.2 mm wide on the metacarpal side and approximately 0.48 mm on the proximal phalangeal side. New bone formation was seen periosteally at the volar and dorsal edges of both resected bone ends (Fig. 25).

Twenty-six-week follow-up

At 26 weeks, most of the filaments of the P(L/D)LA scaffold were unfragmented and only few cracks were observed (Fig. 25B and b). The invasion of the granulation tissue into the cracked filament structure was still very minor. The 4-ply multifilament structure of the scaffold could no longer be clearly identified. The mean diameter of the P(L/D)LA filaments was 116 µm (SD 6.3) in the scaffold. The porosity volarly in the scaffold had remained similar (mean 64%, SD 3.0, $p = 0.67$), but dorsally it had increased (mean 78%, SD 4.6, $p = 0.02$) compared with the 10-week specimens (Fig. 24). The connective tissue inside the scaffold had matured and condensed into dense connective tissue, which was rich in compacted collagen bundles and contained only a few scattered fibroblast-like spindle-shaped cells. After 10-weeks, an obvious increase in collagen framework was observed inside the P(L/D)LA scaffold (Fig. 25 and 26). Especially in the volar side of the scaffold, the dense collagen bundles were aligned between and around the P(L/D)LA filaments (Fig. 25b). Often only 1-2 fibroblast layers encapsulated each individual filament. However, in the dorsal and peripheral regions of the scaffold, all individual filaments were surrounded by a 1-5 fibroblast thick layer. A few multinucleated phagocytic foreign-body giant cells and macrophages were seen on the surface of the filaments, but no other inflammatory cell infiltrates were present. The mean width of the fibrous bone-scaffold interface was 0.84 mm on the metacarpal and 0.30 mm on the proximal phalangeal side. There was still a periosteal reaction at the edges of both bone ends (Fig. 25).

Fifty-two-week follow-up

At 52 weeks, the configuration of the P(L/D)LA scaffold was identifiable but had softened (Fig. 25C). In histological specimens, increased cracking of the P(L/D)LA filaments was seen, but the volume of granulation tissue penetrating into the filaments was still relatively minor.

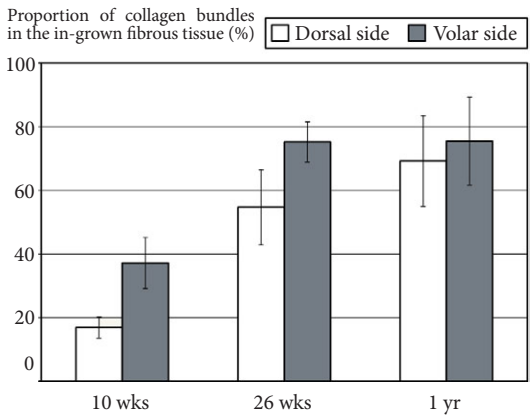

Figure 26. Histomorphometric analysis of the proportion of collagen bundles in the in-grown fibrous tissue shows connective tissue maturation in the dorsal and volar sides of the scaffold as a function of time.

The mean diameter of the cracked P(L/D)LA filaments was 120 µm (SD 7.4) in the scaffold. The degree of porosity remained similar dorsally in the scaffold (mean 77%) compared to the 26-week specimens ($p = 0.80$), but volarly the porosity had slightly reduced (56%, $p = 0.19$, vs. 26 week specimens) (Fig. 24). The difference in the degree of the porosity between the volar and dorsal sides of the scaffold was significant ($p = 0.022$). The dense connective tissue was highly organised throughout the scaffold and formed a nearly acellular, dense collagen framework with only a 1-3 fibroblasts thick layer around each P(L/D)LA filament in most places, especially volarly in the scaffold. The increase in the collagen framework inside the scaffold was significant compared to the 10-week specimens ($p = 0.002$, Fig. 26). Macrophages and a few foreign-body giant cells were seen in close vicinity to the polymer indicating actively ongoing degradation. The number of macrophages had increased compared with 10 and 26 week specimens but they were still few in number. No other inflammatory cell infiltrates were seen. The mean width of the fibrous bone-scaffold interface was 1.33 mm on the metacarpal side and 0.19 mm on the proximal phalangeal side. This difference was statistically significant ($p < 0.001$). Due to new bone formation the bone end of the metacarpal bone had remodelled into a rounded convex shape, whereas the bone edges of the proximal phalanx were "clumped" and so its contour formed a more concavely-shaped bone end.

Three-year follow-up

At 3 years, the P(L/D)LA scaffold had almost completely degraded and disappeared (Fig. 25 and 27). Only a very few tiny polymer particles were seen. The site of the scaffold had mostly been replaced with acellular dense connective tissue, characterised by abundant dense compacted collagen and a paucity of cells. The collagen fibers were mainly orientated in longitudinal direction. Patches of loose connective tissue, with polymer debris apparently being actively phagocytosed by macrophages, and some foreign-body giant cells were seen in some areas, especially dorsally in the reconstructed joint (Fig. 27). Except for a few lymphocytes that were seen in these areas, no lymphocyte or neutrophil infiltrates were evident. Scattered clusters of adipocytes were seen in the marginal areas of the joint. The bone ends were similar to the one-year specimens, except that the clumpy volar edge of the proximal phalanx had become more prominent than the dorsal one.

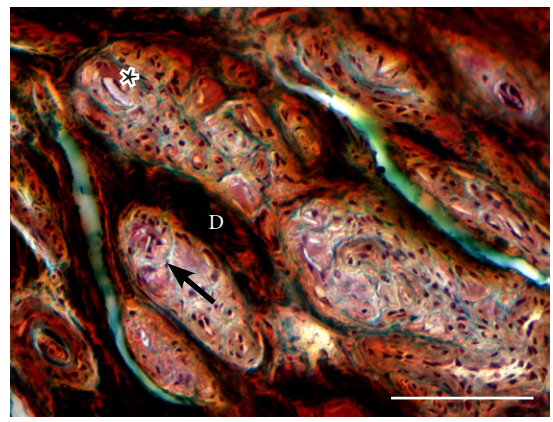

Figure 27. At three years the P(L/D)LA 96/4 joint scaffold had almost totally degraded and was replaced by dense connective tissue (D) with abundant collagen fibres. In some areas there were patches of cell-rich loose connective tissue with tiny P(L/D)LA 96/4 debris particles (star) being phagocytosed by macrophages and foreign body giant cells (arrow). Masson-Goldner trichrome; scale bar 100 µm.

5.2.4 Light microscopy of P(L/D)LA 96/4 scaffold with Polyactive® stem

Ten-week follow-up

Ten weeks after implantation, the intramedullary Polyactive® 1000PEO70PBT30 stems had been fragmented into various sizes of fragments, the diameter of which varied from tens of μm to several millimeters (Fig. 28A). Histological evaluation demonstrated that intramedullary Polyactive® 1000PEO70PBT30 fragments were surrounded by inflammatory cell infiltrates, such as polymorphonuclear neutrophils, macrophages, epitheloid cells, foreign-body giant cells and small lymphocytes organised into separate layers in a centrifugal direction from the center of the granuloma (Fig. 29). Many blood vessels were seen in the outer portions of the granulomas. The granulomas were surrounded by a thin layer of fibrous tissue (10-30 layers of fibroblasts) composed of multiple, slender and spindle-shaped fibroblasts embedded in collagenous matrix. No direct bone - Polyactive® 1000PEO70PBT30 stem contact could be seen. The cortical bone was thin at the stem site, usually less than 500 μm thick. In some places the cortex was perforated and small Polyactive® 1000PEO70PBT30 fragments (< 200 μm in diameter) had been extruded into the extramedullary space over wide areas. A lot of osteoclasts were found at the margins of the osteolytic areas, aggressively resorbing the endosteal bone (Fig. 29). The extramedullary Polyactive® 1000PEO70PBT30 fragments were often embedded in granulomas (Fig. 30). In addition, foreign-body giant cells with a 'foamy' appearance containing Polyactive® 1000PEO70PBT30 fragments in their cytoplasm were present. The histology of the extramedullary inflammatory granulomas resembles the intraosseus foreign-body reaction with polymorphonuclear neutrophils, lymphocytes, and epitheloid cells, but often with a thicker fibrous capsule (10-50 layers of fibroblasts) as the outermost zone. In the arthroplasty joint space, fibrous connective tissue formation was seen inside the P(L/D)LA 96/4 scaffold. New bone formation was seen periosteally at the volar and dorsal edges of both resected bone ends.

Twenty-six-week follow-up

The extent of fragmentation of the Polyactive® 1000PEO70PBT30 stem had not markedly increased. The foreign-body reaction around the Polyactive® 1000PEO70PBT30 fragments was still prominent. However, the inflammatory infiltrates in the granulomatous areas were clearly less numerous and smaller in size, whereas the outermost fibrous capsule was thicker than in the 10 week specimens consisting of up to 70 layers of fibroblasts. The granulomas were at this stage characterised by central Polyactive® 1000PEO70PBT30 particles surrounded by polymorphonuclear neutrophils, epitheloid cells, lymphocytes and only a few mononuclear phagocytic cells that often contained implant material fragments in their cytoplasm. Despite marked osteolytic areas observed adjacent to these inflammatory tissues, no aggressive osteoclast activity was seen any more.

Fifty-two-week follow-up

The degradation of the Polyactive® 1000PEO70PBT30 stems had progressed, but the outline of the stem was still identifiable due to the large intramedullary fragments of the stem that were 1-2 mm in diameter (Fig. 28C). No direct bone - polymer contact could be seen. The

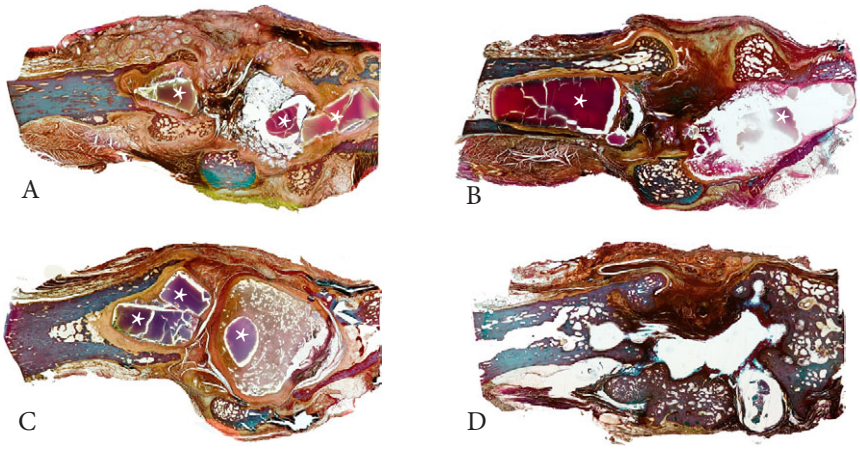

Figure 28. Sagittal photomicrograph of the joints reconstructed by P(L/D)LA 96/4 scaffold with Polyactive® 1000PEO70PBT30 double-sided stem at A) 10, B) 26, C) 52 weeks and D) 3 years post-operatively. The Polyactive® 1000PEO70PBT30 fragments are indicated by stars. Masson-Goldner trichrome.

Figure 29. Intramedullary Polyactive® 1000PEO70PBT30 stem - bone interface at 10 weeks. A lot of osteoclasts are found at the margins of the osteolytic area resorbing aggressively the endosteal bone. Polyactive® 1000PEO70PBT30 stem is indicated by a star, the arrows indicate osteoclasts resorbing endosteal bone. Masson-Goldner trichrome; scale bar 200 μm.

Figure 30. Extramedullarily perforated Polyactive® 1000PEO70PBT30 fragment surrounded by a granuloma at 10 weeks. Polyactive® fragment is indicated by a star. Masson-Goldner trichrome; scale bar 200 μm.

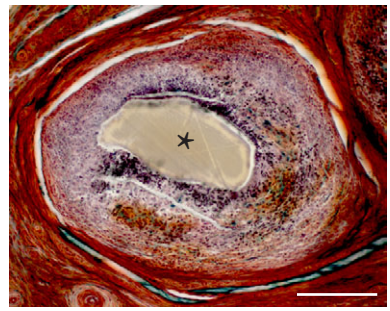

Figure 31. A bone cyst which developed at the site of degraded intramedullary Polyactive® stem. The bone cyst is indicated by a star. Masson-Goldner trichrome; scale bar 500 μm.

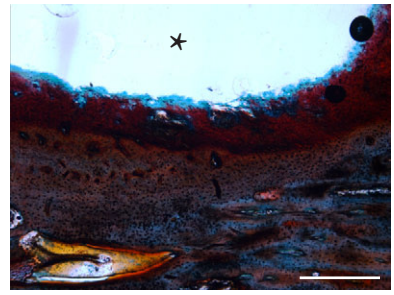

Polyactive® 1000PEO70PBT30 fragments were enclosed in granulomas infiltrated by polymorphonuclear neutrophils, lymphocytes, epitheloid cells and macrophages. However, compared with 10-week and 26-week specimens, the inflammatory infiltration was more moderate and previously separate cell layers inside the granulomas were not clearly identifiable anymore. The fibrous tissue capsule (10-30 layers of fibroblasts) surrounding the granulomas now contained also myofibroblasts. The endosteal surface of the bone was now occupied by osteoblasts forming new bone. The outline of the P(L/D)LA scaffold was identifiable despite the high rate of cracking of filaments.

Three-year follow-up

At three years, the Polyactive® 1000PEO70PBT30 stem had been mostly degraded and previous osteolytic areas had been replaced by new trabecular bone (Fig. 28D). The bones were highly sclerotic having thickened cortices enclosing disorganised and coarse trabeculae. A few large cysts without any lining cells were seen both intramedullary and in the fibrous artroplasty joint space (Fig. 31). No polymer material could be discerned. The predominant tissue component was dense fibrous tissue in the arthroplasty joint space. There were no inflammatory infiltrates.

6 DISCUSSION

6.1 Bioabsorbable fixation

In the present study, the initial fixation stabilities provided by bioabsorbable implants in the tubular bones of the hand were studied *ex vivo* and compared with those of metal fixation techniques.

In transversally-osteotomised metacarpals, 2.0 mm SR-PLGA 80/20 or SR-P(L/DL)LA 70/30 plate systems provided bending stability comparable with that obtained with a 1.7 mm titanium plate system. In dorsal apex bending, the rigidity of the dorsal bioabsorbable plate system was higher than those of crossed Kirschner wires. However, in palmar apex bending, Kirschner wire fixation was superior to the bioabsorbable and titanium plate fixations. The reason for this is the direction of force, which isolates and leaves the plate alone to carry the load. The lateral placement of the plate may be, from an extensor mechanism point of view, more favourable. By placing the bioabsorbable plate dorsolaterally rather than dorsally, the rigidity was increased in palmar apex bending but decreased in dorsal apex bending. Torsional rigidity provided by 2.0 mm bioabsorbable plate systems was higher than those provided by 1.7 mm titanium plate system, and no significant difference was found when comparing them with Kirschner wire fixation. Previously in transverse proximal phalangeal osteotomy, the rigidity provided by crossed 1.5 mm SR-PGA pins coated with PDS has been reported to be comparable with that of crossed 1.5 mm Kirschner wires in bending and compression tests, but the torsional rigidity achieved by the bioabsorbable pins was minor [46]. In biomechanical testing with non-SR plates and screws, the results have shown low strength characteristics [22].

In obliquely-osteotomised pig metacarpals, the main advantage of using bioabsorbable plates was the increased bending stability for the bioabsorbable construct. However, a single interfragmentary bioabsorbable screw with a plate provided relatively limited torsional rigidity due to deficient interfragmentary compression. Two 1.5 mm SR-PLLA pins provided fixation rigidity comparable with that of 1.5 mm Kirschner wires in dorsal and palmar apex bending, whereas in torsion the rigidity was comparable with that of 1.25 mm Kirschner wires. Two interfragmentary SR-P(L/DL)LA 70/30 screws (outer Ø 2.0 mm, inner Ø 1.45 mm) provided similar fixation rigidity to two 1.5 mm Kirschner wires in all directions, but lower rigidity than the titanium lag screws. The titanium plate with an interfragmentary lag screw showed to be mechanically superior to all other modes of fixation.

The bending and torsional forces are those likely to occur in metacarpal and phalangeal bones during *in vivo* loading of the hand. Therefore, bending and torsion tests were applied to osteotomised bones in these biomechanical studies. The bone specimens utilised in these studies were fresh frozen human cadaver metacarpal bones (paper I) and pig second metacarpal bones (paper II). The diaphyseal part of the pig metacarpal resembles human metacarpal bones and proximal phalanges [106]. Pig bones provided lower variance in dimentions and biomechanical properties compared to human cadaver bones. This is because cadaver bones were harvested from donors of variable age and bone densities.

Ex vivo biomechanical testing provides important data on fixation methods, although there are limitations as regards to clinical applications. The use of denuded bones underestimates the natural contribution of surrounding soft tissues to bone stability and deformities. There are no solid data indicating how much rigidity is required to achieve functional stability of a hand fracture. The conditions *in vivo* involve cyclic and sometimes sudden loading. While these biomechanical studies indicated satisfactory relative initial fixation stability compared to metal fixation techniques, they did not address the possibility of fatigue failure of fixation. The fatigue properties of bioabsorbable fixation systems have been insuffiently studied and need to be the subject of future studies.

The retention of mechanical properties of bioabsorbable fixation systems was not analysed in these studies. However, the behavior of SR-PLLA, SR-P(L/DL)LA 70/30 and SR-PLGA 80/20 fixation implant *in vivo* has been earlier extensively validated in both experimental [73, 101, 145, 206, 208, 209] and clinical [6, 158, 219] studies. These implants have shown good biocompatibility and have controlled strength retention properties. However, the soft-tissue volume available for accommodating implants is relatively small in the hand. Fibrosis and inflammatory tissue reaction related to the bioabsorbable implants and especially to extra-osseal plates is a potential concern in terms of tendon adhesion and soft-tissue irritation. Substantially amorphous SR-P(L/DL)LA 70/30 and SR-PLGA 80/20 co-polymers appears to have reduced the severity of this reaction [6, 73, 101, 145, 182, 219]; that reduces concern about complications. After an experimental trauma in monkeys, a PLGA sheet has been documented to reduce tendon adhesion and fibrosis between extensor tendon and metacarpal bone compared with control hands without implants [38]. SR plates, although small, remain relatively bulky when compared with the very thin equivalent titanium plates. Therefore, before disintegration, bioabsorbable implants may disturb the balance and function of joints and tendons. In the future, the fixation stability of bioabsorbable plate fixation can further increase and profiles can be made lower with three-dimensional plate design.

The biomechanical results and the extensive experience in the craniomaxillofacial region [6, 219] encouraged us to proceed with preliminary clinical studies on SR plate-and-screw systems in the hand. In our three preliminary patients with complex hand injuries, the SR-P(L/DL)LA 70/30 plates combined with 1.5 mm or 2.0 mm screws gave adequate stability for bone fixation and allowed union without infection or deformity or signs of implant failure. With follow-up periods of 12–20 months, union was achieved in all three cases and no clinical signs of adverse reactions were seen. Recently, non-SR PLGA 82/18 plates (LactoSorb®) were used for the fixation of 12 unstable metacarpal fractures [43]. An additional orthosis for 3 weeks was combined with the treatment protocol because of two patients with a secondary implant failure. No further implant failures were observed after this change of the post-operative regimen. Bone consolidation occurred within 6 weeks, and the healing was uneventful except for prolonged transient soft-tissue swelling in 3 patients. The patients demonstrated total active ROM 220°-265° at the six-month follow-up. The authors suggested the bioabsorbable plate-and-screw system with a supplemental orthosis for non-comminuted metacarpal fractures in compliant patients.

Bioabsorbable fixation implants offer potential advantages over the metal implants. When bioabsorbable fixation implants are used, no removal operation is necessitated and still no long-term interference with tendons and the growing skeleton remains [216, 217, 219]. In intra- and periarticular fractures, bioabsorbable pins are of advantage, since pins can be cut flush or beneath the bone surface, minimally violating the articular surface [57, 90, 136, 225]. Bioabsorbable implants do not interfere with clinical imaging. Additionally, the risk of implant-associated stress shielding and peri-implant osteoporosis is reduced [74].

6.2 Bioabsorbable joint scaffold arthroplasty

6.2.1 P(L/D)LA 96/4 joint scaffold

This experimental small joint arthroplasty model in minipigs showed that the P(L/D)LA 96/4 joint scaffold could be successfully used to engineer fibrous tissue joints *in situ*. The scaffold was initially invaded by vascularised and cell-rich loose connective tissue. In rat subcutis the in-growth of connective tissue into the P(L/D)LA 96/4 scaffolds occurred by three weeks [93]. During the follow-up of this study, the loose connective tissue inside the joint scaffold construct matured to dense fibrous connective tissue with an abundant collagen framework, containing only relatively few fibroblasts. The cell-rich interface zone immediately around all P(L/D)LA 96/4 filaments consisted of a fibroblast layer that became thinner during the follow-up. Recently, a somewhat similar connective tissue response to a P(L/D)LA mesh sheet after subcutaneous implantation in rat was described [82]. A type III collagen-rich area was found in the cell-rich interface zone immediately around the implant, whereas type I collagen and α-actin were expressed in the outer dense connective tissue zone. Myofibroblasts rich in α-actin formed a tight framework around the P(L/D)LA material and the type III collagen-rich interface zone, providing contraction and stability [82-84]. A prolonged and enhanced expression of extracellular matrix proteins tenascin and cellular fibronectin has also been demonstrated around P(L/D)LA implants [82-84]. This type of organised tissue architecture may represent the topological equivalent of a wound healing process, including clearance of dead tissue debris, production of a provisional fibronectin, tenascin and type III collagen rich matrix, scar contraction and maturation to type I collagen-rich fibrous tissue. A previous histological study on monkeys' thumb basal joints demonstrated that allograft tendon interposition promoted the repopulation of the artroplasty space with dense fibrous tissue, whereas the specimens without an interposition tendon graft were filled with loose fibroadipose tissue [166].

The collagen framework inside the scaffold became more prominent during the follow-up and provided ultimate structural integrity and strength in the arthroplasty space after scaffold degradation. The collagen framework was more prominent in the scaffold volarly than dorsally, which suggests that compression loading associated with joint flexion serves as a stimulus for fibrogenesis. At 3 years the structure of the P(L/D)LA 96/4 joint scaffold was almost completely disintegrated and replaced by dense fibrous connective tissue with scattered fibroblastic cells embedded in a collagen-rich matrix. As a last sign of the degradation process, there were patches of cell-rich loose connective tissue with tiny polymer debris particles in some areas. In addition to the local resident cells, such as vascular endothelial cells, fibroblasts and mast cells, this cellular reaction was composed of macrophages and foreign-body giant cells which are thought to be responsible for the ultimate digestion of the polymeric debris [128]. No accumulations of lymphocytes, implying an immune-inflammatory process, were seen. These results are consistent with earlier clinical, histological and immunohistological studies on P(L/D)LA 96/4 implants [64, 65, 82-84, 93, 162].

The maintenance of the arthroplasty space and joint alignment after interposition arthroplasty is essential for a successful outcome. *In vitro* compression testing has shown that the P(L/D)LA 96/4 joint scaffolds withstand estimated *in vivo* stresses and axial loading in the human MCP joints [120]. In this study, the arthroplasty space was maintained in the P(L/D)LA 96/4 scaffold group during the three years follow-up despite the scaffold degradation and strength

loosening. It thus seems that this type of joint arthroplasty does not *per se* require that the joint spacer is of biostable material. Apparently, endogenously "engineered" fibrous tissue is able to maintain the arthroplasty space. Probably the daily active use of the small joints of the hand prevents ankylosis and favours formation of a fibrous and functional pseudarthrosis.

The in-growth of fibrous tissue into an implant can be regulated by altering the structural parameters of the scaffold, such as the porosity, pore size, pore interconnectivity, filament orientation and compression modulus of the implant [200]. Because of the knitting and shaping techniques, the P(L/D)LA 96/4 scaffold has open porosity throughout the structure with the pore size ranging from some ten micrometers to more than 1 mm in diameter [64, 120]. This minipig experiment shows that this is enough for the ingrowth of fibroblasts which subsequently are able to replace the relatively loose and vascular connective tissue into cell-poor and well-organised fibrous connective tissue.

The original macroscopic configuration of the P(L/D)LA 96/4 scaffold was identifiable until follow-up of 52 weeks, but some changes on the surface and in the porosity developed during this observation period. The porosity of the scaffold reduced *in situ* volarly, probably due to compression caused by bones and ligaments and due to the reduced strength of the polymer. On the other hand, the mean porosity was dorsally increased at 26 and 52 weeks, which may be due to a distraction force generated on the extension side of the joint during joint motion.

The passive ROM values after the P(L/D)LA 96/4 joint scaffold and Swanson implant arthroplasties were similar in the present experimental study. However, the number of animals in each time group was not sufficient for adequate statistical analysis. The values may appear somewhat high when compared to the ROM values reported in human clinical studies for rheumatoid MCP joints after Swanson silicone arthroplasty [33, 53]. However, the ROM values recorded in most clinical studies are active, not passive. In radiographs, a minimal radiological volar subluxation, without any progression during the follow-up, was seen in the P(L/D)LA 96/4 scaffold group. In the microscopic evaluation, the volar subluxation occurred at the fibrous interface area between the scaffold and the resected metacarpal bone end. It is likely that most of the hybrid joint motion occurs in this hinge area, whereas the scaffold itself functions as a cushion-like absorbing counterforce. In the P(L/D)LA 96/4 scaffold group, the head of the resected metacarpal bone remodeled into a rounded convex shape, whereas the proximal phalanx remodelled into a concave shape. Possibly the joint biomechanics plays a role in this type of remodelling; a similar widening of the base of the proximal phalangeal bone is seen, e.g. in psoriatic arthritis, characterised by new bone formation. The P(L/D)LA 96/4 scaffold degradation did not induce any significant osteolysis or cortical erosion in the adjacent bones.

In the future, the bioabsorbable joint scaffold may be improved by using surface modification of the scaffold, bioactive molecules, cytokines, growth factors and seeded cells, such as chondrocytes, to reconstruct more complex structures [71, 168]. This is possible as PLA-based materials are cyto- and biocompatible with cells and tissues [1, 6, 19, 75, 76, 89, 103, 133, 134, 137, 158, 205-209, 213, 214, 219]. An improved understanding of cell behaviour (i.e., adhesion, proliferation and differentation) is needed for a better understanding of different types of scaffolds and of cell-material interactions. However, in rheumatoid patients, cartilage may be unfavourable because of the inflammatory joint disease, which may to some extent be maintained by an autoimmune attack against autologous cartilage tissue [85].

The fifth minipig MCP joint is a new *in vivo* model for evaluating the implants used in the small joint arthroplasty. The fifth minipig MCP joint is not a main weight-bearing joint, but, however, moves at each step, simulating cyclic hand joint loading. Its shape and passive ROM are close to those of the healthy human MCP joints. As regards the MCP arthroplasties, which are mainly done for rheumatoid arthritis patients, there were no inflammatory cell infiltrates in the reconstructed joints, and their soft-tissue balance was favourable. In the present study, both bone ends of the joint were resected to simulate the end stage of arthritis. Previously, e.g. the rabbit knee has been used as an *in vivo* model for evaluating the implants used in the reconstruction of MCP joints [113] but the model has been criticised [178]. Monkey hands closely resemble human hands in an anatomical sense [166], but the use of the monkey as an experimental animal is more expensive and its availability is limited.

6.2.2 P(L/D)LA 96/4 joint scaffold with Polyactive® stem

The alignment and stability of the P(L/D)LA 96/4 joint scaffold and the reconstructed joint must be maintained post-operatively before the in-grown fibrous tissue provides ultimate stability. Before the scaffold becomes stabilised by the invaded fibrous tissue, a temporary anchorage to adjacent bones using a double-sided intramedullary stem was considered as an alternative. To anchor the P(L/D)LA 96/4 joint scaffold in the resected joint for the early post-operative period, we developed a composite P(L/D)LA 96/4 scaffold with a double-sided intramedullary Polyactive® 1000PEO70PBT30 stem.

Earlier studies suggest that Polyactive® PEO/PBT co-polymer is degradable, elastomeric [78, 164], osteoconductive [21, 88, 149, 151, 153, 163] and has good biocompatibility [21, 88, 109, 149, 151-153, 157, 163, 198]. Hydrogel-like and bone bonding properties of the material, may enable *in situ* locking in bone [78, 195].

The Polyactive® 1000PEO70PBT30 stem caused a deleterious tissue reaction with dramatic signs of osteolysis in this study. The original diameter of the implant tracks (2-3 mm) had an osteolytic extension up to 7 mm seen in the radiographs since the first follow-up of 10 weeks. The bone cortex at the site of the intramedullary stem was often less than 1 mm in thickness and occasionally even perforated during the first post-operative year. In the control Swanson implant group with similar stem dimensions, the radiological stem track averaged only 3 mm in maximum diameter during the three-year follow-up. This diameter around the stems of Swanson implants was similar to or only slightly greater than the original reamed bone channel diameter. However, in clinical studies peri-implant osteolysis around the silicone implants is a common radiological finding, especially in the long-term follow-up [53, 131]. The osteolysis around silicone implants is caused by the pistoning movement of the silicone stems in the intramedullary canal and by the foreign-body reaction to silicone [33, 53, 131, 177].

The Polyactive® co-polymer is initially highly elastomeric [78, 164]. The composite joint implants with a double-sided intramedullary Polyactive® 1000PEO70PBT30 stem were similar to handle and to implant with flexible Swanson silicone rubber implants during the operation. However, the mechanical properties of Polyactive® 1000PEO70PBT30 decrease rapidly in an aqueous environment due to the high swelling typical for hydrogels and later also due to degradation [78]. In this study, the fragmentation of the stem during the first 10 weeks was suggestive of a decrease of elastomeric properties.

In this small joint arthroplasty model, no direct bone – Polyactive® 1000PEO70PBT30 stem bonding could be seen during the 3 years follow-up. Microscopically, the Polyactive® 1000PEO70PBT30 fragments were surrounded by granulomas that showed massive inflammatory foreign-body reactions with numerous polymorphonuclear leukocytes, lymphocytes, mononuclear macrophages and foreign-body giant cells with phagocytozed Polyactive® 1000PEO70PBT30 particles. The foreign-body reaction persisted until 52 weeks but gradually settled down by 3 years. High numbers of osteoclasts were found resorbing the endosteal bone to a large extent near the intramedullary Polyactive® 1000PEO70PBT30 fragments at 10 weeks. Cytokine production by macrophages and foreign-body giant cells can cause recruitment and activation of osteoclasts leading to bone resorption [86]. However, the osteoclast profile persisted only at the ten-week follow-up. At 52 weeks, relatively many osteoblasts, reflecting osteogenic activity, were seen at the endosteal surface of the bone. The bone synthesised was highly sclerotic and contained coarse trabeculae. At three years, no Polyactive® 1000PEO70PBT30 fragments could be seen anymore, but a few large cysts without any lining cells were seen both in the intramedullary and the fibrous artroplasty joint space, as the last sign of the Polyactive® 1000PEO70PBT30 material.

We suppose that the extensive osteolysis and foreign-body reaction induced by the Polyactive® 1000PEO70PBT30 stem in this study were caused by a raise in the intramedullary pressure and the irritation due to hydrogel-like properties of the Polyactive® 1000PEO70PBT30 stems and abrasion phenomenon caused by pistoning movement of a stem due to animal moving feet. The minipig fifth MCP joint moves at each step subjecting the Polyactive® 1000PEO70PBT30 stem to cyclic stress. This biomechanical aspect, not occurring in the earlier studies on the biocompatibility of this material, may have resulted to pistoning of the stem in the intramedullary canal during the early post-operative period and, thus, prevented good initial mechanical contact between the bone and the Polyactive® 1000PEO70PBT30 stem, and subsequent bone implant bonding. Wet PEO/PBT cylinders in a fully swollen state lack the capacity for bone-bonding but are instead encapsulated by thin fibrous capsule interposed between the bone and implant [163]. Cyclic stress to Polyactive® 1000PEO70PBT30 stem may also have accelerated the water up-take and degradation of the polymer. This perhaps led to accelerated swelling of the Polyactive® 1000PEO70PBT30 and tissue reactions, increased intramedullary pressure and excessive formation of degradation products overwhelming the clearance capacity of the surrounding tissue.

These results demonstrating extensive osteolysis and massive foreign-body reactions were unexpected, as in all earlier animal and clinical studies the Polyactive® co-polymer has demonstrated to have good biocompatibility and, in most earlier studies, even osteoconductivity. The reason for the controversial results could be the difference in polymer application to earlier *in vivo* studies in which the co-polymer has been investigated in non-loaded applications. In contrast, in this small joint arthroplasty model, the Polyactive® 1000PEO70PBT30 stem was subjected to cyclic stress associated with joint motion which led to deleterious, osteolytic tissue reaction.

7 CONCLUSIONS

The present study demonstrated that the initial biomechanical properties of SR bioabsorbable plates, screws and pins are comparable to currently-employed metal fixation methods in the small tubular bones. Bioabsorbable plate considerably enhances the bending stability of the bioabsorbable fixation construct. However, the torsional stability provided by these bioabsorbable implants is more limited than that obtained with their metal counterparts. In three cases of complex hand injuries, bioabsorbable plates were applied successfully, resulting in consolidation in a proof-of-principle type of study. In an experimental small joint arthroplasty model, P(L/D)LA 96/4 joint scaffold promoted functionally-adapted fibrous tissue in-growth while the arthroplasty space between the bone ends was maintained. After the degradation of the scaffold, a functional, stable pseudarthrosis with cell-poor and well-organised connective tissue was formed. In the composite joint implant, however, the intramedullary double-sided Polyactive® 1000PEO70PBT30 stem caused a deleterious, osteolytic tissue reaction and thus the Polyactive® 1000PEO70PBT30 stem should not be used in clinical joint reconstruction. The bioabsorbable implants have potential for use in clinical hand surgery, but must await validation in clinical patient series and controlled trials.

ACKNOWLEDGEMENTS

This study was carried out at the Department of Hand Surgery, Helsinki University Central Hospital; Institute of Biomedicine/Anatomy, University of Helsinki; Department of Medicine, Helsinki University Central Hospital; and ORTON Orthopaedic Hospital of the Invalid Foundation, Helsinki, during 2000-2008.

I wish to express my deepest gratitude to the following persons:

Professor Yrjö T. Konttinen, MD, PhD, Department of Medicine, Helsinki University Central Hospital, for supervising this study, for his support and guidance throughout these years. I am grateful for the excellent research facilities and for the possibility to learn the basics of research methods and scientific thinking. I admire his endless energy and vast knowledge in the field of biomaterials. I was truly privileged to join his research group.

Professor Nureddin Ashammakhi, MD, PhD, FRCSEd, Institute of Biomaterials, Tampere University of Technology, for valuable advice and support, and important guidance. His enthusiasm for science is something to really look up to.

Late Professor Seppo Santavirta, MD, PhD, for support and valuable comments and for providing excellent research facilities.

Academy Professor Pertti Törmälä, PhD, MDScihc, and Professor Minna Kellomäki, DrTech, Institute of Biomaterials, Tampere University of Technology, for the fruitful collaboration and for the expertise concerning polymer technology and for providing facilities for biomechanical testing.

Professor Riitta-Mari Tulamo, DVM, PhD, Department of Equine and Small Animal Medicine, Faculty of Veterinary Medicine, University of Helsinki, for facilities for experimental surgical research, and for invaluable help with the operations on the experimental animals.

Docent Timo Raatikainen, MD, PhD, Department of Hand Surgery, Helsinki University Central Hospital, for his interest in and positive attitude to this project, and for giving me the possibility to bring this thesis to its end.

Professor Ismo Virtanen, MD, PhD, Institute of Biomedicine/ Anatomy, University of Helsinki, for research facilities and support. I am also thankful for the chance to have gained extensive experience in teaching while working at the Insitute of Biomedicine/Anatomy.

Professor Christer Sollerman, MD, PhD, and Docent Ilkka Antti-Poika, MD, PhD, for their prompt review of this thesis and for their constructive criticism.

Acting Professor, Docent Jari Salo, MD, PhD, Department of Orthopaedics and Traumatology, Helsinki University Central Hospital, for interest and support especially during the final phase of the study.

The co-authors of the original papers: Professor Milomir Ninkovic, MD, PhD, Marina Ninkovic, MD, Christoph Harpf, MD, for their support and their essential role in the clinical part of this study; Docent Outi Kaarela, MD, PhD, Mauri Lehtimäki, MD, PhD, for their expertise and important contribution.

The other collaborators: Pasi Olkkonen, MSc, for consultation in statistics, Docent Jarkko Vasenius, MD, PhD, for his useful comments, Hanna Kurppa, MA, MSc, for skillful drawings, Pirkko Mäki for processing the histological specimens, and Seppo Koskensalo and the staff for taking good care of the experimental animals.

The co-workers at the Institute of Biomaterial, Tampere University of Technology, and in the company ConMed Linvatec Biomaterials, Inc. (former Bionx Implants Ltd): especially Harri Happonen, Kari Laurikainen, Jouko Ilomäki and Kimmo Lähteenkorva for fruitful cooperation in developing bioabsorbable implants.

The members of the TULES research group: especially Mari Ainola, Mika Hukkanen, Erkki Hänninen, Eija Kaila, Mikko Liljesröm, Guofeng Ma, Jami Mandelin, Pauliina Porola and Ville Waris for their invaluable help and friendship; and the other personnel of the Institute of Biomedicine/Anatomy.

All my surgeon colleagues at the Department of Hand Surgery, Helsinki University Central Hospital, for their support and friendship.

My parents, brother and sisters and their families for their love and support. My parents Timo and Liisa Waris have encouraged and supported me throughout my life, this study project being no exception. Other relatives for their help and support. Collectively, all my friends.

Last, but most I thank my dear wife Krista for her support, patience and love, and our son Juhana being the light of our life.

This study was supported by National Center of Excellence in Biomaterials and Tissue Engineering of Academy of Finland (2000-2005), Finnish Funding Agency for Technology and Innovation (Tekes), European Commission, Ministry of Education (National Graduate School of Biomaterials and its successor National Graduate School of Musculoskeletal Disorders and Biomaterials, National Graduate School of Clinical Investigation), Sigrid Jusélius Foundation, University of Helsinki, University of Helsinki funds, Helsinki University Central Hospital EVO funds, Institute of Biomaterials at Tampere University of Technology, Finnish Medical Society Duodecim, Finnish Medical Foundation, Research Foundation for Orthopaedics and Traumatology in Finland, Finnish Society for Surgery of the Hand, Farmos Science and Research Foundation, Biomedicum Helsinki Foundation, Päivikki and Sakari Sohlberg Foundation, Finnish-Norwegian Medical Foundation, Maud Kuistila Memorial Foundation, Maire Lisko Foundation, and Onni Talas Foundation (the scholarship fund of The Keuruu Murtomäki family association). I am most grateful to each of these institutions.

Helsinki, August 2008

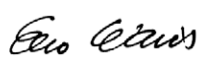

Eero Waris

REFERENCES

1. Akmaz I, Kiral A, Pehlivan O, Mahirogullari M, Solakoglu C, Rodop O. Biodegradable implants in the treatment of scaphoid nonunions. Int Orthop 2004;28:261-266.
2. Alexander H, Langrana N, Massengill JB, Weiss AB. Development of new methods for phalangeal fracture fixation. J Biomech 1981;14:377-387.
3. Anderson ML, Dhert WJ, de Bruijn JD, Dalmeijer RA, Leenders H, van Blitterswijk CA, Verbout AJ. Critical size defect in the goat's os ilium. A model to evaluate bone grafts and substitutes. Clin Orthop Relat Res 1999;364:231-239.
4. Arata J, Ishikawa K, Sawabe K, Soeda H, Kitayama T. Osteosynthesis in digital replantation using bioabsorbable rods. Ann Plast Surg 2003;50:350-353.
5. Arata J, Ishikawa K, Soeda H, Kitayama T. Arthrodesis of the distal interphalangeal joint using a bioabsorbable rod as an intramedullary nail. Scand J Plast Reconstr Surg Hand Surg 2003;37:228-231.
6. Ashammakhi N, Peltoniemi H, Waris E, Suuronen R, Serlo W, Kellomäki M, Törmälä P, Waris T. Developments in craniomaxillofacial surgery: use of self-reinforced bioabsorbable osteofixation devices. Plast Reconstr Surg 2001;108:167-180.
7. Athwal GS, Chenkin J, King GJ, Pichora DR. Early failures with a spheric interposition arthroplasty of the thumb basal joint. J Hand Surg [Am] 2004;29:1080-1084.
8. Barber FA, Snyder SJ, Abrams JS, Fanelli GC, Savoie FH 3rd. Arthroscopic Bankart reconstruction with a bioabsorbable anchor. J Shoulder Elbow Surg 2003;12:535-538.
9. Beevers DJ, Seedhom BB. Metacarpophalangeal joint prostheses. A review of the clinical results of past and current designs. J Hand Surg [Br] 1995;20:125-136.
10. Belcher HJ, Zic R. Adverse effect of porcine collagen interposition after trapeziectomy: a comparative study. J Hand Surg [Br] 2001;26:159-164.
11. Bergsma JE, de Bruijn WC, Rozema FR, Bos RR, Boering G. Late degradation tissue response to poly(L-lactide) bone plates and screws. Biomaterials 1995;16:25-31.
12. Bettinger PC, Linscheid RL, Berger RA, Cooney WP 3rd, An KN. An anatomic study of the stabilizing ligaments of the trapezium and trapeziometacarpal joint. J Hand Surg [Am] 1999;24:786-798.
13. Black D, Mann RJ, Constine R, Daniels AU. Comparison of internal fixation techniques in metacarpal fractures. J Hand Surg [Am] 1985;10:466-472.
14. Black DM, Mann RJ, Constine RM, Daniels AU. The stability of internal fixation in the proximal phalanx. J Hand Surg [Am] 1986;11:672-677.
15. Böhringer G, Schädel-Hopfner M, Junge A, Gotzen L. Die arthroskopische Therapie frischer Discus articularis-Verletzungen bei distalen Radiusfrakturen. Operative Technik und vorläufige Ergebnisse. Handchir Mikrochir Plast Chir 2001;33:245-251.
16. Böhringer G, Schädel-Höpfner M, Petermann J, Gotzen L. A method for all-inside arthroscopic repair of Palmer 1B triangular fibrocartilage complex tears. Arthroscopy 2002;18:211-213.
17. Bosscha K, Snellen JP. Internal fixation of metacarpal and phalangeal fractures with AO minifragment screws and plates: a prospective study. Injury 1993;24:166-168.
18. Böstman OM. Intense granulomatous inflammatory lesions associated with absorbable internal fixation devices made of polyglycolide in ankle fractures. Clin Orthop Relat Res 1992;278:193-199.

19. Böstman OM, Pihlajamäki HK. Adverse tissue reactions to bioabsorbable fixation devices. Clin Orthop Relat Res 2000;371:216-227.
20. Botte MJ, Davis JL, Rose BA, von Schroeder HP, Gellman H, Zinberg EM, Abrams RA. Complications of smooth pin fixation of fractures and dislocations in the hand and wrist. Clin Orthop Relat Res 1992;276:194-201.
21. Bouwmeester SJ, Kuijer R, Sollie-Drees MM, van der Linden AJ, Bulstra SK. Quantitative histological analysis of bony ingrowth within the biomaterial Polyactive implanted in different bone locations: an experimental study in rabbits. J Mater Sci Mater Med 1998;9:181-185.
22. Bozic KJ, Perez LE, Wilson DR, Fitzgibbons PG, Jupiter JB. Mechanical testing of bioresorbable implants for use in metacarpal fracture fixation. J Hand Surg [Am] 2001;26:755-761.
23. Branam BR, Tuttle HG, Stern PJ, Levin L. Resurfacing arthroplasty versus silicone arthroplasty for proximal interphalangeal joint osteoarthritis. J Hand Surg [Am] 2007;32:775-788.
24. Brüser P, Krein R, Larkin G. Fixation of metacarpal fractures using absorbable hemicerclage sutures. J Hand Surg [Br] 1999;24:683-687.
25. Buijs GJ, van der Houwen EB, Stegenga B, Bos RR, Verkerke GJ. Mechanical strength and stiffness of biodegradable and titanium osteofixation systems. J Oral Maxillofac Surg 2007;65:2148-2158.
26. Buijs GJ, van der Houwen EB, Stegenga B, Bos RR, Verkerke GJ. Torsion strength of biodegradable and titanium screws: a comparison. J Oral Maxillofac Surg 2007;65:2142-2147.
27. Burkhart SS. The evolution of clinical applications of biodegradable implants in arthroscopic surgery. Biomaterials 2000;21:2631-2634.
28. Carter PR, Benton LJ, Dysert PA. Silicone rubber carpal implants: a study of the incidence of late osseous complications. J Hand Surg [Am] 1986;11:639-644.
29. Casteleyn PP, Handelberg F, Haentjens P. Biodegradable rods versus Kirschner wire fixation of wrist fractures. A randomised trial. J Bone Joint Surg [Br] 1992;74:858-861.
30. Ceonzo K, Gaynor A, Shaffer L, Kojima K, Vacanti CA, Stahl GL. Polyglycolic acid-induced inflammation: role of hydrolysis and resulting complement activation. Tissue Eng 2006;12:301-308.
31. Chen SH, Wei FC, Chen HC, Chuang CC, Noordhoff S. Miniature plates and screws in acute complex hand injury. J Trauma 1994;37:237-242.
32. Chow SP, Pun WK, So YC, Luk KD, Chiu KY, Ng KH, Ng C, Crosby C. A prospective study of 245 open digital fractures of the hand. J Hand Surg [Br] 1991;16:137-140.
33. Chung KC, Kowalski CP, Myra Kim H, Kazmers IS. Patient outcomes following Swanson silastic metacarpophalangeal joint arthroplasty in the rheumatoid hand: a systematic overview. J Rheumatol 2000;27:1395-1402.
34. Claase MB, de Bruijn JD, Grijpma DW, Feijen J. Ectopic bone formation in cell-seeded poly(ethylene oxide)/poly(butylene terephthalate) copolymer scaffolds of varying porosity. J Mater Sci Mater Med 2007;18:1299-1307.
35. Cohen MS, Turner TM, Urban RM. Effects of implant material and plate design on tendon function and morphology. Clin Orthop Relat Res 2006;445:81-90.
36. Cook SD, Beckenbaugh RD, Redondo J, Popich LS, Klawitter JJ, Linscheid RL. Long-term follow-up of pyrolytic carbon metacarpophalangeal implants. J Bone Joint Surg [Am] 1999;81:635-648.
37. Cooney WP,III, Chao EY. Biomechanical analysis of static forces in the thumb during hand function. J Bone Joint Surg [Am] 1977;59:27-36.
38. Cutright DE, Reid RL. A biodegradable tendon gliding device. Hand 1975;7:228-237.

39. Dabezies EJ, Schutte JP. Fixation of metacarpal and phalangeal fractures with miniature plates and screws. J Hand Surg [Am] 1986;11:283-288.
40. Derkash RS, Niebauer JJ Jr, Lane CS. Long-term follow-up of metacarpal phalangeal arthroplasty with silicone Dacron prostheses. J Hand Surg [Am] 1986;11:553-558.
41. Diwaker HN, Stothard J. The role of internal fixation in closed fractures of the proximal phalanges and metacarpals in adults. J Hand Surg [Br] 1986;11:103-108.
42. Donath K, Breuner G. A method for the study of undecalcified bones and teeth with attached soft tissues. The sage-schliff (sawing and grinding) technique. J Oral Pathol 1982;11:318-326.
43. Dumont C, Fuchs M, Burchhardt H, Appelt D, Bohr S, Stürmer KM. Clinical results of absorbable plates for displaced metacarpal fractures. J Hand Surg [Am] 2007;32:491-496.
44. Faraj AA, Davis TR. Percutaneous intramedullary fixation of metacarpal shaft fractures. J Hand Surg [Br] 1999;24:76-79.
45. Firoozbakhsh KK, Moneim MS, Howey T, Castaneda E, Pirela-Cruz MA. Comparative fatigue strengths and stabilities of metacarpal internal fixation techniques. J Hand Surg [Am] 1993;18:1059-1068.
46. Fitoussi F, Lu W, Ip WY, Chow SP. Biomechanical properties of absorbable implants in finger fractures. J Hand Surg [Br] 1998;23:79-83.
47. Foliart DE. Swanson silicone finger joint implants: a review of the literature regarding long-term complications. J Hand Surg [Am] 1995;20:445-449.
48. Ford DJ, el-Hadidi S, Lunn PG, Burke FD. Fractures of the metacarpals: treatment by A. O. screw and plate fixation. J Hand Surg [Br] 1987;12:34-37.
49. Fusetti C, Meyer H, Borisch N, Stern R, Santa DD, Papaloizos M. Complications of plate fixation in metacarpal fractures. J Trauma 2002;52:535-539.
50. Fyfe IS, Mason S. The mechanical stability of internal fixation of fractured phalanges. Hand 1979;11:50-54.
51. Gangopadhyay S, Ravi K, Packer G. Dorsal plating of unstable distal radius fractures using a bio-absorbable plating system and bone substitute. J Hand Surg [Br] 2006;31:93-100.
52. Givissis P, Kapoutsis D, Ditsios K, Christidoulou A. Upper limb fractures treated with bioabsorbable materials. J Hand Surg [Eur] 2008;32:26.
53. Goldfarb CA, Stern PJ. Metacarpophalangeal joint arthroplasty in rheumatoid arthritis. A long-term assessment. J Bone Joint Surg [Am] 2003;85:1869-1878.
54. Goldner J. A modification of the Masson trichrome technique for routine laboratory purposes. Am J Pathol 1938;14:237-243.
55. Goodsett JR, Pahl AC, Glaspy JN, Schapira MM. Kirschner wire embolization to the heart: an unusual cause of pericardial tamponade. Chest 1999;115:291-293.
56. Gray KV, Meals RA. Hematoma and distraction arthroplasty for thumb basal joint osteoarthritis: minimum 6.5-year follow-up evaluation. J Hand Surg [Am] 2007;32:23-29.
57. Guo W, Liu K, Zhuang G, Chen Z, Guo T. Treatment of intra-articular fracture with absorbable screws and rods. Zhongguo Xiu Fu Chong Jian Wai Ke Za Zhi 2006;20:268-271.
58. Haapaniemi TA, Hermansson US. Cardiac arrhythmia caused by a Kirschner wire inside the heart. An unusual complication of finger osteosynthesis. J Hand Surg [Br] 1997;22:402-404.
59. Haas HG. PDS-Splinte zur Frakturbehandlung. Handchir Mikrochir Plast Chir 1986;18:295-297.
60. Hallab N, Merritt K, Jacobs JJ. Metal sensitivity in patients with orthopaedic implants. J Bone Joint Surg [Am] 2001;83:428-436.
61. Harris ED, Budd RC, Firestein GS, Genovese MC, Sergent JS, Ruddy S, Sledge CB, editors. Kelley's Textbook of Rheumatology, 7th edition. Philadelphia: Saunders; 2004.

62. Helling HJ, Prokop A, Schmid HU, Nagel M, Lilienthal J, Rehm KE. Biodegradable implants versus standard metal fixation for displaced radial head fractures. A prospective, randomized, multicenter study. J Shoulder Elbow Surg 2006;15:479-485.
63. Hidaka S, Gustilo RB. Refracture of bones of the forearm after plate removal. J Bone Joint Surg [Am] 1984;66:1241-1243.
64. Honkanen PB, Kellomäki M, Lehtimäki MY, Törmälä P, Mäkelä S, Lehto MU. Bioreconstructive joint scaffold implant arthroplasty in metacarpophalangeal joints: short-term results of a new treatment concept in rheumatoid arthritis patients. Tissue Eng 2003;9:957-965.
65. Honkanen PB, Konttinen YT, Kellomäki M, Mäkelä S, Lehto MUK. Bioreconstructive polylactide scaffold implant in metacarpophalangeal joint arthroplasty in rheumatoid arthritis: midterm follow-up study. J Hand Surg [Eur]; in press.
66. Hope PG, Williamson DM, Coates CJ, Cole WG. Biodegradable pin fixation of elbow fractures in children. A randomised trial. J Bone Joint Surg [Br] 1991;73:965-968.
67. Horton TC, Hatton M, Davis TR. A prospective randomized controlled study of fixation of long oblique and spiral shaft fractures of the proximal phalanx: closed reduction and percutaneous Kirschner wiring versus open reduction and lag screw fixation. J Hand Surg [Br] 2003;28:5-9.
68. Huang C, Li J, Zhu J, Li P, Xie G, Gong Y. A comparative study on two different absorbable intramedullary nails in treating metacarpal and phalanx fractures. Zhongguo Xiu Fu Chong Jian Wai Ke Za Zhi 2004;18:360-363.
69. Huang C, Li J, Zhu J, Xie G, Chen D, Li Q. Clinical study of phalange fractures treated by absorbable intramedullary nail in replantation of severed finger. Zhongguo Xiu Fu Chong Jian Wai Ke Za Zhi 2005;19:204-206.
70. Ikävalko M, Skyttä ET, Belt EA. One-year results of use of poly-L/D-lactic acid joint scaffolds and bone packing in revision metacarpophalangeal arthroplasty. J Hand Surg [Eur] 2007;32:427-433.
71. Isogai N, Landis W, Kim TH, Gerstenfeld LC, Upton J, Vacanti JP. Formation of phalanges and small joints by tissue-engineering. J Bone Joint Surg [Am] 1999;81:306-316.
72. Jensen CH, Jensen CM. Biodegradable pins versus Kirschner wires in hand surgery. J Hand Surg [Br] 1996;21:507-510.
73. Joukainen A, Pihlajamäki H, Mäkelä EA, Ashammakhi N, Viljanen J, Pätiälä H, Kellomäki M, Törmälä P, Rokkanen P. Strength retention of self-reinforced drawn poly-L/DL-lactide 70/30 (SR-PLA70) rods and fixation properties of distal femoral osteotomies with these rods. an experimental study on rats. J Biomater Sci Polym Ed 2000;11:1411-1428.
74. Juutilainen T, Hirvensalo E, Majola A, Partio EK, Pätiälä H, Rokkanen P, Kinnunen J. Bone mineral density in fractures treated with absorbable or metallic implants. Ann Chir Gynaecol 1997;86:51-55.
75. Juutilainen T, Pätiälä H. Arthrodesis in rheumatoid arthritis using absorbable screws and rods. Scand J Rheumatol 1995;24:228-233.
76. Juutilainen T, Vihtonen K, Pätiälä H, Rokkanen P, Törmälä P. Reinsertion of the ruptured ulnar collateral ligament of the metacarpophalangeal joint of the thumb with an absorbable self-reinforced polylactide mini tack. Ann Chir Gynaecol 1996;85:364-368.
77. Kallela I, Tulamo RM, Hietanen J, Pohjonen T, Suuronen R, Lindqvist C. Fixation of mandibular body osteotomies using biodegradable amorphous self-reinforced (70L:30DL) polylactide or metal lag screws: an experimental study in sheep. J Craniomaxillofac Surg 1999;27:124-133.
78. Kellomäki M, Paasimaa S, Grijpma DW, Kolppo K, Törmälä P. In vitro degradation of Polyactive 1000PEOT70PBT30 devices. Biomaterials 2002;23:283-295.

79. Kellomäki M, Törmälä P. Processing of resorbable poly-a-hydroxy acids for use as tissue-engineering scaffolds. In: Hollander AP, Hatton PV, editors. Methods in Molecular Biology: Biopolymer Methods in Tissue Engineering, vol. 238. Totowa, NJ: The Humana Press Inc; 2003. p. 1-10.
80. Ketchum LD, Thompson D, Pocock G, Wallingford D. A clinical study of forces generated by the intrinsic muscles of the index finger and the extrinsic flexor and extensor muscles of the hand. J Hand Surg [Am] 1978;3:571-578.
81. Khoo CT. Silicone synovitis. The current role of silicone elastomer implants in joint reconstruction. J Hand Surg [Br] 1993;18:679-686.
82. Kontio R, Ruuttila P, Lindroos L, Suuronen R, Salo A, Lindqvist C, Virtanen I, Konttinen YT. Biodegradable polydioxanone and poly(l/d)lactide implants: an experimental study on peri-implant tissue response. Int J Oral Maxillofac Surg 2005;34:766-776.
83. Kontio R, Salo A, Suuronen R, Lindqvist C, Meurman JH, Virtanen I. Fibrous wound repair associated with biodegradable poly-L/D-lactide copolymer implants: study of the expression of tenascin and cellular fibronectin. J Mater Sci Mater Med 1998;9:603-609.
84. Kontio R, Suuronen R, Konttinen YT, Hallikainen D, Lindqvist C, Kommonen B, Kellomäki M, Kylmä T, Virtanen I, Laine P. Orbital floor reconstruction with poly-L/D-lactide implants: clinical, radiological and immunohistochemical study in sheep. Int J Oral Maxillofac Surg 2004;33:361-368.
85. Konttinen YT, Li TF, Lassus J, Waris V, Santavirta S, Virtanen I. Removal of hyaline articular cartilage reduces lymphocyte infiltration and activation in rheumatoid synovial membrane. J Rheumatol 2001;28:2184-2189.
86. Konttinen YT, Zhao D, Beklen A, Ma G, Takagi M, Kivelä-Rajamäki M, Ashammakhi N, Santavirta S. The microenvironment around total hip replacement prostheses. Clin Orthop Relat Res 2005;430:28-38.
87. Krein R, Richter M, Brüser P. Osteosynthesen mit resorbierbaren Hemizerklagen bei Metakarpalfrakturen. Handchir Mikrochir Plast Chir 2000;32:102-106.
88. Kuijer R, Bouwmeester SJ, Drees MM, Surtel DA, Terwindt-Rouwenhorst EA, Van Der Linden AJ, Van Blitterswijk CA, Bulstra SK. The polymer Polyactive as a bone-filling substance: an experimental study in rabbits. J Mater Sci Mater Med 1998;9:449-455.
89. Kujala S, Raatikainen T, Kaarela O, Ashammakhi N, Ryhänen J. Successful treatment of scaphoid fractures and nonunions using bioabsorbable screws: report of six cases. J Hand Surg [Am] 2004;29:68-73.
90. Kumta SM, Leung PC. The technique and indications for the use of biodegradable implants in fractures of the hand. Tech Orthop 1998;13:160-163.
91. Kumta SM, Spinner R, Leung PC. Absorbable intramedullary implants for hand fractures. Animal experiments and clinical trial. J Bone Joint Surg [Br] 1992;74:563-566.
92. Kurzen P, Fusetti C, Bonaccio M, Nagy L. Complications after plate fixation of phalangeal fractures. J Trauma 2006;60:841-843.
93. Länsman S, Pääkkö P, Ryhänen J, Kellomäki M, Waris E, Törmälä P, Waris T, Ashammakhi N. Poly-L/D-lactide (PLDLA) 96/4 fibrous implants: histological evaluation in the subcutis of experimental design. J Craniofac Surg 2006;17:1121-1128.
94. Lehtimäki M, Lehto M, Kellomäki M, Paasimaa S, Mäkelä S, Honkanen P, Törmälä P. Resorboituva tekonivel reumapotilaiden rystysnivelten hoidossa. SOT 1998;21:368-370.
95. Li P, Bakker D, van Blitterswijk CA. The bone-bonding polymer Polyactive 80/20 induces hydroxycarbonate apatite formation in vitro. J Biomed Mater Res 1997;34:79-86.
96. Linscheid RL. Implant arthroplasty of the hand: retrospective and prospective considerations. J Hand Surg [Am] 2000;25:796-816.
97. Lionelli GT, Korentager RA. Biomechanical failure of metacarpal fracture resorbable plate fixation. Ann Plast Surg 2002;49:202-206.

98. Liu C, Tian D, Zhang Y, Zhang Y, Liu L. Treatment of old scaphoid fracture with absorbable screw. Zhongguo Xiu Fu Chong Jian Wai Ke Za Zhi 2008;22:450-452.
99. Lutz M, Sailer R, Zimmermann R, Gabl M, Ulmer H, Pechlaner S. Closed reduction transarticular Kirschner wire fixation versus open reduction internal fixation in the treatment of Bennett's fracture dislocation. J Hand Surg [Br] 2003;28:142-147.
100. Majola A, Vainionpää S, Rokkanen P, Mikkola HM, Törmälä P. Absorbable self-reinforced polylactide (SR-PLA) composite rods for fracture fixation: strength and strength retention in the bone and subcutaneous tissue of rabbits. J Mater Sci Mater Med 1992;3:43-47.
101. Mäkelä E, Mäkelä EA, Partio EK, Juutilainen T, Lähteenkorva K, Törmälä P, Rokkanen P. Fixation of experimental osteotomies with bioabsorbable SR-polylactide-polyglycolide (80/20) polymeric rods. J Mater Sci Mater Med 2008;19:1061-1067.
102. Mäkelä EA, Böstman O, Kekomäki M, Södergård J, Vainio J, Törmälä P, Rokkanen P. Biodegradable fixation of distal humeral physeal fractures. Clin Orthop Relat Res 1992;283:237-243.
103. Manninen MJ, Pohjonen T. Intramedullary nailing of the cortical bone osteotomies in rabbits with self-reinforced poly-L-lactide rods manufactured by the fibrillation method. Biomaterials 1993;14:305-312.
104. Maruyama T, Saha S, Mongiano DO, Mudge K. Metacarpal fracture fixation with absorbable polyglycolide rods and stainless steel K wires: a biomechanical comparison. J Biomed Mater Res 1996;33:9-12.
105. Massengill JB, Alexander H, Langrana N, Mylod A. A phalangeal fracture model – quantitative analysis of rigidity and failure. J Hand Surg [Am] 1982;7:264-270.
106. Massengill JB, Alexander H, Parson JR, Schecter MJ. Mechanical analysis of Kirschner wire fixation in a phalangeal model. J Hand Surg [Am] 1979;4:351-356.
107. Matloub HS, Jensen PL, Sanger JR, Grunert BK, Yousif NJ. Spiral fracture fixation techniques. A biomechanical study. J Hand Surg [Br] 1993;18:515-519.
108. Matsusue Y, Nakamura T, Iida H, Shimizu K. A long-term clinical study on drawn poly-L-lactide implants in orthopaedic surgery. J Long Term Eff Med Implants 1997;7:119-137.
109. Meijer GJ, van Dooren A, Gaillard ML, Dalmeijer R, de Putter C, Koole R, van Blitterwijk CA. Polyactive as a bone-filler in a beagle dog model. Int J Oral Maxillofac Surg 1996;25:210-216.
110. Merle M, Voche PH. L'ostéosynthèse résorbable: approche expérimentale et clinique en chirurgie de la main. Bull Mem Acad R Med Belg 1994;149:329-339.
111. Meyer-Clement M, Brüser P, Bönninghoff N, Stober R. Dexon-Cerclagen am Handskelett. Handchir Mikrochir Plast Chir. 1984;16:189-191.
112. Miller RA, Brady JM, Cutright DE. Degradation rates of oral resorbable implants (polylactates and polyglycolates): rate modification with changes in PLA/PGA copolymer ratios. J Biomed Mater Res 1977;11:711-719.
113. Minamikawa Y, Peimer CA, Ogawa R, Fujimoto K, Sherwin FS, Howard C. In vivo experimental analysis of silicone implants used with titanium grommets. J Hand Surg [Am] 1994;19:567-574.
114. Miot S, Scandiucci de Freitas P, Wirz D, Daniels AU, Sims TJ, Hollander AP, Mainil-Varlet P, Heberer M, Martin I. Cartilage tissue engineering by expanded goat articular chondrocytes. J Orthop Res 2006;24:1078-1085.
115. Möller K, Sollerman C, Geijer M, Brånemark PI. Osseointegrated silicone implants. 18 patients with 57 MCP joints followed for 2 years. Acta Orthop Scand 1999;70:109-115.
116. Möller K, Sollerman C, Geijer M, Kopylov P, Tägil M. Avanta versus Swanson silicone implants in the MCP joint – A prospective, randomized comparison of 30 patients followed for 2 years. J Hand Surg [Br] 2005;30:8-13.

117. Morgan WJ, Slowman LA, Wotton HM 3rd, Nairus J. Comparison of metal versus absorbable implants in tension-band wiring: a preliminary study. Orthopedics 2001;24:383-384.
118. Moroni L, Hendriks JA, Schotel R, de Wijn JR, van Blitterswijk CA. Design of biphasic polymeric 3-dimensional fiber deposited scaffolds for cartilage tissue engineering applications. Tissue Eng 2007;13:361-371.
119. Muermans S, Coenen L. Interpositional arthroplasty with Gore-Tex, Marlex or tendon for osteoarthritis of the trapeziometacarpal joint. A retrospective comparative study. J Hand Surg [Br] 1998;23:64-68.
120. Mutanen M. Studies of bioreconstructive small-joint prostheses. Master of science thesis, Tampere University of Technology, 2004. 100pp.
121. Nakamura K, Oda H, Tanaka S, Kuga Y, Yamamoto M, Nishikawa T, Juji T, Shimizu M. Usefulness of absorbable screws in the Sauvé–Kapandji procedure for rheumatoid wrist reconstruction. Mod Rheumatol 2002;12:144-147.
122. Nilsson A, Liljensten E, Bergström C, Sollerman C. Results from a degradable TMC joint spacer (Artelon) compared with tendon arthroplasty. J Hand Surg [Am] 2005;30:380-389.
123. Nusem I, Goodwin DR. Excision of the trapezium and interposition arthroplasty with gelfoam for the treatment of trapeziometacarpal osteoarthritis. J Hand Surg [Br] 2003;28:242-245.
124. Ouellette EA, Dennis JJ, Milne EL, Latta LL, Makowski AL. Role of soft tissues in metacarpal fracture fixation. Clin Orthop Relat Res 2003;412:169-175.
125. Ouellette EA, Freeland AE. Use of the minicondylar plate in metacarpal and phalangeal fractures. Clin Orthop Relat Res 1996;327:38-46.
126. Paavolainen P, Karaharju E, Slätis P, Ahonen J, Holmström T. Effect of rigid plate fixation on structure and mineral content of cortical bone. Clin Orthop Relat Res 1978;136:287-293.
127. Page SM, Stern PJ. Complications and range of motion following plate fixation of metacarpal and phalangeal fractures. J Hand Surg [Am] 1998;23:827-832.
128. Päivärinta U, Böstman O, Majola A, Toivonen T, Törmälä P, Rokkanen P. Intraosseous cellular response to biodegradable fracture fixation screws made of polyglycolide or polylactide. Arch Orthop Trauma Surg 1993;112:71-74.
129. Parkkila T, Belt EA, Hakala M, Kautiainen H, Leppilahti J. Comparison of Swanson and Sutter metacarpophalangeal arthroplasties in patients with rheumatoid arthritis: a prospective and randomized trial. J Hand Surg [Am] 2005;30:1276-1281.
130. Parkkila T, Hakala M, Kautiainen H, Leppilahti J, Belt EA. Osteolysis after sutter metacarpophalangeal arthroplasty: a prospective study of 282 implants followed up for 5.7 years. Scand J Plast Reconstr Surg Hand Surg 2006;40:297-301.
131. Parkkila TJ, Belt EA, Hakala M, Kautiainen HJ, Leppilahti J. Grading of radiographic osteolytic changes after silastic metacarpophalangeal arthroplasty and a prospective trial of osteolysis following use of Swanson and Sutter prostheses. J Hand Surg [Br] 2005;30:382-387.
132. Partio EK, Hirvensalo E, Böstman O, Rokkanen P. A prospective controlled trial of the fracture of the humeral medial epicondyle – how to treat? Ann Chir Gynaecol 1996;85:67-71.
133. Peltoniemi HH, Tulamo RM, Pihlajamäki HK, Kallioinen M, Pohjonen T, Törmälä P, Rokkanen PU, Waris T. Consolidation of craniotomy lines after resorbable polylactide and titanium plating: a comparative experimental study in sheep. Plast Reconstr Surg 1998;101:123-133.

134. Peltoniemi HH, Tulamo RM, Toivonen T, Hallikainen D, Törmälä P, Waris T. Biodegradable semirigid plate and miniscrew fixation compared with rigid titanium fixation in experimental calvarial osteotomy. J Neurosurg 1999;90:910-917.
135. Pelto-Vasenius K, Hirvensalo E, Böstman O, Rokkanen P. Fixation of scaphoid delayed union and non-union with absorbable polyglycolide pin or Herbert screw. Consolidation and functional results. Arch Orthop Trauma Surg 1995;114:347-351.
136. Pelto-Vasenius K, Hirvensalo E, Rokkanen P. Absorbable pins in the treatment of hand fractures. Ann Chir Gynaecol 1996;85:353-358.
137. Pihlajamäki H, Böstman O, Hirvensalo E, Törmälä P, Rokkanen P. Absorbable pins of self-reinforced poly-L-lactic acid for fixation of fractures and osteotomies. J Bone Joint Surg [Br] 1992;74:853-857.
138. Pohjonen T, Törmälä P. In vitro hydrolysis behaviour of self-reinforced 80/20 polylactide-co-glycolide copolymer. 2000:504.
139. Prevel CD, Eppley BL, Ge J, Winkler MM, Katona TR, D'Alessio K, Sarver D. A comparative biomechanical analysis of resorbable rigid fixation versus titanium rigid fixation of metacarpal fractures. Ann Plast Surg 1996;37:377-385.
140. Prevel CD, Eppley BL, Jackson JR, Moore K, McCarty M, Wood R. Mini and micro plating of phalangeal and metacarpal fractures: a biomechanical study. J Hand Surg [Am] 1995;20:44-49.
141. Prevel CD, McCarty M, Katona T, Moore K, Jackson JR, Eppley BL, Sood R. Comparative biomechanical stability of titanium bone fixation systems in metacarpal fractures. Ann Plast Surg 1995;35:6-14.
142. Pun WK, Chow SP, So YC, Luk KD, Ip FK, Chan KC, Ngai WK, Crosby C, Ng C. A prospective study on 284 digital fractures of the hand. J Hand Surg [Am] 1989;14:474-481.
143. Pun WK, Chow SP, So YC, Luk KD, Ngai WK, Ip FK, Peng WH, Ng C, Crosby C. Unstable phalangeal fractures: treatment by A.O. screw and plate fixation. J Hand Surg [Am] 1991;16:113-117.
144. Puttlitz CM, Adams BD, Brown TD. Bioabsorbable pin fixation of intercarpal joints: an evaluation of fixation stiffness. Clin Biomech 1997;12:149-153.
145. Pyhältö T, Lapinsuo M, Pätiälä H, Niiranen H, Törmälä P, Rokkanen P. Fixation of distal femoral osteotomies with self-reinforced poly(L/DL)lactide 70:30 and self-reinforced poly(L/DL)lactide 70:30/bioactive glass composite rods. an experimental study on rabbits. J Biomater Sci Polym Ed 2005;16:725-744.
146. Qi JH, Zhu BL, Yin DZ. Treatment of fracture involved articular surface with absorbable screws and rods. Zhongguo Xiu Fu Chong Jian Wai Ke Za Zhi 2003;17:453-455.
147. Radder AM, Davies JE, Leenders H, van Blitterswijk CA. Interfacial behavior of PEO/PBT copolymers (Polyactive®) in a calvarial system: an in vitro study. J Biomed Mater Res 1994;28:269-277.
148. Radder AM, Davies JE, Sodhi RNS, van der Meer SAT, Wolke JGC, van Blitterswijk CA. Postoperative carbonate-apatite formation in PEO/PBT copolymers (Polyactive®). Cells Mater 1995;5:55-62.
149. Radder AM, Leenders H, van Blitterswijk CA. Interface reactions to PEO/PBT copolymers (Polyactive®) after implantation in cortical bone. J Biomed Mater Res 1994;28:141-151.
150. Radder AM, Leenders H, van Blitterswijk CA. Bone-bonding behaviour of poly(ethylene oxide)-polybutylene terephthalate copolymer coatings and bulk implants: a comparative study. Biomaterials 1995;16:507-513.
151. Radder AM, Leenders H, van Blitterswijk CA. Application of porous PEO/PBT copolymers for bone replacement. J Biomed Mater Res 1996;30:341-351.
152. Radder AM, Loon JA, Puppels GJ, Blitterswijk CA. Degradation and calcification of a PEO/PBT copolymer series. J Mater Sci Mater Med 1995;6:510-517.

153. Radder AM, van Blitterswijk CA. Abundant postoperative calcification of an elastomer: matrix calcium phosphate-polymer composite for bone regeneration. J Mater Sci Mater Med 1994;5:320-325.
154. Reed AM, Gilding DK. Biodegradable polymers for use in surgery — poly(ethylene oxide)/poly(ethylene terephthalate) (PEO/PET) copolymers: 2. In vitro degradation. Polymer 1981;22:499-504.
155. Reilly DT, Burstein AH. The elastic and ultimate properties of compact bone tissue. J Biomech 1975;8:393-405.
156. Riordan DC, Fowler SB. Arthroplasty of the metacarpophalangeal joints: review of resection-type arthroplasty. J Hand Surg [Am] 1989;14:368-371.
157. Roessler M, Wilke A, Griss P, Kienapfel H. Missing osteoconductive effect of a resorbable PEO/PBT copolymer in human bone defects: a clinically relevant pilot study with contrary results to previous animal studies. J Biomed Mater Res 2000;53:167-173.
158. Rokkanen PU, Böstman O, Hirvensalo E, Mäkelä EA, Partio EK, Pätiälä H, Vainionpää SI, Vihtonen K, Törmälä P. Bioabsorbable fixation in orthopaedic surgery and traumatology. Biomaterials 2000;21:2607-2613.
159. Roure P, Ip WY, Lu W, Chow SP, Gogolewski S. Intramedullary fixation by resorbable rods in a comminuted phalangeal fracture model. A biomechanical study. J Hand Surg [Br] 1999;24:476-481.
160. Rubel IF, Seligson D, Lai JL, Voor MJ, Wang M. Pullout strengths of self-reinforced poly-L-lactide (SR-PLLA) rods versus Kirschner wires in bovine femur. J Orthop Trauma 2001;15:429-432.
161. Rustemeier M, Ganßmann M. Treatment of osseous ruptures of the flexor tendons with resorbable materials. Handchir Mikrochir Plast Chir 1986;18:302-303.
162. Saikku-Bäckström A, Tulamo RM, Räihä JE, Kellomäki M, Toivonen T, Törmälä P, Rokkanen P. Intramedullary fixation of cortical bone osteotomies with absorbable self-reinforced fibrillated poly-96L/4D-lactide (SR-PLA96) rods in rabbits. Biomaterials 2001;22:33-43.
163. Sakkers RJ, Dalmeyer RA, de Wijn JR, van Blitterswijk CA. Use of bone-bonding hydrogel copolymers in bone: an in vitro and in vivo study of expanding PEO-PBT copolymers in goat femora. J Biomed Mater Res 2000;49:312-318.
164. Sakkers RJ, de Wijn JR, Dalmeyer RA, van Blitterswijk CA, Brand R. Evaluation of copolymers of polyethylene oxide and polybutylene terephthalate (Polyactive): mechanical behaviour. J Mater Sci Mater Med 1998;9:375-379.
165. Santavirta S, Konttinen YT, Saito T, Grönblad M, Partio E, Kemppinen P, Rokkanen P. Immune response to polyglycolic acid implants. J Bone Joint Surg [Br] 1990;72:597-600.
166. Schmidt CC, McCarthy DM, Arnoczky SP, Herndon JH. Basal joint arthroplasty using an allograft tendon interposition versus no interposition: a radiographic, vascular, and histologic study. J Hand Surg [Am] 2000;25:447-457.
167. Schmidt K, Willburger R, Ossowski A, Miehlke RK. The effect of the additional use of grommets in silicone implant arthroplasty of the metacarpophalangeal joints. J Hand Surg [Br] 1999;24:561-564.
168. Sedrakyan S, Zhou ZY, Perin L, Leach K, Mooney D, Kim TH. Tissue engineering of a small hand phalanx with a porously casted polylactic acid-polyglycolic acid copolymer. Tissue Eng 2006;12:2675-2683.
169. Shetty V, Caputo AA, Kelso I. Torsion-axial force characteristics of SR-PLLA screws. J Craniomaxillofac Surg 1997;25:19-23.
170. Short WH, Werner FW, Sutton LG. Treatment of scapholunate dissociation with a bioresorbable polymer plate: a biomechanical study. J Hand Surg [Am] 2008;33:643-649.

171. Sohn RC, Jahng KH, Curtiss SB, Szabo RM. Comparison of metacarpal plating methods. J Hand Surg [Am] 2008;33:316-321.
172. Sollerman CJ, Geijer M. Polyurethane versus silicone for endoprosthetic replacement of the metacarpophalangeal joints in rheumatoid arthritis. Scand J Plast Reconstr Surg Hand Surg 1996;30:145-150.
173. Squitieri L, Chung KC. A systematic review of outcomes and complications of vascularized toe joint transfer, silicone arthroplasty, and PyroCarbon arthroplasty for posttraumatic joint reconstruction of the finger. Plast Reconstr Surg 2008;121:1697-1707.
174. Stahl S, Schwartz O. Complications of K-wire fixation of fractures and dislocations in the hand and wrist. Arch Orthop Trauma Surg 2001;121:527-530.
175. Stern PJ, Wieser MJ, Reilly DG. Complications of plate fixation in the hand skeleton. Clin Orthop Relat Res 1987;214:59-65.
176. Suuronen R, Pohjonen T, Hietanen J, Lindqvist C. A 5-year in vitro and in vivo study of the biodegradation of polylactide plates. J Oral Maxillofac Surg 1998;56:604-14.
177. Swanson AB. Flexible implant arthroplasty for arthritic finger joints: rationale, technique, and results of treatment. J Bone Joint Surg [Am] 1972;54:435-455.
178. Swanson AB. Silicone implants and titanium grommets. J Hand Surg [Am] 1995;20:515-516.
179. Takigawa S, Meletiou S, Sauerbier M, Cooney WP. Long-term assessment of Swanson implant arthroplasty in the proximal interphalangeal joint of the hand. J Hand Surg [Am] 2004;29:785-795.
180. Tegnander A, Engebretsen L, Bergh K, Eide E, Holen KJ, Iversen OJ. Activation of the complement system and adverse effects of biodegradable pins of polylactic acid (Biofix) in osteochondritis dissecans. Acta Orthop Scand 1994;65:472-475.
181. Terjesen T, Apalset K. The influence of different degrees of stiffness of fixation plates on experimental bone healing. J Orthop Res 1988;6:293-299.
182. Tiainen J, Soini Y, Törmälä P, Waris T, Ashammakhi N. Self-reinforced polylactide/polyglycolide 80/20 screws take more than 1(1/2) years to resorb in rabbit cranial bone. J Biomed Mater Res B Appl Biomater 2004;70:49-55.
183. Tomaino MM, Pellegrini VD,Jr, Burton RI. Arthroplasty of the basal joint of the thumb. long-term follow-up after ligament reconstruction with tendon interposition. J Bone Joint Surg [Am] 1995;77:346-355.
184. Tonino AJ, Davidson CL, Klopper PJ, Linclau LA. Protection from stress in bone and its effects. Experiments with stainless steel and plastic plates in dogs. J Bone Joint Surg [Br] 1976;58:107-113.
185. Törmälä P. Biodegradable self-reinforced composite materials; manufacturing structure and mechanical properties. Clin Mater 1992;10:29-34.
186. Törmälä P, Paasimaa S, Lehto M, Lehtimäki M. Reconstructive bioabsorbable joint prosthesis, US Patent no. 6,113,640, 2000.
187. Törmälä P, Pohjonen T, Rokkanen P. Bioabsorbable polymers: materials technology and surgical applications. Proc Inst Mech Eng [H] 1998;212:101-111.
188. Trail IA, Martin JA, Nuttall D, Stanley JK. Seventeen-year survivorship analysis of silastic metacarpophalangeal joint replacement. J Bone Joint Surg [Br] 2004;86:1002-1006.
189. Trevisan C, Morganti A, Casiraghi A, Marinoni EC. Low-severity metacarpal and phalangeal fractures treated with miniature plates and screws. Arch Orthop Trauma Surg 2004;124:675-680.
190. Trumble TE, Rafijah G, Gilbert M, Allan CH, North E, McCallister WV. Thumb trapeziometacarpal joint arthritis: partial trapeziectomy with ligament reconstruction and interposition costochondral allograft. J Hand Surg [Am] 2000;25:61-76.

191. Tupper JW. The metacarpophalangeal volar plate arthroplasty. J Hand Surg [Am] 1989;14:371-375.
192. Turner CH, Burr DB. Basic biomechanical measurements of bone: a tutorial. Bone 1993;14:595-608.
193. Vainio K. Vainio arthroplasty of the metacarpophalangeal joints in rheumatoid arthritis. J Hand Surg [Am] 1989;14:367-368.
194. Vainio K, Reiman I, Pulkki T. Results of arthroplasty of the metacarpophalangeal joints in rheumatoid arthritis. Wiederherstellungschir Traumatol 1967;9:1-7.
195. van Blitterswijk CA, Bakker D, Leenders H, Brink JVD, Hesseling SC, Bovell YP, Radder AM, Sakkers RJ, Gaillard ML, Heinze PH, Beumer GJ. Interfacial reactions leading to bone-bonding with PEO/PBT copolymers (Polyactive®). In: Ducheyne P, Kokubo T, van Blitterswijk CA, eds. Bone-Bonding Biomaterials. Leidertorp, The Netherlands: Reed Healthcare Communications; 1992:13-30.
196. van Blitterswijk CA, de Wijn J, Leenders H, Bakker DJ. The effect of PEO ratio on degradation, calcification and bonebonding of PEO-PBT copolymer. Cells Mater 1993;3:23-26.
197. van Blitterswijk CA, de Wijn JR, Leenders H, van den Brink J, Hesseling SC, Bakker D. A comparative study of the interactions of two calcium phosphates, PEO/PBT copolymer (Polyactive) and a silicone rubber with bone and fibrous tissue. Cells Mater 1993;3:11-22.
198. van Loon JA. Biocompatibility testing of degradable polymers. Ph.D. Thesis, Rijksuniversiteit Leiden, The Netherlands, 1995.
199. van Onselen EB, Karim RB, Hage JJ, Ritt MJ. Prevalence and distribution of hand fractures. J Hand Surg [Br] 2003;28:491-495.
200. van Tienen TG, Heijkants RG, Buma P, de Groot JH, Pennings AJ, Veth RP. Tissue ingrowth and degradation of two biodegradable porous polymers with different porosities and pore sizes. Biomaterials 2002;23:1731-1738.
201. Vandenberk P, De Smet L, Fabry G. Finger fractures in children treated with absorbable pins. J Pediatr Orthop B 1996;5:27-30.
202. Vanik RK, Weber RC, Matloub HS, Sanger JR, Gingrass RP. The comparative strengths of internal fixation techniques. J Hand Surg [Am] 1984;9:216-221.
203. Vasenius J, Vainionpää S, Vihtonen K, Mäkelä A, Rokkanen P, Mero M, Törmälä P. Comparison of in vitro hydrolysis, subcutaneous and intramedullary implantation to evaluate the strength retention of absorbable osteosynthesis implants. Biomaterials 1990;11:501-504.
204. Viegas SF, Ferren EL, Self J, Tencer AF. Comparative mechanical properties of various Kirschner wire configurations in transverse and oblique phalangeal fractures. J Hand Surg [Am] 1988;13:246-253.
205. Vihtonen K, Juutilainen T, Pätiälä H, Rokkanen P, Törmälä P. Reinsertion of the ruptured ulnar collateral ligament of the metacarpophalangeal joint with an absorbable self-reinforced polylactide tack. J Hand Surg [Br] 1993;18:200-203.
206. Viljanen J, Kinnunen J, Bondestam S, Majola A, Rokkanen P, Törmälä P. Bone changes after experimental osteotomies fixed with absorbable self-reinforced poly-L-lactide screws or metallic screws studied by plain radiographs, quantitative computed tomography and magnetic resonance imaging. Biomaterials 1995;16:1353-1358.
207. Viljanen J, Pihlajamäki H, Kinnunen J, Bondestam S, Rokkanen P. Comparison of absorbable poly-L-lactide and metallic intramedullary rods in the fixation of femoral shaft osteotomies: an experimental study in rabbits. J Orthop Sci 2001;6:160-166.
208. Viljanen J, Pihlajamäki H, Majola A, Törmälä P, Rokkanen P. Absorbable polylactide pins versus metallic Kirschner wires in the fixation of cancellous bone osteotomies in rats. Ann Chir Gynaecol 1997;86:66-73.

209. Viljanen JT, Pihlajamäki HK, Törmälä PO, Rokkanen PU. Comparison of the tissue response to absorbable self-reinforced polylactide screws and metallic screws in the fixation of cancellous bone osteotomies: an experimental study on the rabbit distal femur. J Orthop Res 1997;15:398-407.
210. Voche P, Merle M. Utilisation d'implants résorbables intraosseux. Évaluation experimentale et applications cliniques en chirurgie de la main. Chirurgie 1992;118:131-136.
211. Voche P, Merle M, Membre H, Fockens W. Bioabsorbable rods and pins for fixation of metacarpophalangeal arthrodesis of the thumb. J Hand Surg [Am] 1995;20:1032-1036.
212. Vom Saal FH. Intramedullary fixation in fractures of the hand and fingers. J Bone Joint Surg [Am] 1953;35:5-16.
213. Voutilainen N, Juutilainen T, Pätiälä H, Rokkanen P. Arthrodesis of the wrist with bioabsorbable fixation in patients with rheumatoid arthritis. J Hand Surg [Br] 2002;27:563-567.
214. Voutilainen NH, Pätiälä HV, Juutilainen TJ, Rokkanen PU. Long-term results of wrist arthrodeses fixed with self-reinforced polylevolactic acid implants in patients with rheumatoid arthritis. Scand J Rheumatol 2001;30:149-153.
215. Wachtl SW, Guggenheim PR, Sennwald GR. Cemented and non-cemented replacements of the trapeziometacarpal joint. J Bone Joint Surg [Br] 1998;80:121-125.
216. Waris E, Ashammakhi N, Kaarela O, Raatikainen T, Vasenius J. Use of bioabsorbable osteofixation devices in the hand. J Hand Surg [Br] 2004;29:590-598.
217. Waris E, Ashammakhi N, Kelly CP, Andrus L, Waris T, Jackson IT. Transphyseal bioabsorbable screws cause temporary growth retardation in rabbit femur. J Pediatr Orthop 2005;25:342-345.
218. Waris E, Konttinen YT. Letter to the editor: on the use of Lactosorb plate for fixation of a metacarpal shaft fracture. Ann Plast Surg 2004;52:111-112.
219. Waris E, Konttinen YT, Ashammakhi N, Suuronen R, Santavirta S. Bioabsorbable fixation devices in trauma and bone surgery: current clinical standing. Expert Rev Med Devices 2004;1:229-240.
220. Waris E, Pakkanen M, Lassila K, Törmälä P, Konttinen YT, Suuronen R, Ashammakhi N. Alloplastic injectable biomaterials for soft tissue augmentation: a report on two cases with complications associated with a new material (DermaLive) and a review of the literature. Eur J Plast Surg 2003;26:350-355.
221. Weigel T, Schinkel G, Lendlein A. Design and preparation of polymeric scaffolds for tissue engineering. Expert Rev Med Devices 2006;3:835-851.
222. Weightman B, Amis AA. Finger joint force predictions related to design of joint replacements. J Biomed Eng 1982;4:197-205.
223. Wüstner MC, Partecke BD, Buck-Gramcko D. Resorbierbare PDS-Splinte zur Frakturstabilisierung und für Arthrodesen an der Hand. Handchir Mikrochir Plast Chir 1986;18:298-301.
224. Yajima H, Kobata Y, Yamauchi T, Takakura Y. Advanced Kienböck's disease treated with implantation of a tendon roll and temporary partial fixation of the wrist. Scand J Plast Reconstr Surg Hand Surg 2004;38:340-346.
225. Yamamuro T, Matsusue Y, Uchida A, Shimada K, Shimozaki E, Kitaoka K. Bioabsorbable osteosynthetic implants of ultra high strength poly-L-lactide. A clinical study. Int Orthop 1994;18:332-340.